Fakultät für Medizin

Institut für Virologie

Role and regulation of IL-1α production by human T helper cells in health and disease

Ying-Yin Chao

Vollständiger Abdruck der von der Fakultät für Medizin der Technischen Universität München zur Erlangung des akademischen Grades eines

Doctor of Philosophy (Ph.D.)

genehmigten Dissertation.

Vorsitzende/r: Prof. Dr. Stefan Engelhardt

Betreuer/in: Prof. Dr. Christina Zielinski

Prüfer der Dissertation:

1. Prof. Dr. Olaf Groß

2. Prof. Dr. Marc Schmidt-Supprian

Die Dissertation wurde am 22.07.2020 bei der Fakultät für Medizin der Technischen Universität München eingereicht und durch die Fakultät für Medizin am 18.10.2020 angenommen.

Table of contents

Abstract

Over the last few years Th17 cells have been recognized as major drivers of several inflammatory diseases. Th17 cells also display heterogeneity and plasticity, which translates into distinct functions in settings of health and disease and which can be exploited for therapeutic purposes. In our previous studies, we have validated the existence of pro-inflammatory and anti-inflammatory human Th17 cell subsets. They differ in their ability of IL-10 expression, their microbial antigen specificities and their priming requirement for IL-1α (Zielinski CE et al. Nature 2012). Our novel insights indicated that the pro-inflammatory Th17 cell subset can also produce IL-1α, an innate danger signal and alarmin that might confer pathogenicity to this T cell population. The expression of IL-1α by an adaptive immune cell subset therefore prompted us to investigate its characteristics and regulation in detail, as well as to explore innate-like properties of human T helper cells in general. We found that Th17-inducing cytokines and transcriptional networks promote IL-1α production. We found that the activity of calpain, a protease known to cleave IL-1α, was increased in activated T cells and the secretion of IL-1α was calpain-dependent. Surprisingly, we could demonstrate a role for NLRP3 activation in the secretion of IL-1α. It was preferentially expressed in the Th17 cell subset and correlated with pro-IL-1α cleavage. Interestingly, Th17 cell-restricted NLRP3 activation does not activate caspase-1 for the extracellular release of IL-1α, thus engaging in an alternative pathway of inflammasome activation. We also uncovered that the presence of the pore forming protein GSDME in T cells, and that the cleavage of this protein correlate with the secretion level of IL-1α. Taken together, we demonstrate that IL-1α represents a novel, so far overlooked effector cytokine of human Th17 cells that is regulated by calpain and alternatively activated inflammasome. This demonstrates that innate signaling mechanisms can be adopted by adaptive T cells to exert pro-inflammatory functions. After IL-1 blocking therapy, autoinflammatory patients showed diminished production of IL-1α, thus suggesting a potential role of pro-inflammatory Th17 cells in human disease.

Kurzfassung

Seit einigen Jahren ist der große Einfluss von TH17-Zellen in der Entstehung verschiedener entzündlicher Erkrankungen bekannt. Die TH17-Zell Population ist geprägt von einer großen Heterogenität und Plastizität. Die daraus resultierenden Funktionen der Zellen, sowohl im Gesunden als auch in der Krankheit, lassen sich zu Therapiezwecken nutzen. In unseren früheren Studien konnten wir die Existenz von proinflammatorischen und antiinflammatorischen humanen TH17-Zell Subpopulationen bestätigen. Diese unterscheiden sich in ihrer Fähigkeit IL-10 zu produzieren, ihrer mikrobiellen Antigenspezifität und in ihren Priming-Voraussetzungen (Zielinski CE et al. Nature 2012). Neue Erkenntnisse deuten an, dass auch die proinflammatorische TH17-Subpopulation IL-1α produzieren kann. IL-1α ist ein Gefahren- und Alarmsignal des angeborenen Immunsystem, das möglicherweise zur Pathogenität dieser TH17-Subpopulation beiträgt. Die Expression von IL-1α durch eine Subpopulation des erworbenen Immunsystems hat uns veranlasst, die Charakteristika und Regulation dieser Zytokinexpression, sowie Eigenschaften des angeborenen Immunsystems in humanen T-Helfer Zellen im Allgemeinen zu untersuchen. Wir haben herausgefunden, dass TH17-induzierende Zytokine und Transkriptionswege die Produktion von IL-1α begünstigen. Überraschenderweise konnten wir zeigen, dass NLRP3-Aktivierung eine Rolle in der Sekretion von IL-1α spielt. NLRP3 wird in der TH17-Zell Subpopulation verstärkt exprimiert und korreliert mit der Spaltung von pro-IL-1α. Interessanterweise wird durch die auf TH17-Zell begrenzte NLRP3-Aktivierung jedoch nicht Caspase-1 für die extrazelluläre Freisetzung von IL-1α aktiviert, sodass es über einen alternativen Signalweg für die Inflammasom-Aktivierung wirken muss. Wir haben auch einen neuartigen GSDME-assoziierten Weg der Pyroptose für die IL-1α-Freisetzung von TH17-Zellen entdeckt. Zusammenfassend zeigen wir, dass IL-1α ein neues, bisher übersehenes Effektor-Zytokin von TH17-Zellen darstellt, das über einen alternativen Weg der Inflammasom-Aktivierung und derGSDME-assoziierten Pyroptose reguliert wird. Das beweist, dass Signalmechanismen des angeborenen Immunsystems von T-Zellen aus dem erworbenen Immunsystem übernommen werden können, um

proinflammatorische Funktionen auszuführen. Nach einer Therapie mit IL-1 Blockade zeigten Patienten mit auto-inflammatorischen Krankheiten eine verringerte IL-1α Produktion, was auf eine potenzielle Beteiligung proinflammatorischer TH17-Zellen in diesen Erkrankungen hindeuten könnte.

Abbreviations

2-ME	2-Mercaptoethanol
AICD	activation-induced cell death
AIM2	Absent In Melanoma 2
AOSD	Adult-onset Still's disease
APC	allophycocyanin
ASC	Apoptosis-associated Speck-like Protein
ATP	Adenosine triphosphate
BCA	Bicinchoninic acid assay
CAPS	Cryopyrin-associated periodic syndrome
CARD	caspase activation and recruitment domains
Cat#	catalogue number
CathG	cathepsin G
CCR	CC chemokine receptors
CD	cluster of differentiation
cDNA	complementary DNA
CoRegNet	reconstruction and integrated analysis of co-regulatory
CpG-ODNs	CpG oligodeoxynucleotides
CTLs	cytotoxic T lymphocytes
Ctrl	control
CXCL	The chemokine (C-X-C motif) ligand
CXCR	CXC chemokine receptors
Cy7	Cyanine7
DAMPs	Damage-associated molecular patterns
DMSO	dimethyl sulfoxide
DPBS	Dulbecco's phosphate-buffered saline
EDTA	Ethylenediaminetetraacetic acid
ELISA	The enzyme-linked immunosorbent assay
ER	endoplasmic reticulum
Fas	first apoptosis signal receptor
FDR	false discovery rate

FITC	Fluorescein isothiocyanate
FLICA	Fluorescent-Labeled Inhibitor of Caspases
GAPDH	Glyceraldehyde 3-phosphate dehydrogenase
GM-CSF	Granulocyte-macrophage colony-stimulating factor
GSDM	Gasdermin
GSDMD	Gasdermin D
GSDME	Gasdermin E
GSEA	Gene Set Enrichment Analysis
GzmB	Granzyme B
HIV	human immunodeficiency viruses
hrs	hours
IBD	Inflammatory bowel disease
IFN-	Interferon
IL-	Interleukin
IL-1R	Interleukin-1 receptor
JAK	Janus kinase
JIA	Juvenile idiopathic arthritis
kDa	kilodalton
KEGG	Kyoto Encyclopedia of Genes and Genomes
LDH	Lactate dehydrogenase
LPS	Lipopolysaccharides
MACS	Magnetic-activated cell sorting
min	minutes
mL	milliliter
mM	millimolar
MS	Multiple sclerosis
MyD88	Myeloid differentiation primary response 88
NAC	N-Acetyl Cysteine
NE	Neutrophil elastase
NF-kB	Nuclear Factor kappa-light-chain-enhancer of activated B cells
ng	nanogram
NLRP3	NOD-, LRR- and pyrin domain-containing protein 3

NLS	Nuclear localization sequence
nm	nanometer
ns	not significant
PAMPs	Pathogen-associated molecular patterns
PBMC	peripheral blood mononuclear cell
PBS	Phosphate-buffered saline
PCR	Polymerase chain reaction
PE	Phycoerythrin
PMA	Phorbol 12-myristate 13-acetate
PR-3	Proteinase 3
PVDF	Polyvinylidene fluoride
PYD	PYRIN domain
RA	Rheumatoid arthritis
RIPA	Radioimmunoprecipitation assay
RNA	Ribonucleic acid
RORγt	RAR-related orphan receptor gamma
ROS	Reactive oxygen species
SDS-PAGE	sodium dodecyl sulfate–polyacrylamide gel electrophoresis
SEM	standard error of the mean
STAT	signal transducer and activator of transcription
TBST	Tris-Buffered Saline, 0.1% Tween®20 Detergent
Tc	cytotoxic T cell
TCR	T-cell receptor
TGF-	Transforming growth factor
Th	T helper cells
TLRs	Toll-like receptors
TNF-	tumor necrosis factor
v	volt
µL	microliter
µm	micrometer
µM	micromolar

1 Introduction

1.1 Innate and adaptive immunity

To adapt to complicated environments, the human body has evolved several strategies for reacting to the pathogens we encounter in our daily lives. The immune system is a complex network of tissues, cells, and proteins that help to clear the body of pathogens and foreign substances. The immune system can be subdivided into the innate and adaptive immune systems. Briefly, an innate immune response, once activated, exerts rapid broad-recognition of pathogens. Whereas, an adaptive immune response requires a longer period of time to develop and provides highly specialized elimination of pathogens and long-term protection through immunological memory. Classification of cells as either innate or adaptive often depends on their reactions to microbial challenge. For example, macrophages and neutrophils are considered to be innate immune cells because of their rapid and broad-acting responses to pathogens, whereas T cells and B cells are classed as being adaptive immune cells on account of their longer reaction times and high specificity towards particular antigens. Beyond classifying the immune system at the cellular level, soluble factors are also crucial for determining its functions. Cytokines and chemokines are important soluble factors that can be secreted by both types of immune cells and are also important for establishing complicated communication networks in the immune system (Cohen, Bigazzi, & Yoshida, 1974; Lever, 1953). Cytokines and chemokines orchestrate the immune system by recruiting and regulating neighboring and distant cells. Cytokines that are produced to initiate an inflammatory response are believed to be innate-like, whereas those that are produced by adaptive immune cells, or appear later, are adaptive-like. The cells and cytokines involved in these two arms of the immune system have been extensively-studied. However, the division into the innate and adaptive immune systems is not clear-cut and there is often some overlap. This thesis aims to investigate a new and unexpected role of IL-1α, a cytokine that has previously been classified as innate-like. In the current study, the IL-1α was identified in a subset of adaptive immune cells was further elucidated for its mode of regulation and function.

1.2 T helper cell subsets

T helper cells (also known as CD4 T cells and Th cells) are adaptive immune cells that can modulate several other immune cell populations. They are capable of helping B cells with antibody production; boosting the immune functions of first-line defense cells, such as macrophage/monocytes; and recruiting granulocytes to specific sites for enhanced clearance of pathogens (Zhu & Paul, 2008). T helper cells can be further divided into Th1 and Th2 cells. Since the discovery of these two subgroups in the murine immune system by Mosmann and Coffman in 1986 (Mosmann, Cherwinski, Bond, Giedlin, & Coffman, 1986), there have been extensive efforts in determining the full diversity of the T helper subsets. Until now, it has been commonly appreciated that T helper cells are not a homogeneous population, but are composed of several distinct cell subpopulations with distinct functions.

1.2.1 Classification of T helper subsets

In their groundbreaking work, Mosmann and Coffman defined Th1- and Th2-type cells by the cytokines they produced; Th1 cells produce IFN-γ and Th2 cells produce IL-4 (Mosmann et al., 1986). Since that original study, the definition of the Th lineages has depended primarily on the signature cytokines that the cells produce. There are also different classification systems commonly used to identify T helper subsets. One such system is based on detecting lineage-specific transcription factors, which regulate T helper lineage programs and indicate the lineage before the cells are terminally differentiated. Another frequently used system is based on the expression profiles of chemokine receptors (Mahnke, Brodie, Sallusto, Roederer, & Lugli, 2013), which implies the migratory property of the cells. One of the advantages of chemokine receptor-based classification is the easier access to the cell surface and cell preservation because the cell membrane does not need to be destroyed. This is critical for downstream clinical applications. It is not always the case that a subpopulation fits perfectly into a subgroup classification, therefore, the heterogeneity of the T helper subsets causes more challenges to the classification systems. In addition, there are still undiscovered functions of the existing subsets in health and disease settings.

Despite their diversity, these T helper subsets originate from the same pool of naïve CD4 T cells, all emerging from the thymus. The T helper cell fate depends on the configuration of signals they receive during their interactions with other cells. The cytokine combinations that cause the differentiation of naïve CD4 T cells into specific cell types are shown in Figure 1.1 (Eyerich & Zielinski, 2014; Mangan et al., 2006; Zhu & Paul, 2008).

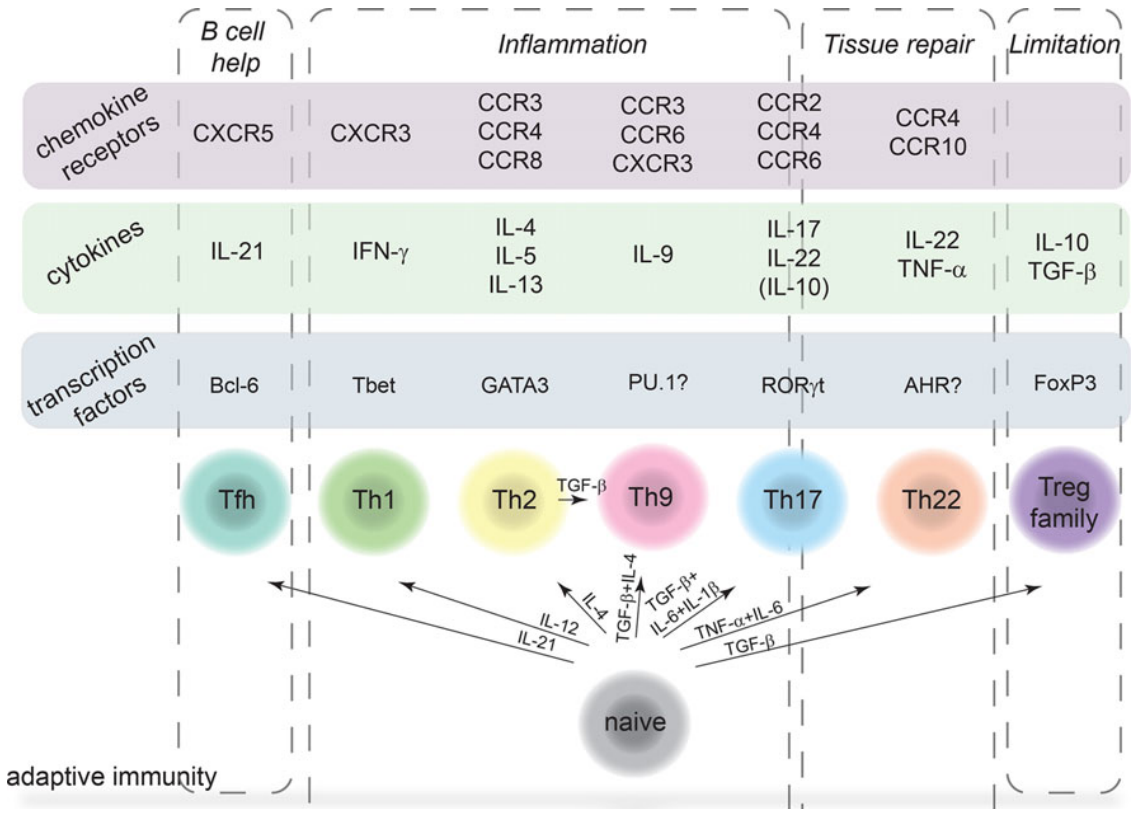

Figure 1.1. Classification of T helper subsets.

Classification of T helper cell subsets with (from top to bottom) chemokine receptor expression, major secreted cytokines, and the lineage-specific transcription factors. The cytokine requirements for the differentiation of T helper cell subsets is also shown. Image modified from Eyerich & Zielinski, 2014.

1.2.2 Th17 cells and their heterogeneity

Th17 cells are a subset of T helper cells that are known to be behave differently from the classical Th1/Th2 (Harrington et al., 2005). Th17 cells are regulated by the RORγt transcription factor (Ivanov et al., 2006), and they mainly secrete IL-17, which gives this population its name, but also IL-22, IL-21, and GM-CSF (Zheng et al., 2007). The role of Th17 cells in the immune system is quite complicated as they not only contribute to the clearance of extracellular bacteria and fungi but are also important in some autoimmune diseases, such as multiple sclerosis (MS), rheumatoid arthritis (RA), juvenile idiopathic arthritis (JIA), and Inflammatory bowel disease (IBD) (Weaver, Harrington, Mangan, Gavrieli, & Murphy, 2006; Yasuda, Takeuchi, & Hirota, 2019). Because there is ample evidence indicating that Th17 cells contribute to the initiation of these diseases, studying how Th17 cells are transformed from protective immune cells to pathogenic lymphocytes has become an area of intensive investigation. Studies have shown that the pro-inflammatory cytokines IL-1 and IL-23 are capable of stabilizing and differentiating Th17 cells in autoimmune models (Chung et al., 2009; Cua et al., 2003; Langrish et al., 2005; Sutton, Brereton, Keogh, Mills, & Lavelle, 2006).

Previously, our laboratory identified a novel type of human IL-10-producing Th17 cell (Noster et al., 2016; Zielinski et al., 2012). IL-1β, a critical cytokine that also drives Th17 cells differentiation (Wilson et al., 2007) showed the ability to modulate the anti-inflammatory cytokine IL-10. We have previously shown that the IL-10-producing Th17 cells act similarly to Treg cells, a well-recognized immunosuppressive subset that mainly produces IL-10 (Noster et al., 2016). In line with our findings, Aschenbrenner et al recently showed that IL-10 production is a property of a human Th17 subset., IL-10^{+} Th17 cells upregulated a variety of genes encoding immunoregulatory molecules as well as genes modulating the tissue-residency program, whereas IL-10^{-} Th17 expressed genes encoding pro-inflammatory cytokines. The evidence that pro-inflammatory and immunoregulatory phenotypes coexist as a stable feature of two subsets of Th17 cells revealed the heterogeneity of Th17 cells (Aschenbrenner et al., 2018).

The immunosuppressive properties of IL-10-producing-Th17 cells thus prompted us to investigate the identities and genetic profiles of this cell subset. Surprisingly, the *IL1A* gene is significantly up-regulated in so-called pro-inflammatory Th17 cells (Results, Figure 2.1C). The *IL1A* gene-encoded IL-1α cytokine is an alarmin, which is primarily expressed in first-line defense cells during the early response toward pathogens.

1.3 Interleukin-1-alpha

1.3.1 Interleukin-1

Interleukin-1 (IL-1) is unique in immunology because IL-1 and Toll-like receptors (TLRs) share the same downstream signaling molecule, myeloid differentiation primary response 88 (MyD88), and hence give rise to similar functions. IL-1 contributes to non-sterile inflammation, and TLRs contribute to sterile inflammation. The discovery of IL-1 is attributed to its effect of increasing body temperature during the initiation phase of the immune response (Dinarello, Goldin, & Wolff, 1974). IL-1 has been associated with innate immunity. It was subsequently discovered that this cytokine contains two isoforms, IL-1α and IL-1β, which share several similarities. The unprocessed forms and processed forms of both proteins are 31 kDa and 17 kDa, respectively. Both lack a leader sequence and are secreted via an unconventional pathway that uses ER-Golgi-independent machinery (Daniels & Brough, 2017). IL-1α and IL-1β both use IL-1R1 as their receptor for signaling, suggesting that they have similar bioactive functions. Despite these similarities, they also show many distinctive features. For example, IL-1α and IL-1β are encoded by two different genes, namely *IL1A* and *IL1B*. In addition, the mechanisms by which these two isoforms are processed are different. The IL-1β secretion mechanism has been extensively studied in monocytes and macrophages over the past few years. The cleavage of IL-1β before secretion is critical for its bioactivity, and is performed by a delicate multi-protein complex called the inflammasome, which engages two signals to activate the entire mechanism. Cysteine protease caspase-1 is the best-known protease that is activated by the inflammasome and cleaves IL-1β to render it bioactive. Besides caspase-1, other enzymes have been

found to cleave IL-1β and are shown in Figure 1.2. Among all the proteases, caspase-8 has gained most attention recently for its potential to replace caspase-1 when it is absent or when its enzymatic-activity is abrogated. Therefore, the caspase-8 inflammasome is described as a “non-canonical inflammasome mechanism” (M. Chen et al., 2015; Gaidt et al., 2016).

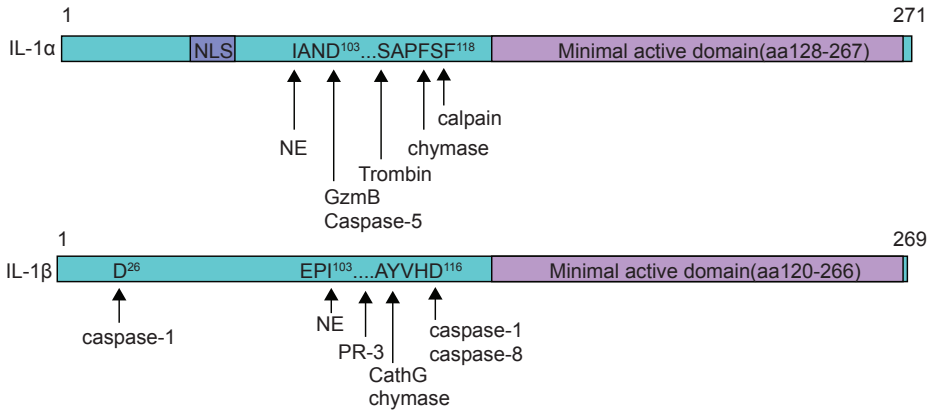

Figure 1.2. Schematic representation showing the cleavage sites of different proteases in IL-1α and IL-1β proteins

(NE, neutrophil elastase; GzmB, granzyme B; CathG, cathepsin G; PR-3, proteinase-3). The minimal active domain in IL-1α and IL-1β and nuclear localization signal (NLS) are also indicated (Purple). Image modified from Afonina, Muller, Martin&Beyaert, 2015.

1.3.2 Regulation of IL-1α

Unlike IL-1β, which has not been found in the nucleus, IL-1α has a nuclear localization sequence in the precursor region and acts as a dual function cytokine. This means that IL-1α not only functions as a conventional cytokine but can also act as a transcription factor (Ariel Werman, 2004). IL-1α has been found to be constitutively expressed in

several cell types, especially in barrier cells (e.g., epithelial cells and endothelial cells) and innate immune cells, when these cells receive stress-associated stimuli. Stress-associated stimuli include oxidative stress, exposure to cytokines (including IL-1 itself); and danger signals, such as pathogen- or damage-associated molecular patterns (PAMPs or DAMPs) (Di Paolo & Shayakhmetov, 2016). Because of its rapid production and importance in sterile inflammation, IL-1α has been regarded as an “alarmin” that alerts the immune system of potential injury and damage. Pro-IL-1α, the precursor form, has bioactivity, yet cleavage of pro-IL-1α into the mature form helps to increase its bioactivity. The well-established cleavage sites are shown in Figure 1.2. Pro-IL-1α can be cleaved inside the cell or in the extracellular space (Di Paolo & Shayakhmetov, 2016). It can be cleaved by a calcium-dependent neutral protease known as calpain (Carruth LM, 1991; Y Kobayashi, 1990). Several studies have also indicated that when pro-IL-1α is cleaved by granzyme B, elastase, or chymase, a more biologically active form of IL-1α is generated (Afonina et al., 2011). More recent studies have shown similar results; thrombin and caspase-5 (caspase-11 in mice), as well as the protease mentioned above, can also cleave pro-IL-1α and produce a more active form of IL-1α (Burzynski et al., 2019; Wiggins et al., 2019).

IL-1α signaling is known to induce the expression of the downstream IL-8 (*CXCL8*) and IL-6 (*IL6*) genes (Di Paolo & Shayakhmetov, 2016; Garlanda, Dinarello, & Mantovani, 2013; Robson, Westwick, & Brown, 1995). Besides signaling through IL-1R1, there is also an inhibitory type 2 IL-1 receptor (IL-1R2) in the cytosol, which acts as a decoy receptor to inhibit amplification of the IL-1 signaling loop (Peters, Joesting, & Freund, 2013). Furthermore, upon binding to IL-1R2, pro-IL-1α is protected from cleavage. Caspase-1 is able to cleave IL-1R2 and release the binding of pro-IL-1α, indicating the participation of the inflammasome in IL-1α processing and its secretion pathway (Zheng, Humphry, Maguire, Bennett, & Clarke, 2013).

Another feature that makes IL-1α distinct from IL-1β is that IL-1α can function as a membrane-bound cytokine in innate immune cells, and regulation of the membrane-bound form and the secreted form are different. The former requires only NF-κB

activation, whereas the latter requires the additional activation of the inflammasome (Fettelschoss et al., 2011; Kurt-Jones, Beller, Mizel, & Unanue, 1985).

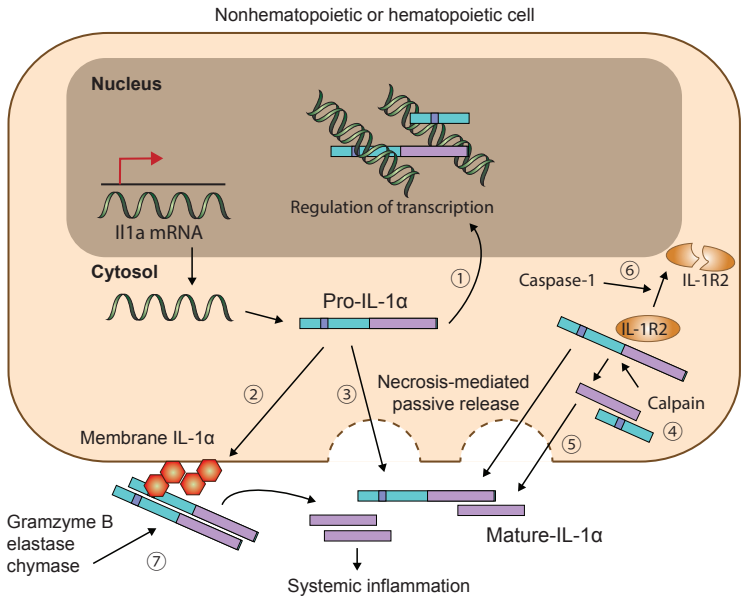

Figure 1.3. Mechanism of IL-1α secretion.

(1) IL-1α has a nuclear localization sequence and translocates to the nucleus as a transcription factor. (2) IL-1α can function as a membrane-bound cytokine. (3) Passive release of pro-IL-1α during necrosis. (4) Calpain cleaves pro-IL-1α and increases IL-1α activity. (5) Mature-IL-1α is secreted via membrane rupture. (6) IL-1R2 in the cytosol interferes with pro-IL-1 alarmin function. Caspase-1-dependent proteolysis of IL-1R2 releases pro-IL-1α and exposes the cleavage site of calpain. (7) Granzyme B, elastase, and chymase cleave the extracellular pro-IL-1α. Image modified from Di Paolo & Shayakhmetov, 2016.

1.3.3 Inflammasome and IL-1α

The inflammasome was first described in 2002 by Tschopp's group as an enormous molecular complex in stimulated innate immune cell lines (Martinon, Burns, & Tschopp, 2002). The inflammasome complex is composed of pattern-recognition receptors and an adaptor protein (named ASC) that contains a pyrin domain (PYD) and a caspase recruitment domain (CARD). It is the ASC protein that brings the caspase-1 and the inflammasome together to form the active structure of the complex. The proximity of caspase-1 triggers the auto-processing by caspase-1 itself (Broz & Dixit, 2016). So far, five receptors have been identified that assemble inflammasomes; NLRP1, NLRP3, NLRC4, absent in melanoma 2 (AIM2), and pyrin (Agostini et al., 2004; Broz & Dixit, 2016; Mariathasan et al., 2004). The NLRP3 inflammasome is the most well-characterized and is known to be involved in several diseases. Its activation requires two signals; the first priming signal is usually provided by extracellular inflammatory stimuli, such as microbial or endogenous molecules, resulting in the induction of NLRP3 and pro-IL1β expression; the second activation signal is stimulated by substances such as ATP, pore-forming toxins, or viral RNA and causes a unique type of cell death termed pyroptosis (Y. He, Hara, & Nunez, 2016). To date, we know that the process that leads to pyroptosis is due to the pores forming in the cell membrane, brought about by gasdermin-D (GSDMD). The N-terminal domain of GSDMD is cleaved by activated caspase-1 and caspase-4/5 and inserts into lipid membranes, causing cell membrane rupture. These non-selective pores then induce pyroptosis, enabling the secretion of cytokines, including cleaved IL-1β, IL-18, and IL-1α (Y. He et al., 2016; Shi et al., 2015). Based on the mechanism described above, it is thought that the mechanism of IL-1α secretion can be either inflammasome-dependent or -independent. Evidence in support of inflammasome-dependent secretion is that the stimuli that induce IL-1β secretion and inflammasome activation also induce IL-1α secretion, and dendritic cells from IL-1β-deficient mice also failed to secrete IL-1α upon stimulation (Fettelschoss et al., 2011). In addition, IL-1α release was shown to be reduced in caspase-1-deficient mice (Keller, Ruegg, Werner, & Beer, 2008), even

though IL-1α is not a substrate of caspase-1. There is also data showing that a small molecule drug, MCC950, inhibits NLRP3 inflammasome formation and inhibits the secretion of IL-1α by bone marrow-derived macrophages (Coll et al., 2015). However, there is still some contradictory data showing that NLRP3-deficient macrophages produce a considerable amount of IL-1α (Coll et al., 2015). The passive release of IL-1α brought about by different types of cell death, which is not associated with the inflammasome, can also contribute to its secretion. This is discussed in greater detail in the following section.

1.3.4 IL-1 and cell viability

Several studies have indicated that cell death stimuli regulate the processing and release of IL-1. Apart from pyroptosis, which we have discussed earlier, IL-1β is suggested to be released via a caspase-8 dependent apoptosis mechanism (Bossaller et al., 2012; England, Summersgill, Edye, Rothwell, & Brough, 2014; Shimada et al., 2012), whereas IL-1α release is believed to be necrosis-associated. Both the pro-form and the mature-form of IL-1α are observed in necrotic cells, implying that during the secretion process, the cytokine is passively released after necrotic membrane rupture. (Afonina et al., 2011; Zheng et al., 2013). Whether cells can remain alive after secreting IL-1 is still under active debate. There is some evidence showing that IL-1s can be released from living macrophages and that IL-1α can be emitted from gasdermin pores instead of plasma membrane rupture (Evavold et al., 2018; Tapia et al., 2019). It remains unclear how cells regulate gasdermin activation or pore formation. Interesting questions still need to be answered, such as could pore formation be reversible? and can cells remain alive after pore formation?

1.3.5 Inflammasome and pyroptosis in T cells

It is well known that the NLRP3 inflammasome regulates interleukin-1β maturation and controls cell pyroptosis in innate immune cells, yet a direct role for NLRP3 in human adaptive immune cells has rarely been described. Recently it was shown that NLRP3 expressed in T cells, albeit inflammasome-unrelated, controls the differentiation of T

helper cells (Bruchard et al., 2015). Caspase-1, the key executor protein in the NLRP3 inflammasome, has also been shown to promote the differentiation of Th17, independent of its enzymatic activity or inflammasome activation (Gao et al., 2020). Regarding the presence of the NLRP3 inflammasome in T helper cells, it has been suggested that the assembly of the NLRP3 inflammasome in T helper cells is driven by complement receptor signaling (Arbore et al., 2016). Of note, NLRP3 inflammasome-triggered pyroptosis is observed in human CD4 T cells infected with HIV and CD4 T cells of rheumatoid arthritis (RA) patients (Doitsh et al., 2014; Li et al., 2019).

1.4 Pathological role of Th17 cells in autoinflammatory syndromes

The proinflammatory functions of Th17 cells can be profitable to the host during bacterial or fungal infections. However, Th17 cells are also notorious for their pathogenicity in several autoimmune diseases, such as psoriasis, arthritis, multiple sclerosis, and IBD. Therapies targeting IL-17 have been widely used and achieved attenuation of autoimmune disease scores.

Recently, Th17 cells have also been associated with several autoinflammatory diseases. Autoinflammatory diseases are characterized by the excess production of IL-1β. The causes of these diseases are mostly associated with gene mutations in the inflammasome, which leads to an abnormal amount of downstream cytokines, such as IL-1β and IL-18. The diseases that have been studied and linked to Th17 cells so far are Schnitzler syndrome (Noster et al., 2016) and the autoinflammatory disorder adult-onset Still's disease (AOSD) (Waite & Skokos, 2012). It has previously been shown that in patients with Schnitzler syndrome, production of the anti-inflammatory cytokine IL-10 is abrogated in Th17 cells, but this effect can be restored with IL-1β-blocking treatment (Noster et al., 2016). These data support that IL-1 signaling triggers the pro-inflammatory phenotypes of Th17 cells and aggravates disease severity.

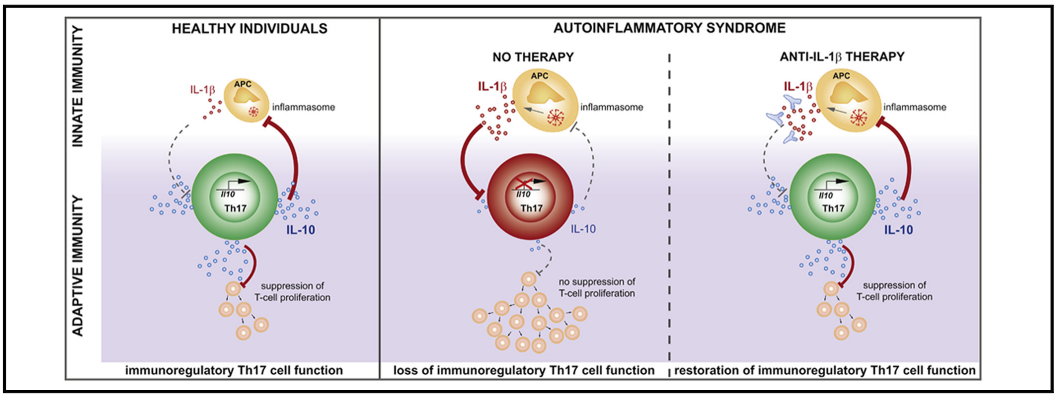

Figure 1.4. Schematic representation depicting that patients with auto-inflammatory syndromes have systemic IL-1β overproduction and defects in Th17 cell production of IL-10.

This abrogation in anti-inflammatory Th17 cell functions can be restored following therapy with IL-1β binding antibodies (Canakinumab). Image derived from Noster et al., 2016.

AOSD is another disease model that has been studied for its potential association with Th17 cells. The rationale for this model is the elevated levels of IL-1β, IL-18, and IL-6 observed in the serum of AOSD patients. These cytokines are able to promote the differentiation of Th17 cells. Indeed, increased numbers of Th17 cells and higher levels of related cytokines are observed in AOSD patients (D. Y. Chen et al., 2010). Currently, the treatments for autoinflammatory patients are IL-1 blocking drugs, such as Canakinumab (blocking IL-1β) or Anakinra (blocking IL-1R). The outcomes have been mostly promising (Goldbach-Mansky & Kastner, 2009); however, there is little research on the underlying mechanisms of the therapy regarding the regulation of adaptive immune cells. Together, the role of Th17 cells in autoinflammatory diseases is as interesting as it is in autoimmune diseases. Understanding the regulation of pro- and auto-inflammatory Th17 cells in autoinflammatory disease models may provide better targeted therapies for clinical applications.

1.5 Aim of this Thesis

The discovery of IL-1α production by human Th17 cells highlights a novel function of this cytokine in immune responses driven by T helper subsets. The innate-like properties of IL-1α prompt us to investigate the whole picture of how this cytokine is regulated in an adaptive Th17 cell lineage. The aims for this thesis are to characterize this novel property of Th17 cells in detail, to resolve the mechanism of IL-1α regulation in T helper cells, including the upstream priming conditions and the processing and releasing mechanisms. Finally, I aim to elucidate the clinical relevance of these novel Th17 cells in human disease settings.

In detail, firstly, I would like to determine whether IL-1α production is T helper cell-type dependent. Since little is known about the IL-1α that is produced by adaptive immune cells, I will isolate different T cell types to identify T cell populations that produce IL-1α. Further, I will test the migration properties of the IL-1α producing cells; the migration properties of the cells will indicate the functions and effector sites of the IL-1α producing cells.

Secondly, I would like to determine what the priming signals are for IL-1α production in T cells. As we know that IL-1α is an alarmin cytokine, its secretion must be strictly regulated to prevent the unwanted amplification of inflammatory responses. Besides the stimulation conditions (TCR stimulation and costimulation) conventionally used to activate T cells, the role of additional signals, such as cytokines and TLRs, in the context of promoting IL-1α production intracellularly will be investigated. Concerning the secretion mechanism, which is currently explored-studied in innate immune cells, I would like to start with the knowledge we obtain from innate immune cells and then refer to T helper cells.

Thirdly, I aim to determine whether IL-1α secreting T cells contribute to the pathogenicity of some known disease models that are Th17-related. Previously, it was demonstrated that the alteration of pro- and anti-inflammatory Th17 cells might

influence the pathological outcome in autoinflammatory syndromes (Noster et al., 2016). I plan to investigate the role of IL-1α-producing Th17 cells in the same disease settings and observe the effects of IL-1 blocking therapies on IL-1α production.

2 Results

2.1 The existence of heterogeneity among human Th17 cells with pro- and anti-inflammatory properties.

We have previously identified two types of T helper 17 (Th17) cells in human peripheral blood, which differ in their polarization requirements for Interleukin (IL)-1β and cytokine profiles [e.g., interferon (IFN)-γ or IL-10)] (Noster et al., 2016; Zielinski et al., 2012). The anti-inflammatory cytokine IL-10 was significantly downregulated after IL-1β treatment. (Figure 2.1B) To obtain a better overview of these two distinct subpopulations, we performed gene array analysis (Figure 2.1C). In line with our previous publications, we found that *IL10* is enriched in anti-inflammatory Th17 cells. Surprisingly, in the current study, I found that *IL1A* gene expression was strongly upregulated in pro-inflammatory Th17 cells in our transcriptome data. The microarray has been performed by colleagues at the Charité University Hospital Berlin and was analyzed by a bioinformatic collaborator (Pawl Durek). IL-1α has been associated with innate immune cells, as a first-line danger signal, also known as an alarmin, but the role of this cytokine in adaptive immune cells remained unclear. To better understand the role played by *IL1A in* our transcriptome analysis, we attempted to extract additional information from the top 20 up- and down-dysregulated genes (Figure 2.1A). However, drawing conclusions regarding potential mechanisms was difficult based on the data regarding differentially expressed genes. We also attempted to perform gene set enrichment analysis (GSEA), using published data regarding the pro- or anti-inflammatory program of human Th17 subsets (Aschenbrenner et al., 2018)(Figure 2.2B). The gene expression profile of our IL-1β-treated Th17 cells showed a high correlation with the pro-inflammatory gene-expression profile of IL-10^{neg} Th17 cells published by Aschenbrenner et al. Similarly, in their study they showed that *IL1A* gene was also highly expressed in the IL-10^{neg} Th17 cells in their study (Figure 2.2C).

2.1.1 IL-1α is expressed in human T cell subsets, especially in Th17 cells

To validate the transcriptome data from our analysis, I attempted to detect IL-1α at the protein level in human T cells. Firstly, I started with the whole CD4 and CD8 memory

T-cells. $CD4^+CD45RA^-$ (CD4 memory) and $CD8^+CD45RA^-$ (CD8 memory) cells were isolated and stimulated with anti-CD3/CD28 beads, which was the same protocol used for Th17 cells to obtain our transcriptome data. IL-1β was also administered, to promote IL-1α expression. However, IL-1α could only be detected in approximately 1% of cells in either population, even with IL-1β treatment (Figure 2.3A and B). I attempted to further add transforming growth factor (TGF)-β, a cytokine that is crucial for the stabilization of the Th17 program, which resulted in a significant increase in the frequencies of IL-$1\alpha^+$ to 3–4% in CD4 but not CD8 memory cells (Figure 2.3C). The proportion of IL-$1\alpha^+$ cells was also rather low (below 2%) in CD4 naive T cells. (Figure 2.3D)

To determine which T helper subset produced the most IL-1α, I isolated Th1 ($CD45RA^-CXCR3^+CCR4^-CCR6^-$), Th2 ($CD45RA^-CXCR3^-CCR4^+CCR6^-$), Th17 ($CD45RA^-CXCR3^-CCR4^+CCR6^-$), and T-regulatory (Treg) ($CD25^{hi}CD127^-$) cells from $CD4^+$ cells, based on the expression level of chemokine receptors and surface markers as indicated (Figure 2.3E). Approximately 8% of Th17 cells and approximately 6% of Th1 cells produced IL-1α, which is significantly higher than Treg cells (Figure 2.3F). Interestingly, among all the subsets, Th17 cells produced the largest amounts of extracellular IL-1α (Figure 2.3G) as I detected IL-1α concentration in the supernatants by using ELISA. IL-1β treatment further increased IL-1α secretion by Th17 cells from ~8 pg/mL to 40 pg/mL (Figure 2.3H). The secreted IL-1α could also be observed in Th1 cells (~10 pg/mL with IL-1β treatment) but not in Th2 or Treg cells. These results implied that IL-1α production may correlate with the Th17 program, which deserves further investigation.

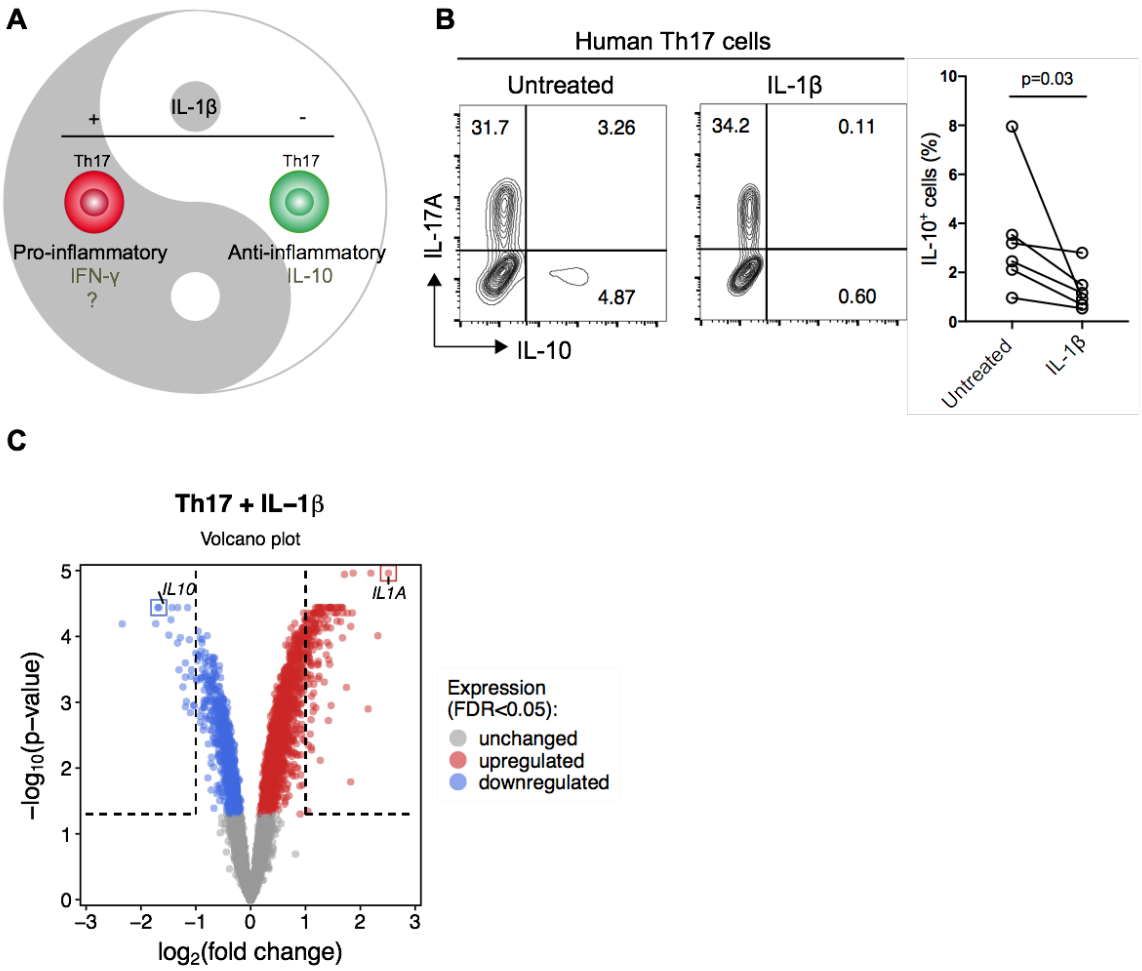

Figure 2.1 Two types of Th17 cells, which differ in pro- and anti- inflammatory functionalities.

(A) The functions of human helper T cells can be regulated by cytokines released from innate antigen-presenting cells. One cytokine, IL-1β, is essential for Th17 differentiation and plays a role in modifying Th17 cells toward pro-inflammatory phenotypes. (B) The downregulation of IL-10 by IL-1β. Human Th17 cells were stimulated with anti-CD3/CD28, in the presence of IL-1β (20 ng/mL) for 5 days (n=6, paired t-test). (C) Microarray analysis between pro- and anti- inflammatory Th17 subsets. Pro- and anti- inflammatory Th17 subsets were generated in the presence or absence of IL-1β and were stimulated, as described in (B) (n=3).

A

Summary

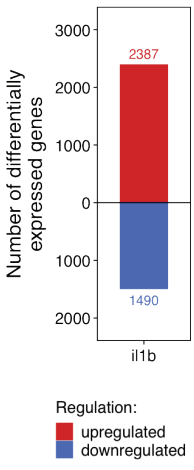

Top 20 dysregulated genes

gene	description	AveExpr	logFC
IL1A	interleukin 1 alpha	6.932	2.512
GJB2	gap junction protein beta 2	6.608	2.32
CCL1	C-C motif chemokine ligand 1	9.603	2.19
UBD	ubiquitin D	6.008	2.141
TUBA1A	tubulin alpha 1a	10.238	1.868
SPC25	kinetochore complex component	6.644	1.853
DPYSL2	dihydropyrimidinase like 2	7.427	1.825
OLAH	oleoyl-ACP hydrolase	4.779	1.824
DHCR24	24-dehydrocholesterol reductase	7.306	1.764
CCL18	C-C motif chemokine ligand 18	5.605	1.746
ACAT2	acetyl-CoA acetyltransferase 2	8.934	1.71
E2F8	E2F transcription factor 8	6.868	1.68
KIF20A	kinesin family member 20A	5.534	1.679
KIF23	kinesin family member 23	6.596	1.673
CDC20	cell division cycle 20	7.187	1.66
TUBB	tubulin beta class I	9.681	1.644
DLGAP5	DLG associated protein 5	6.427	1.641
ANLN	anillin actin binding protein	5.49	1.583
PTPRK	tyrosine phosphatase, receptor type K	5.399	1.58
DHRS2	dehydrogenase/reductase 2	5.824	1.577

gene	description	AveExpr	logFC
TXK	TXK tyrosine kinase	6.262	-2.342
TNIP3	TNFAIP3 interacting protein 3	8.447	-1.731
ADA2	adenosine deaminase 2	7.363	-1.693
IL10	interleukin 10	11.931	-1.676
IL18RAP	interleukin 18 receptor accessory protein	9.149	-1.493
IL21	interleukin 21	10.356	-1.454
MIAT	myocardial infarction associated transcript	9.632	-1.436
KLRB1	killer cell lectin like receptor B1	11.233	-1.333
DUSP22	dual specificity phosphatase 22	9.203	-1.331
IL4	interleukin 4	10.56	-1.305
LOC107984485	uncharacterized LOC107984485	8.269	-1.281
CD160	CD160 molecule	7.478	-1.233
B3GALT2	beta-1,3-galactosyltransferase 2	5.043	-1.191
PTX3	pentraxin 3	4.219	-1.191
CGA	glycoprotein hormones, alpha polypeptide	6.3	-1.191
STXBP5-AS1	STXBP5 antisense RNA 1	7.204	-1.172
AREG	amphiregulin	11.022	-1.149
CCR5	C-C motif chemokine receptor 5 (gene/pseudogene)	6.435	-1.119
SRPX	sushi repeat containing protein X-linked	5.691	-1.1
EXOC2	exocyst complex component 2	9.815	-1.09

B

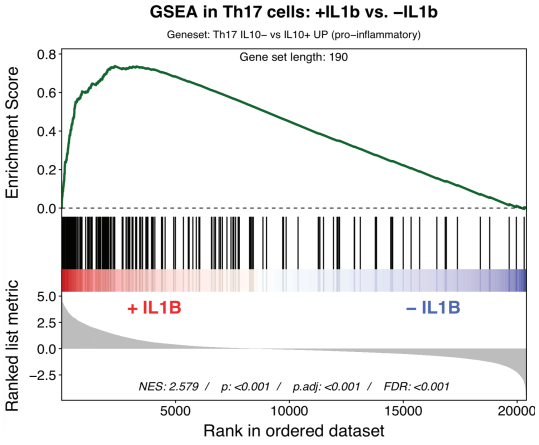

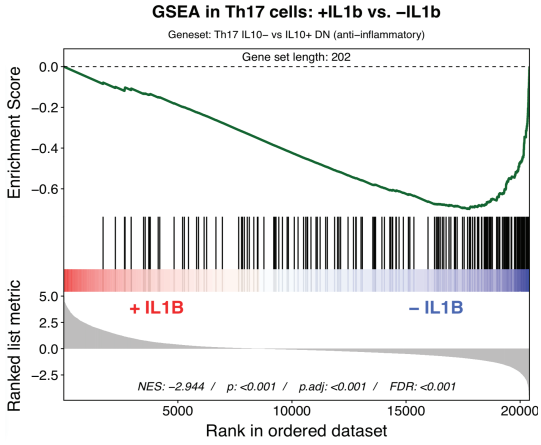

C

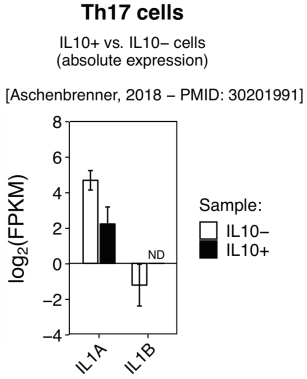

Figure 2.2 Gene set enrichment analysis shows that IL-1β-treated Th17 cells are enriched in pro-inflammatory genes.

(A) The top 20 dysregulated genes were extracted from the microarray analysis of Th17 cells stimulated and treated with or without IL-1β. (B) Gene set enrichment analysis from a previously published dataset (Th17 IL10- vs IL-10+)(Aschenbrenner et al., 2018), showing genes related to the pro-inflammatory and anti-inflammatory signatures of Th17 cells that were stimulated as described in Figure 2.1. (C) *IL1A* is significantly downregulated in $IL10^+$ Th17 cells in comparison to $IL10^-$ Th17 cells from published data set (PMID: 30201991)(Aschenbrenner et al., 2018)

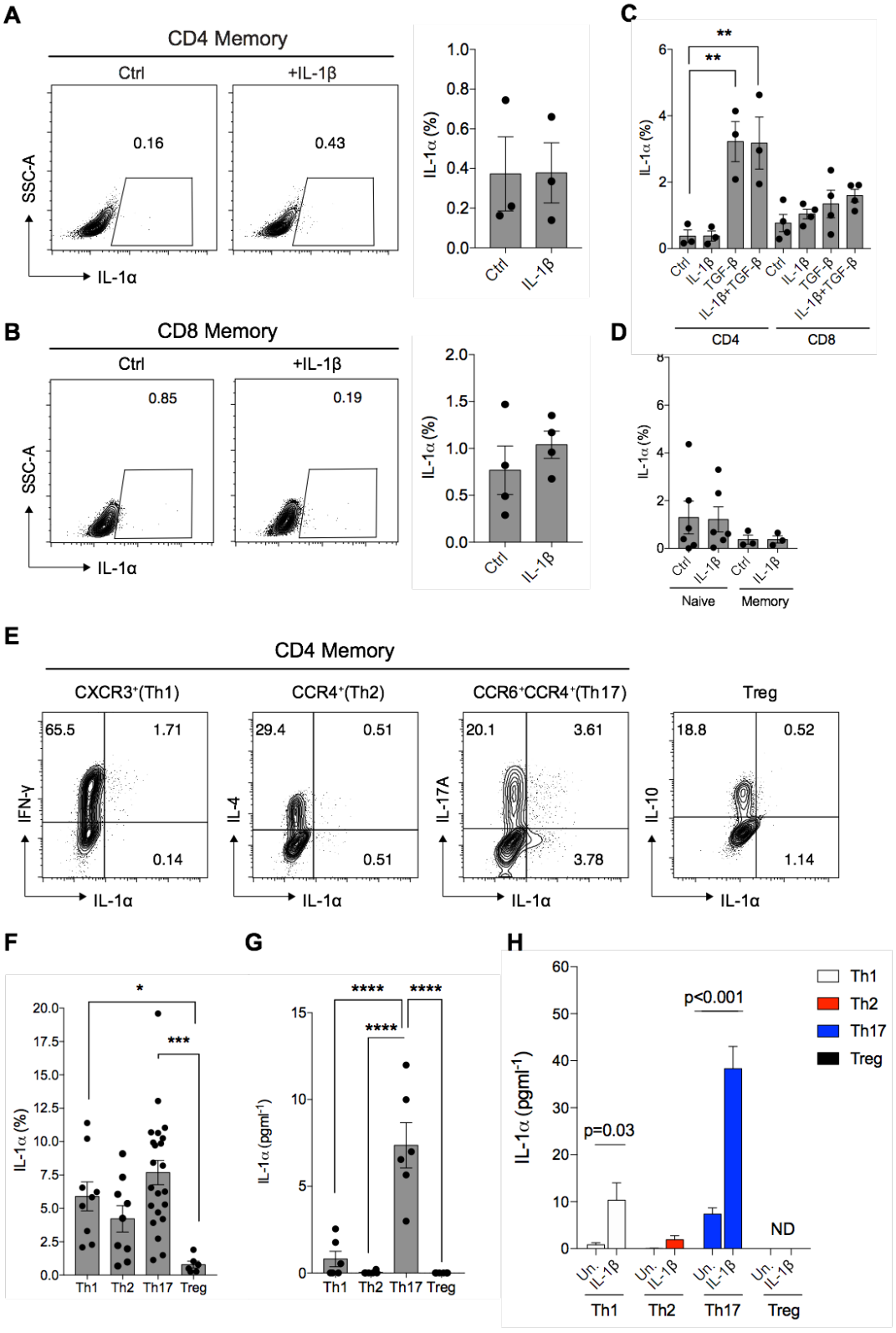

Figure 2.3 See next page for caption.

Figure 2.3 IL-1α producing cells are enriched in CCR4$^+$CCR6$^+$ Th17 cells.

(A) IL-1α expression in CD4$^+$CD45RA$^-$ memory cells. Cells were stimulated with plate-coated CD3/D28 (2, 2 μg/mL), in the presence or absence of IL-1β (20 ng/mL), for 5 days. Flow cytometry evaluation of IL-1α production after intracellular staining. Left, a representative plot showing little IL-1α production by CD4 memory cells. Right, quantification of the percentage of IL-1α-producing cells. Data are presented as the mean ± Standard error of the mean (SEM) (n=3, paired Student's t-test) (B) IL-1α expression in CD8$^+$CD45RA$^-$ memory cells. Cells were stimulated and treated as described in (A). Data are presented as the mean ± SEM (n=4, paired Student's t-test) (C) CD4 and CD8 memory T cells were isolated and treated with IL-1β (20 ng/mL), TGF-β (20 ng/mL), or both, and stimulated as described in (A). IL-1α production comparison is shown. (For CD4, n=3, for CD8, n=4, one-way ANOVA, * $p < 0.05$). (D) CD4$^+$CD45RA$^+$ naïve and CD4$^+$CD45RA$^-$ memory T cells were isolated. IL-1α expression was assessed by intracellular staining, followed by flow cytometry (n = 6, 6, 3, 3 per group). (E) The frequencies of IL-1α expression in Th1, Th2, Th17, and Treg cells. Cells were isolated from human CD4-magnetic beads-enriched cells. Cells were sorted according to the differential expression of the chemokine receptors (CCR6, CCR4, and CXCR3). Treg cells were sorted as CD25$^+$CD127$^-$ cells. All isolated subsets were stimulated for 5 days, in the presence of IL-1β (20 ng/mL). Representative plots showing the percentages of IL-1α-positive cells in different subsets. (F) Quantification of the percentage of IL-1α-producing cells. Data are presented as the mean ± SEM (Th1, n = 9; Th2, n = 9; Th17, n = 22; Treg, n = 6, one-way ANOVA, * $p < 0.05$, ** $p < 0.01$, *** $p < 0.001$) (G) Supernatants were collected on day 5. The secretion of IL-1α was measured by ELISA. Data are presented as the mean ± SEM (n = 6, one-way ANOVA, * $p < 0.05$, ** $p < 0.01$, *** $p < 0.001$) (H) T cell subsets were cultured with IL-1β. Supernatants were collected on day 5 and analyzed by ELISA. Data are presented as the mean ± SEM (n = 6, paired Student's t-test).

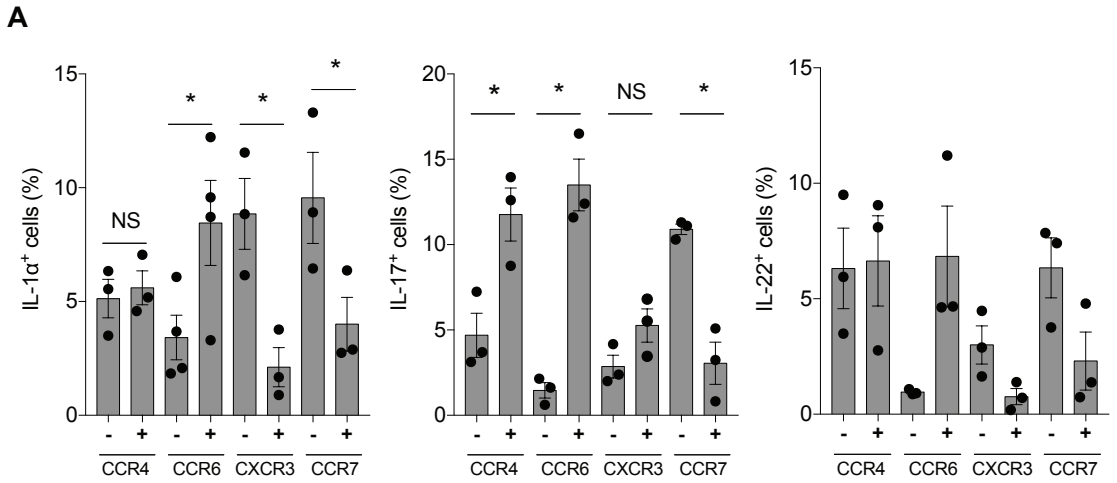

Figure 2.4 IL-1α+ cells are enriched in the CCR6$^+$CXCR3$^-$CCR7$^-$ population.

(A) CD45RA$^-$ CD4$^+$ memory cells were sorted according to the chemokine receptor expression, via surface staining. Sorted cells were then stimulated with plate-coated CD3/D28 (2, 2 μg/mL) for 2 days, and rested for 3 days. Cytokine production from the cells was assessed by intracellular staining. Data are presented as the mean ± SEM (n = 3, paired Student's t-test, ns, not significant, * $p < 0.05$).

Effector functions and migratory capacity are known to be co-regulated during Th cell differentiation. Identifying IL-1α producing Th cells, with their distinct chemokine receptor profiles, may indicate their migratory destinations and could be used for their ex vivo isolation. The chemokine receptors CCR6, CCR4, CXCR3, and CCR7 were used to identify their corresponding migration sites, skin, lung, liver, and lymph nodes. CCR7 expression also suggests its function, as it contributes to the homing of T cells to lymph nodes. Cells expressing IL-1α were present at significantly higher frequencies within the CCR6$^+$, CXCR3$^-$ and CCR7$^-$ compartments (compared with CCR6$^-$, CXCR3$^+$ and CCR7$^+$, respectively), whereas no significant differences in IL-1α$^+$ cell frequencies were observed between the CCR4$^+$ and CCR4$^-$ populations. CCR4, however, can distinguish IL-17-expressing cells and is commonly used to identify Th17 cells (Figure 2.4A). The chemokine receptor profile of IL-1α-expressing cells also shows a similar

pattern to that observed in IL-22 expressing cells. Taken together, the chemokine receptor profile associated with IL-1α expression agrees with our previous finding that Th17 cells express the largest amounts of IL-1α among all Th subsets. Therefore, I extensively investigated the co-regulation between of IL-1α expression and the Th17 differentiation program.

2.1.2 Distinct IL-1α production patterns in adaptive and innate immune cells

IL-1α in human monocytes has both a surface form and a secreted form, which are differentially regulated. The nuclear factor (NF)-κB signaling pathway is necessary for surface IL-1α expression, whereas the additional activation of the inflammasome is necessary for IL-1α secretion (Fettelschoss et al., 2011). To determine which form of IL-1α is detected in human T cells, surface and intracellular fluorescence-activated cell sorting (FACS) staining was performed in isolated Th1, Th2, and Th17 cells (Figure 2.5A). Because IL-1α expression in innate immune cells is upregulated rapidly after activation (< 24 hours), I first isolated Th subsets from fresh peripheral blood and performed IL-1α staining immediately after isolation (*ex vivo*). I found that neither surface nor intracellular IL-1α was detectable from *ex vivo* isolated (unstimulated) Th subsets, whereas intracellular and secreted IL-1α were measurable after the Th subsets were stimulated through CD3/CD28 for 5 days (*in vitro*). The proportion of IL-1α$^+$ cells was increased from ~0% to 7–8% in Th17 cells. The same effects were observed in Th1 and Th2 (Figure 2.5B). However, surface IL-1α expression was still not observed after Th17 cells stimulation (below 1%) (Figure 2.5C). As a control, human monocytes were isolated and stimulated with danger signals. Both surface and intracellular forms of IL-1α were robustly expressed, in line with published reports (Fettelschoss et al., 2011)(Fig 2.5D). Taken together, these data suggested that IL-1α production in Th cells is distinct from that in innate cells. Because IL-1α$^+$ cells could only be detected when Th cells were stimulated with anti-CD3/CD28 for 5 days, I hypothesize that T-cell receptor (TCR) activation and longer culture times are essential for IL-1α production in Th subsets.

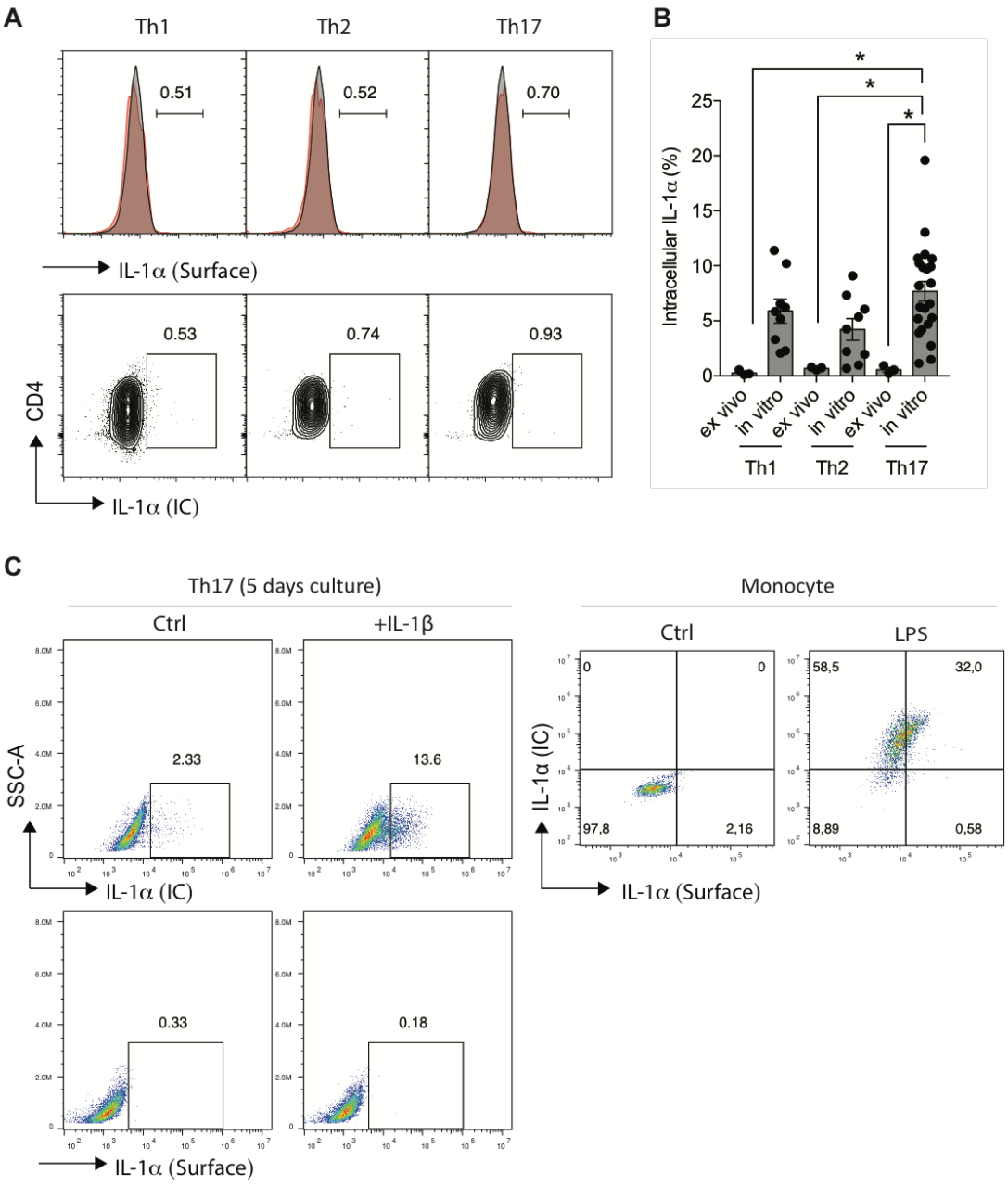

Figure 2.5 See next page for caption.

Figure 2.5 IL-1α is not expressed by ex vivo Th subsets without stimulation.

(A) Flow cytometry evaluation of IL-1α production in sorted Th1, Th2, and Th17 cells, after intracellular staining. Cells were sorted as described previously. Surface and intracellular staining were performed immediately after cell sorting (*ex vivo*). (B) Quantification of the percent of intracellular IL-1α-producing cells from *ex vivo* and *in vitro* cultures (cells were stimulated with anti-CD3/CD28 for 5 days). Graphs show the percentage of IL-1α positive cells. Data are presented as the mean ± SEM (*ex vivo*, n = 3; in vitro, n = 6, one-way ANOVA, *p < 0.05, **p < 0.01). (C) No surface expression of IL-1α from cultured Th17 cells (representative plot from more than 3 experiments). (D) Surface IL-1α expression is observed on $CD14^+$ monocytes after cells were stimulated with lipopolysaccharide (LPS). (n = 3, representative plot).

2.1.3 The priming conditions for IL-1α production in naïve CD4 T cells

The results showing that IL-1α is produced predominantly by Th17 cells and that IL-1α production strongly correlates with the chemokine receptor profile of Th17 cells raise the possibility that the Th17 polarization conditions may promote IL-1α production. To test this hypothesis, I isolated CD4 naïve T cells and stimulated them with Th1-, Th2- and Th17-differentiation cytokines. For Th1 and Th2 differentiation, the cytokines IL-12 and IL-4, respectively, have been relatively well-established. However, the differentiation of human Th17 cells from naïve T cells has been very difficult to accomplish, *in vitro*. The cytokines IL-6 and IL-23 are thought to play important roles in the promotion of Th17 differentiation (McGeachy et al., 2009; Veldhoen, Hocking, Atkins, Locksley, & Stockinger, 2006); therefore, these cytokines were also included in the Th17 polarization condition, together with IL-1β and TGF-β, which have previously been used as Th17 polarizing cytokines (Sallusto, Zielinski, & Lanzavecchia, 2012) (Figure 2.6). Notably, the proportion $IL\text{-}1\alpha^+$ cells increased significantly by the Th17 polarization condition (IL-1β+TGF-β+IL-23) but not by the Th1 and the Th2 polarization conditions (Figure 2.6A and B). Because T cells have previously been reported to express Toll-like receptors (TLRs), which provide additional signals to promote

pathogenicity in murine Th17 cells (Bhan et al., 2013; Marta, Andersson, Isaksson, Kampe, & Lobell, 2008), and because TLRs share the same downstream myeloid differentiation primary response 88 (MyD88) signaling pathway as the IL-1 receptor, I next investigated the contributions of innate TLR signaling signals to IL-1α, within the adaptive Th cell lineage. For this purpose, CpG-ODNs was administered, along with the Th17 polarization cytokines (IL-1β+TGF-β). The proportion IL-1α^+ cells increased when cells were differentiated into Th17 cells with CpG-ODNs (Figure 2.6C). In addition to testing the intracellular expressions, I also tested the secretion level of IL-1α, and the Th1 and Th17 polarization increased IL-1α secretion from ~7 pg/mL to ~25 pg/mL and ~45 pg/mL, respectively (Figure 2.6D). The differentiation outcome was determined by the secreted cytokines IL-17A and IFN-γ (IL-4 is not shown because it added to the Th2-differentiation medium). The polarizing cytokines successfully transformed naïve T cells towards Th1 and Th17 differentiation pathways (Figure 2.6E and F), and the addition of IL-6 or IL-23 did not increase IL-17A production (Figure 2.6E). Together, these results demonstrate that the proportion of IL-1α^+ cells increased with Th17 polarization conditions, and that IL-1α secretion into the supernatant increased with Th17 polarization conditions. However, Th1 and Th2 polarization conditions did not increase IL-1α production.

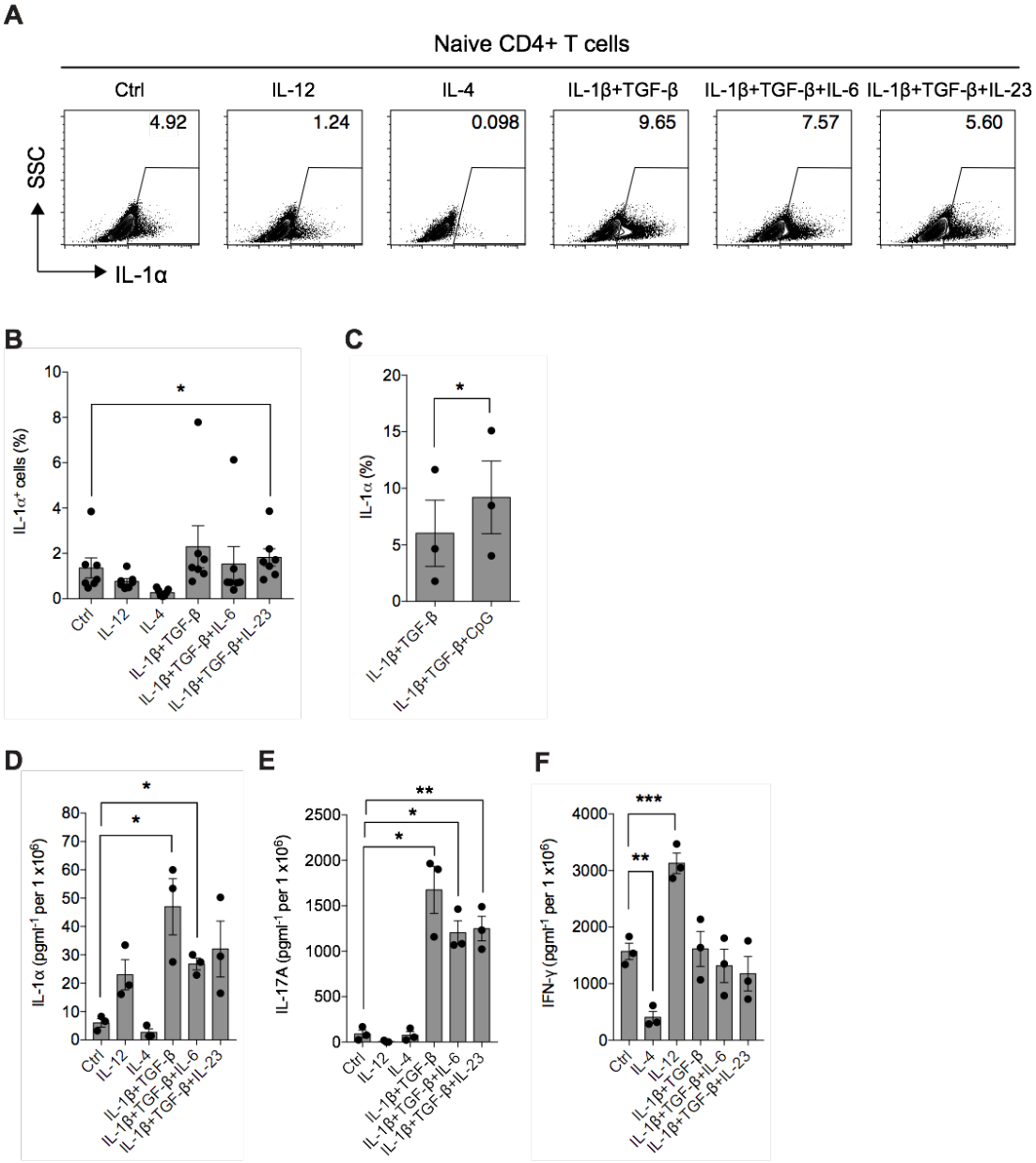

Figure 2.6 The proportion of IL-1α$^+$ cells and IL-1α secretion from naïve CD4 T cells with different Th cell polarizing conditions.

(A) Flow cytometry evaluations of intracellular IL-1α-production in CD45RA$^+$ CD4 naïve T cells, stimulated with anti-CD3/CD28, in the presence of polarizing cytokines for 5 days. (B) The graphs show the percentage of IL-1α-positive cells in total. Data are presented

as the mean ± SEM (n = 7, one-way ANOVA, * $p < 0.05$, ** $p < 0.01$). (C) $CD45RA^+$ CD4 naïve cells were stimulated in the presence of the indicated cytokines plus TLR9 ligand (CpG-ODNs) at 10 μg/mL for 5 days. Graphs show the percentage of IL-1α-positive cells. Data are presented as the mean ± SEM (n = 3, paired Student's t-test, * $p < 0.05$). (D-F) Supernatants were collect on day 5. Secreted levels of IL-1α, IL-17A and IFN-γ were analyzed by ELISA and normalized against total cell numbers (n = 3, one-way ANOVA, * $p < 0.05$, ** $p < 0.01$, *** $p < 0.001$).

2.1.4 Stability and plasticity of IL-1α production in Th17 cells

To determine whether IL-1α expression in T cells is maintained long-term in terminally differentiated cells or whether expression remains contingent on external signals, I isolated differentiated Th17 cells from peripheral blood and cultured them with the cytokines of Th1-or-Th2-oriented milieus (IL-12 and IL-4, respectively). The proportion of $IL\text{-}1\alpha^+$ cell was approximately 8% in isolated Th17 cells, and the treatments of IL-12 and IL-4 did not show a difference (Figure 2.7A). Next, the cytokines that have been identified as being crucial for Th17 functional priming or stability (IL-1β+TGF-β) were added to the Th17 cells. IL-1β and TGF-β promoted IL-1α expression from ~8% to ~35%, whereas IL-6 does not affect IL-1α expression (Figure 2.7B). Adding IL-6 or IL-23, in combination with IL-1β and TGF-β, did not induce the frequencies of $IL\text{-}1\alpha^+$ cells (Figure 2.7B). To investigate the role played by TLR signaling in differentiated Th17 cells, the TLR ligands, CpG-ODNs and lipopolysaccharide (LPS) were added to Th17 cytokine milieus. CpG-ODNs but not LPS was able to increase the frequencies of IL-1α (Figure 2.7C).

Transcriptional factors from the retinoic acid receptor (RAR)-related orphan nuclear receptor (ROR) family are known to be expressed in Th17 cells and have been suggested to play roles in Th17 differentiation. By treating Th17 cells with a highly selective, potent, small-molecule inhibitor of RORγ, GSK2981278 inhibited IL-17A secretion in human T cells grown under Th17-skewing conditions in a previous study (Smith et al., 2016). I also found that GSK2981278 significantly reduced the proportions of $IL\text{-}17A^+$ cells and $IL\text{-}1\alpha^+$ cells in Th17 cells (Figures 2.7D and E).

However, IL-10 and IFN-γ were unaffected. These data indicated that RORγ affected IL-1α production by Th17 cells.

Next, I investigated the co-expression pattern between IL-17A and IL-1α in Th17 cells, as these two cytokines may be co-regulated by RORγ. Th17 clones were generated according to our established protocol. In brief, Th17 cells were sorted and stimulated with irradiated allogenic PBMC and phytohemgglutinin (PHA). Determining the cytokine profiles of each clone can help us to narrow our investigation to the single-cell level, because each individual clone proliferated from a single cell, and may have similar cytokine regulation profile. However, no co-expression pattern between IL-17A and IL-1α was observed in individual clones, the IL-17A high producing clones have nonsignificant higher proportion of IL-1α$^+$ cells (Figure 2.8A), suggesting that IL-1α production is regulated independently from IL-17A production in Th17 cells.

To investigate whether IL-1α production in Th17 cells is maintained long-term even without restimulation or just temporarily after activation, I attempted to stimulated IL-1α-producing clones repeatedly and examined the IL-1α production. Before the setup of the experiments, I observed that the stimulated clones expressed increased amount of IL-1α (Figure 2.9A). Next, I stimulated the clones and measured IL-1α production over time. Although IL-17A exhibited a relatively stable expression pattern, IL-1α expression was upregulated on day 4 and then decreased on day 16 (Figure 2.19B). The same clones were then rested for longer than 10 days and re-stimulated with the same stimuli for the next 33 days (timeline see Figure 2.9C). The clones were stimulated with plate-bound anti-CD3/CD28 twice, at day 0 and day 16, for 48 hours each time and transferred to 96 well U-bottom plates. The production of IL-1α was conserved at day 4, after the second round of stimulation; however, the production of IL-1α was lower at day 20 in some clones after the third round of stimulation (Figure 2.9C). These results indicated that IL-1α, similar to IL-17A, can be produced as a signature cytokine, rather than reflecting short-term effects after T-cell activation. IL-1β, which has been shown to upregulate IL-1α production, based on transcriptome

data from the bulk Th17 population, also regulated IL-1α production at the single-cell level (Figure 2.9D).

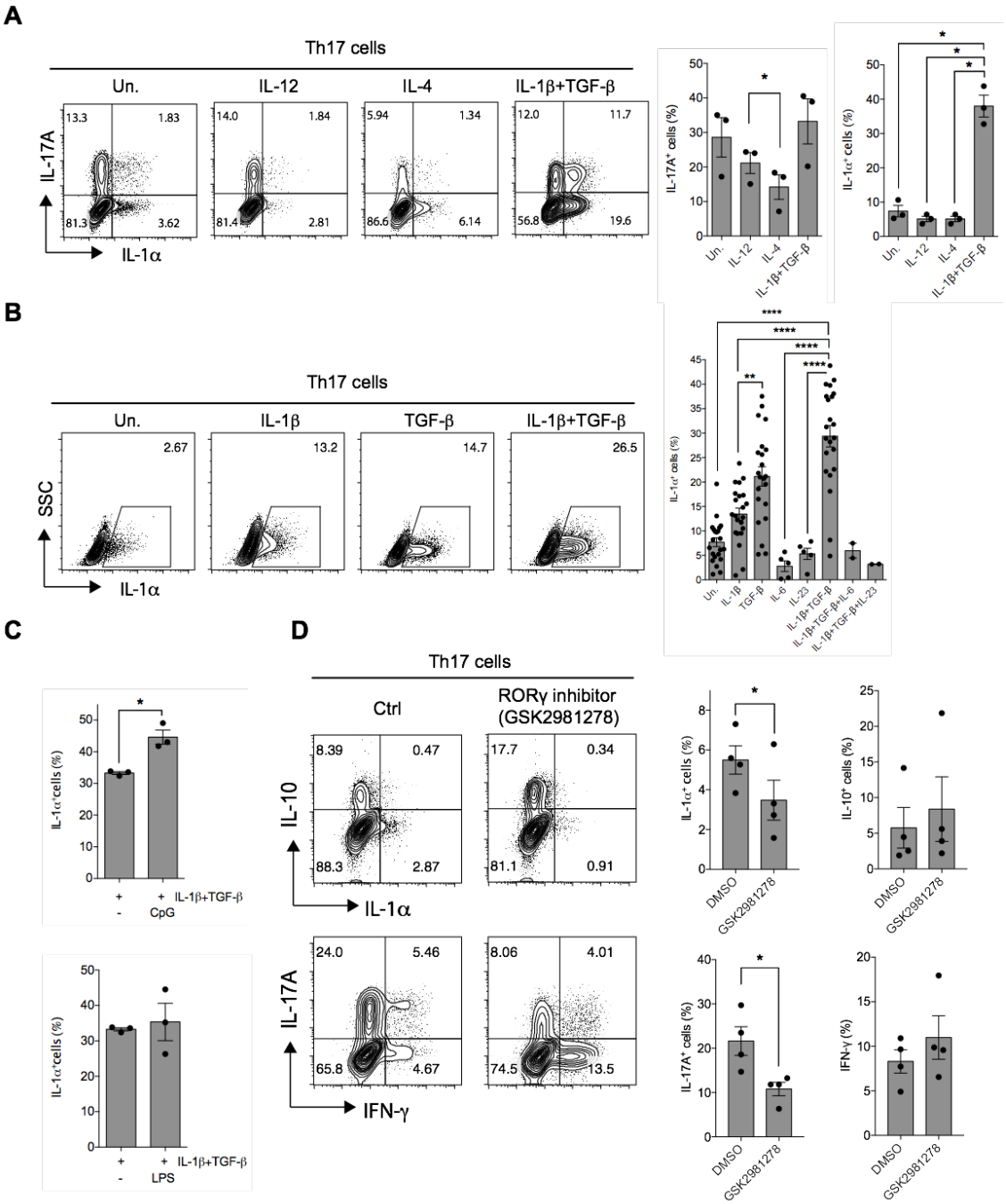

Figure 2.7 See next page for caption.

Figure 2.7 The Th17 polarizing cytokines IL-1β and TGF-β, induce IL-1α production by Th17 in a cooperative manner.

(A) Isolated $CXCR3^{-}CCR4^{+}CCR6^{+}CD45RA^{-}CD4^{+}$ cells (Th17) were stimulated with anti-CD3/CD28 and cultured in Th1-Th2- and Th17- differentiation conditions for 5 days. The bar graphs show the frequencies of IL-17A and IL-1α in the total cell population. Data are presented as the mean ± SEM (n=3, one-way ANOVA, * $p < 0.05$, ** $p < 0.01$) (B) Th17 cells were cultured with different Th17-polarizing cytokine combinations. The bar graph shows the frequencies of IL-1α in the total cell population. Data are presented as the mean ± SEM (n=2–21, one-way ANOVA, * $p < 0.05$, ** $p < 0.01$, *** $p < 0.001$, **** $p < 0.0001$). (C) Isolated Th17 cells were treated with IL-1β and TGF-β, in the presence or absence of CpG-ODNs (10 μg/mL) or LPS (10 μg/mL) for 5 days. The bar graph shows the frequencies of IL-1α in the total cell population. Data are presented as the mean ± SEM (n = 3, paired Student's t-test, * $p < 0.05$, ** $p < 0.01$, *** $p < 0.001$). (D) Isolated Th17 cells were pre-incubated with the RORγ inhibitor GSK2981278 (10 μM), for 3 hours, and stimulated with anti-CD3/CD28 for 5 days. (E) The bar graphs show the percentages of IL-1α, IL-17A, IL-10 and IFN-γ in the total cell population. Data are presented as the mean ± SEM (n = 4, paired Student's t-test, * $p < 0.05$).

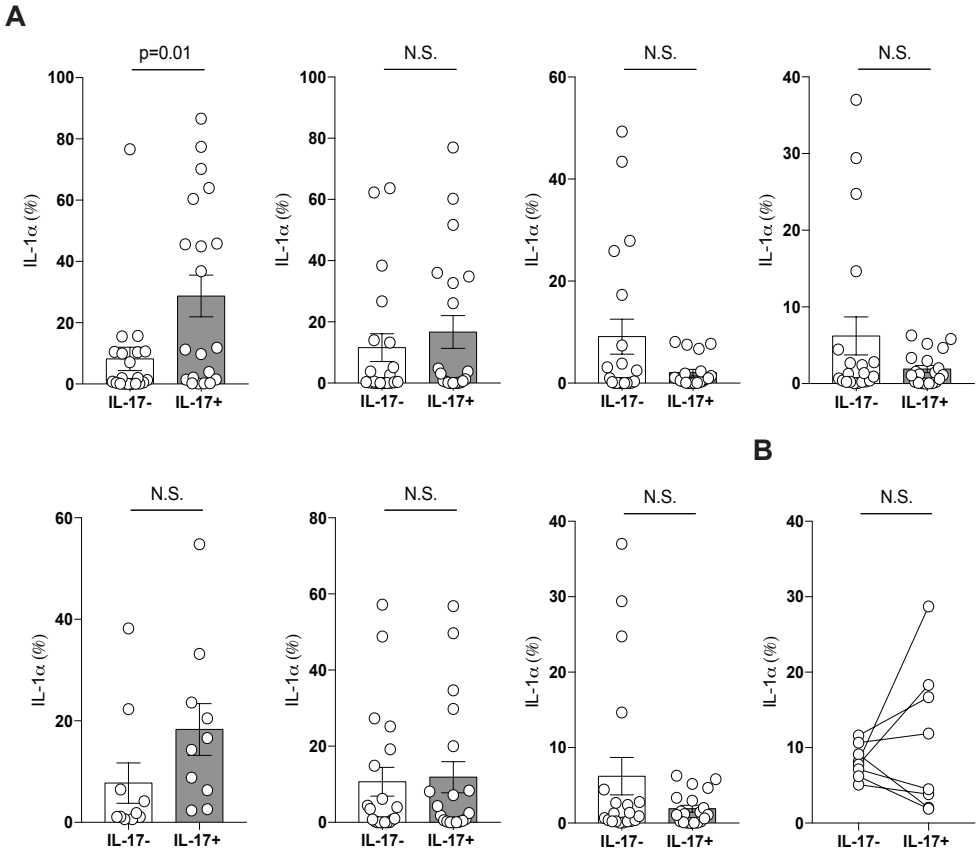

Figure 2.8 Clones do not show correlations between IL-1α and IL-17 expression.

(A) Th17 clones were generated by the direct cloning of $CCR6^{+}CCR4^{+}$ memory $CD4^{+}$ T cells. Cytokine staining was performed on day 12. The top 10 or 20 IL-17A-expressing clones ($IL\text{-}17^{+}$) were selected from each individual experiment, and IL-1α production was compared between the top-expressing clones and the IL-17A-nonproducing clones. Data are presented as the mean ± SEM (n = 10 or 20, unpaired Student's t-test). (B) Average IL-1α expression levels were compared between 7 cloning experiments (n = 7, paired Student's t-test).

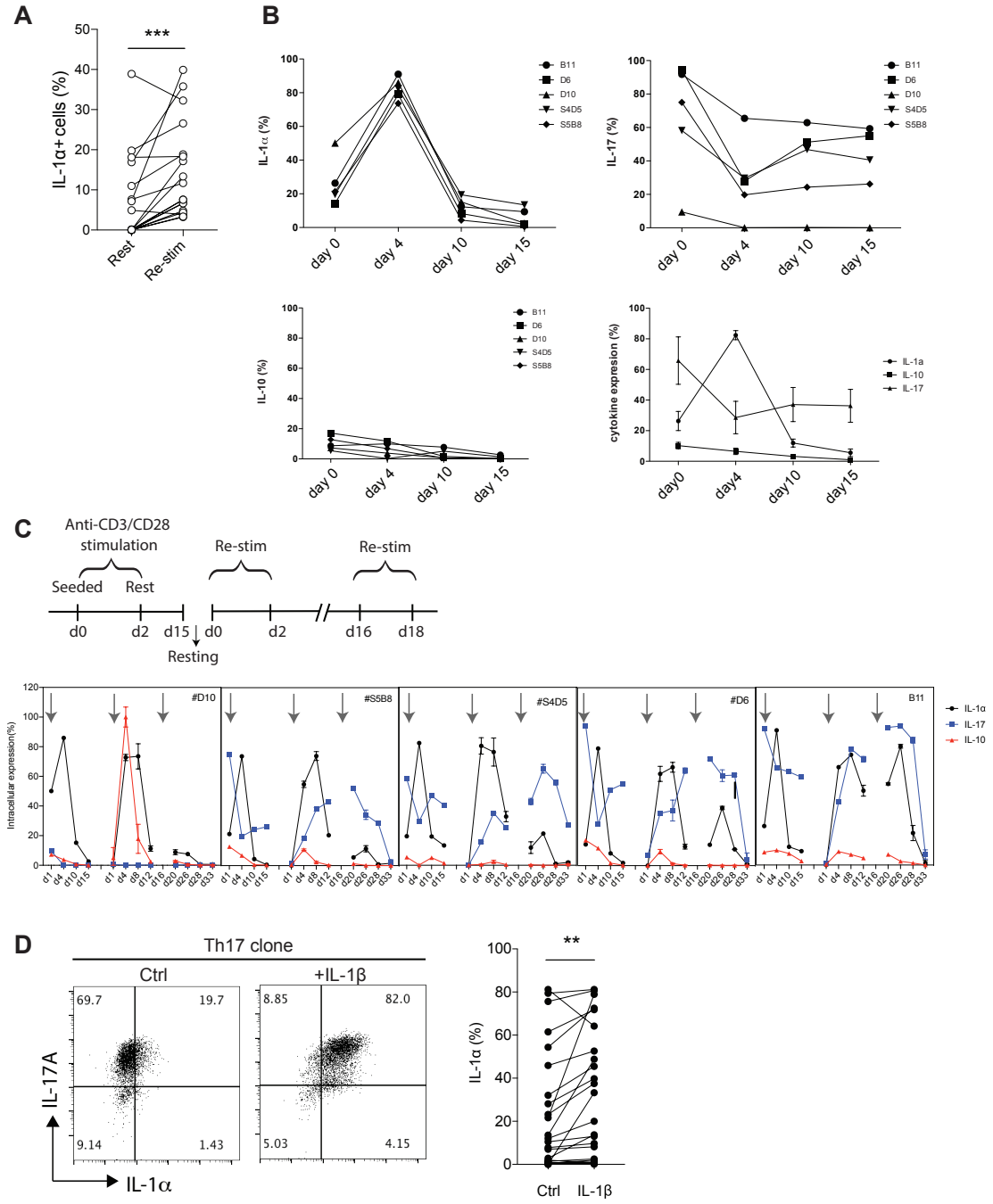

Figure 2.9 The stability and plasticity of IL-1α production.

(A) Clones expressing different levels of IL-1α were selected and analyzed in the resting state (>10 days after cloning) and then re-stimulated with anti-CD3/CD28 for 5 days. The IL-1α percentage was determined by intracellular staining. (n = 13, paired Student's t-test, * $p < 0.05$, ** $p < 0.01$, *** $p < 0.001$). (B) Five representative Th17 cell resting clones

were selected, re-stimulated with anti-CD3/CD28, and analyzed at different times. Graphs show the percentages of IL-1α, IL-17A, and IL-10 in the total cell population. (C) Five representative Th17 cells were then rested (>10 days) and re-stimulated again, at days 0 and day16s with anti-CD3/CD28 to examine their capacities to produce IL-1α, IL-17 and IL-10. Graphs show the percentages of IL-1α, IL-17A, and IL-10 in the total cell population. (D) Different levels of IL-1α-producing clones were selected and re-stimulated with anti-CD3/CD28, in the presence or absence of IL-1β for 5 days. IL-1α was evaluated using intracellular staining (n = 26, paired Student's t-test).

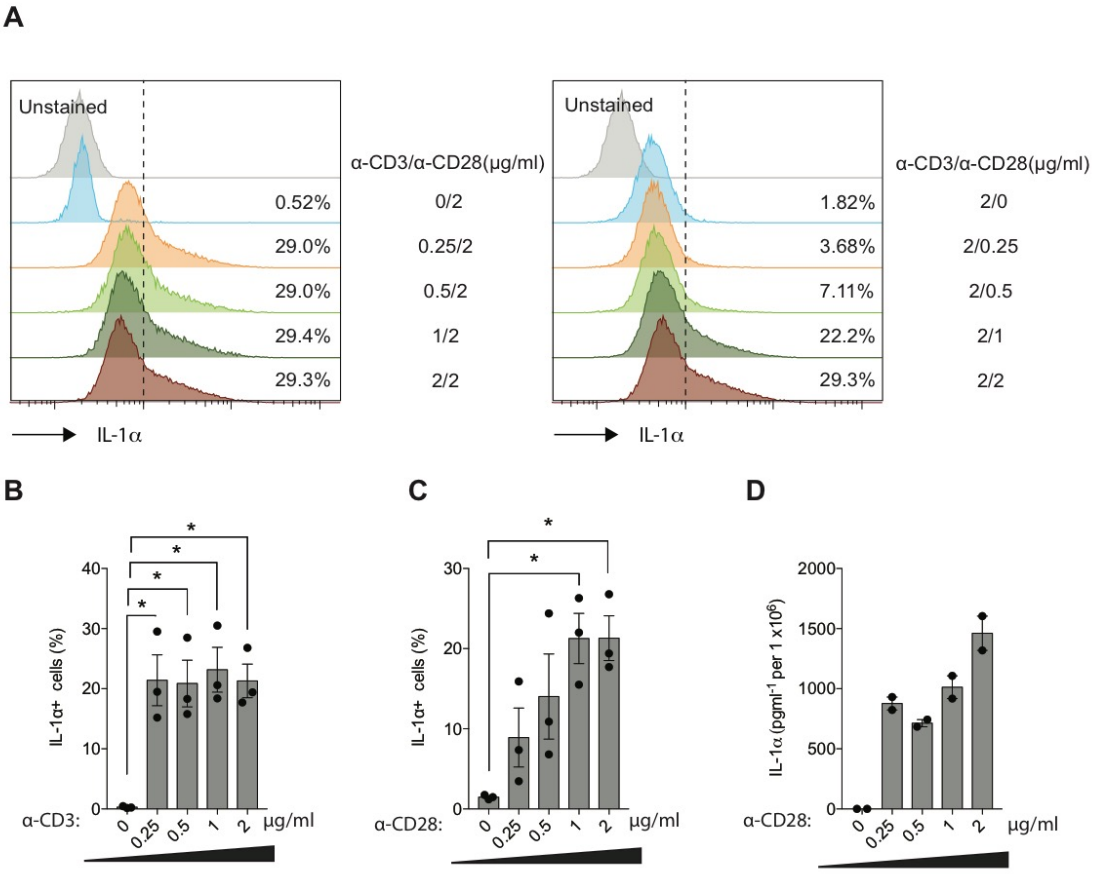

Figure 2.10 The role of TCR signaling in inducing IL-1α induction.

(A) Isolated Th17 cells were stimulated with different concentrations of anti-CD3 and anti-CD28, in the presence of IL-1β and TGF-β. (B and C) IL-1α percentage is shown in bar graphs (n = 3, one-way ANOVA, * $p < 0.05$, ** $p < 0.01$). (D) Supernatants were collected on day 5 and analyzed by ELISA and normalized against cell number (n = 2, mean ± SEM).

Next, I dissected the signals that determine the differentiation of Th17 cells with IL-1α production properties, by examining TCR signal strength and the costimulatory and cytokine requirements. Th17 cells were isolated, as previously described, and stimulated with different doses of anti-CD3 (0-2 μg/mL) and anti-CD28 (0-2 μg/mL). IL-1β and TGF-β were added, to maximize the intracellular level of IL-1α (Figures 2.10A–C). Interestingly, compared with anti-CD3, which required lower amounts (0.25 μg/mL) to trigger full IL-1α expression, anti-CD28 showed a dose-dependent effect and was indispensable for IL-1α production and secretion (Figure 2.10D). The increased production of IL-1α following increased TCR signaling and costimulatory activation suggested that the cytokines produced by activated T cells might be responsible for the induction of IL-1α by Th17 cells. IL-2 is known to be produced by activated T cells and to activate the STAT5 signaling pathway. To test the impact of IL-2 on IL-1α induction in Th17 cells, recombinant IL-2 (produced in-house) was added to the culture, which significantly enhanced IL-1α production (Figure 2.11A). However, the blockade of the downstream molecule signal transducer and activator of transcription (STAT)5 did not alter the IL-1α levels, which indicated that the effects of IL-2 might be regulated through a STAT5-independent pathway (Figure 2.11B).

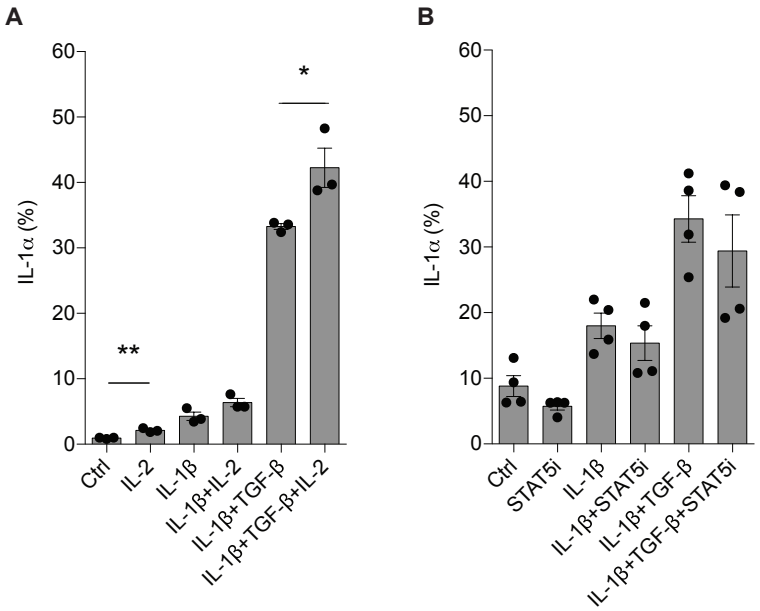

Figure 2.11 See next page for caption.

Figure 2.11 Regulation of IL-1α by IL-2 signaling.

(A) Isolated Th17 cells were stimulated and treated with different cytokines, for 5 days. The IL-1α percentage was determined by intracellular staining. The bar graph shows the IL-1α percentage in the total cell population. (n = 3, paired Student's t-test, * $p<0.05$, ** $p < 0.01$) (B) Isolated Th17 cells were pre-treated with a STAT5 inhibitor (200 μM), for 3 hours, and stimulated with anti-CD3/CD28 plus the indicated cytokines, for 5 days. The IL-1α percentage was determined by intracellular staining. The bar graph shows the IL-1α percentage in the total cell population (n = 4, paired Student's t-test).

2.2 The molecular mechanism of IL-1α production by human Th17 cells

2.2.1 The underlying mechanism of IL-1α secretion

Previous publications have shown that IL-1α can be secreted from innate cells, either in a pro-form (31 kDa) or a mature form (17 kDa). The pro-form is secreted due to leakage from the injured cell membrane (C. J. Chen et al., 2007; Eigenbrod, Park, Harder, Iwakura, & Núñez, 2008), whereas the mature form requires protease-mediated cleavage. Both the pro- and mature forms have bioactivities. Identifying the form of IL-1α that is secreted from Th cells may reveal the mechanisms underlying the secretion process. Our previous data revealed that IL-1α production cannot be detected in the absence of TCR stimulation, suggesting a requirement for concomitant TCR signaling to initiate IL-1α production by Th cells, whereas innate cells lack this requirement. This requirement for TCR signaling may be associated with TCR-induced calcium release, which is required for calpain activation, a process that is important for one possible cleavage of pro-IL-1α. Calpains have been described to be expressed in T cells (Perez et al., 2016). To assess the role played by calpains in human T cell IL-1α production, I first identified the secreted form of IL-1α and found that IL-1α is dominantly secreted in the mature from (Figure 2.12A and B). Calpain inhibitor I and II were used, which showed different inhibitor constants toward μ-calpain and m-calpain [Calpain inhibitor I: μ-calpain (Ki = 190 nM), m-calpain (Ki = 220 nM); Calpain inhibitor

II; μ-calpain (Ki = 120 nM), m-calpain (Ki = 230 nM)], and IL-1α secretion was significantly hindered by both inhibitors (Figure 2.13 A–D). I also observed the cell-killing effects of calpain inhibitor I (but not calpain inhibitor II), when I treated cells with a higher dose of the compound (Figure 2.13 C). To avoid cell number effects, secreted IL-1α data was compared with raw data (Figure 2.13 B and D). Calpain inhibitor II has not demonstrated negative effects on cell viability. Therefore, I normalized the secreted IL-1α amount against total cell number (Figure 2.13E). Moreover, in line with our hypothesis, calpain activity was doubled with T cell stimulation (Figure 2.13F), which supported our hypothesis that activated calpain can initiate IL-1α cleavage and promote its secretion.

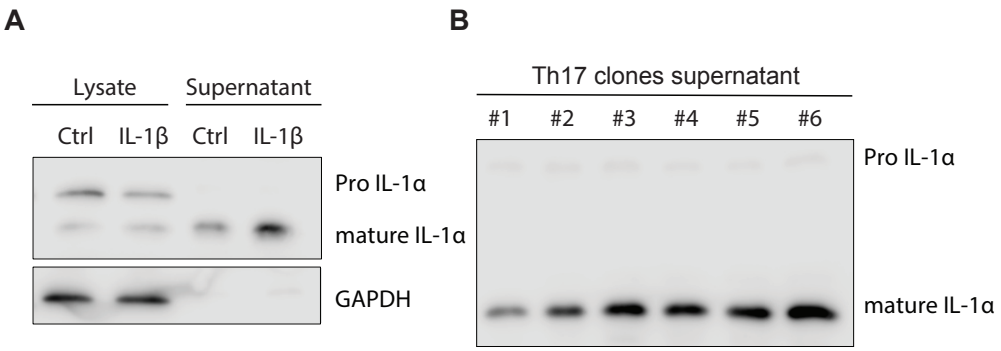

Figure 2.12 Secreted IL-1α represents the processed form.

(A) Immunoblots analysis of IL-1α and glyceraldehyde 3-phosphate dehydrogenase (GAPDH) in Th17 cell lysates and supernatants. Th17 cells were stimulated and treated, either with or without IL-1β, for 5 days. (B) Immunoblot analysis of IL-1α in the supernatant from Th17 clones. Selected Th17 clones were re-stimulated with anti-CD3 and anti-CD28. Supernatants were collected on day 5.

Another T cell-derived serine protease, granzyme B (GzmB), has been shown to cleave pro-IL-1α, and the proteolysis effectively enhanced the biological activity of IL-1α, both *in vitro* and *in vivo* (Afonina et al., 2011). Activated memory CD4 T cells secrete comparable amounts of GzmB as memory CD8 T cells (L. Lin et al., 2014). To determine whether activated Th17 cells secreted granzyme B, which, in turn, induced IL-1α secretion, I first measured GzmB levels in the cell culture supernatant from Th17 cells following anti-CD3 and anti-CD28 stimulation. Surprisingly, the level of GzmB declined at 48-72 hours (from ~1800 pg/mL to ~1500 pg/mL) after cells activation (Figure 2.14A); however, this phenomenon was not observed for the IL-17A levels (Figure 2.14B). GzmB is well-known for its role in the promotion of CTL-target cell death (Pardo et al., 2004), and the receptor required for GzmB uptake, mannose-6-phosphate receptor (M6PR), has been found to be expressed on proliferating T cells (Ara, Ahmed, & Xiang, 2018). The increased expression of M6PR was associated with increased susceptibility to GzmB-mediated apoptosis. In light of these findings, I therefore hypothesized that GzmB can facilitate pro-IL-1α cleavage and secretion. To test this hypothesis, the supernatant from stimulated cells, containing GzmB, was added on top of the unstimulated cells for 3 days. Following the addition of the supernatant to cell culture, IL-1α could be detected in unstimulated cells (from 0% to ~10% in total IL-17$^+$cells), suggesting that the soluble factors in the supernatant are potent inducers of IL-1α production (Figure 2.14C). However, removing the “stimulated” supernatant from the culture system largely suppressed IL-1α production (from ~30% to 10% in total IL-17$^+$cells) (Figure 2.14D). Furthermore, the intracellular and extracellular levels of IL-1α were reduced by adding a GzmB inhibitor, Z-IETD-FMK (Figure 2.14E). Together, these data indicated that calpain and GzmB both participates in the IL-1α secretion mechanism.

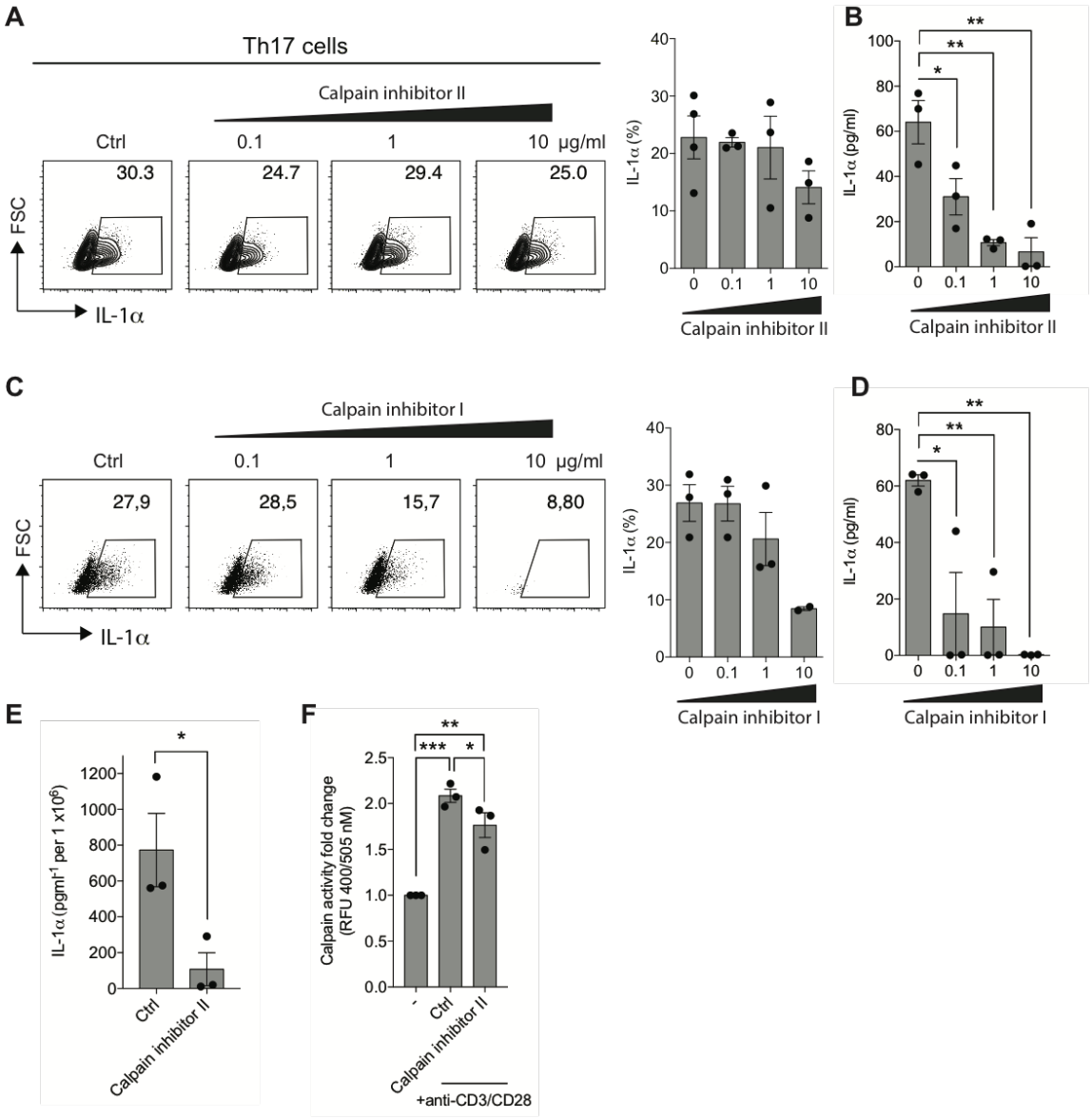

Figure 2.13 The secretion of IL-1α from Th17 cells is Calpain-dependent.

(A and C) Th17 cells were isolated as described previously. Cells were pretreated for 3 hours, with different doses of Calpain I or Calpain II inhibitors, and stimulated with anti-CD3/CD28 in the presence of IL-1β and TGF-β. IL-1α percentage was determined by intracellular staining. The bar graph shows the IL-1α percentage in the total cell population. (n = 3, one-way ANOVA). (B and D) Supernatants were collected on day 5 and were analyzed by ELISA. (n = 3, one-way ANOVA, * $p < 0.05$, ** $p < 0.01$, *** $p <$

0.001) (E) The concentration of IL-1α was normalized by cell number in cells treated with Calpain inhibitor II (10 μg/mL). (n = 3, paired Student's t-test, * $p < 0.05$) (F) Th17 cells lysates were extracted after 3 days, with or without stimulation. Calpain inhibitor II (10 μg/mL) was added to the cells overnight, before CD3/CD28 stimulation. Cell lysates were normalized against total protein concentration. Fluorescence intensity was measured after 1-hour incubation with calpain substrate Ac-LLY-AFC. Data are presented as the fold change in relative fluorescence units (RFU) 400/505 (excitation/emission wavelengths) (n = 3, one-way ANOVA, * $p < 0.05$, ** $p < 0.01$).

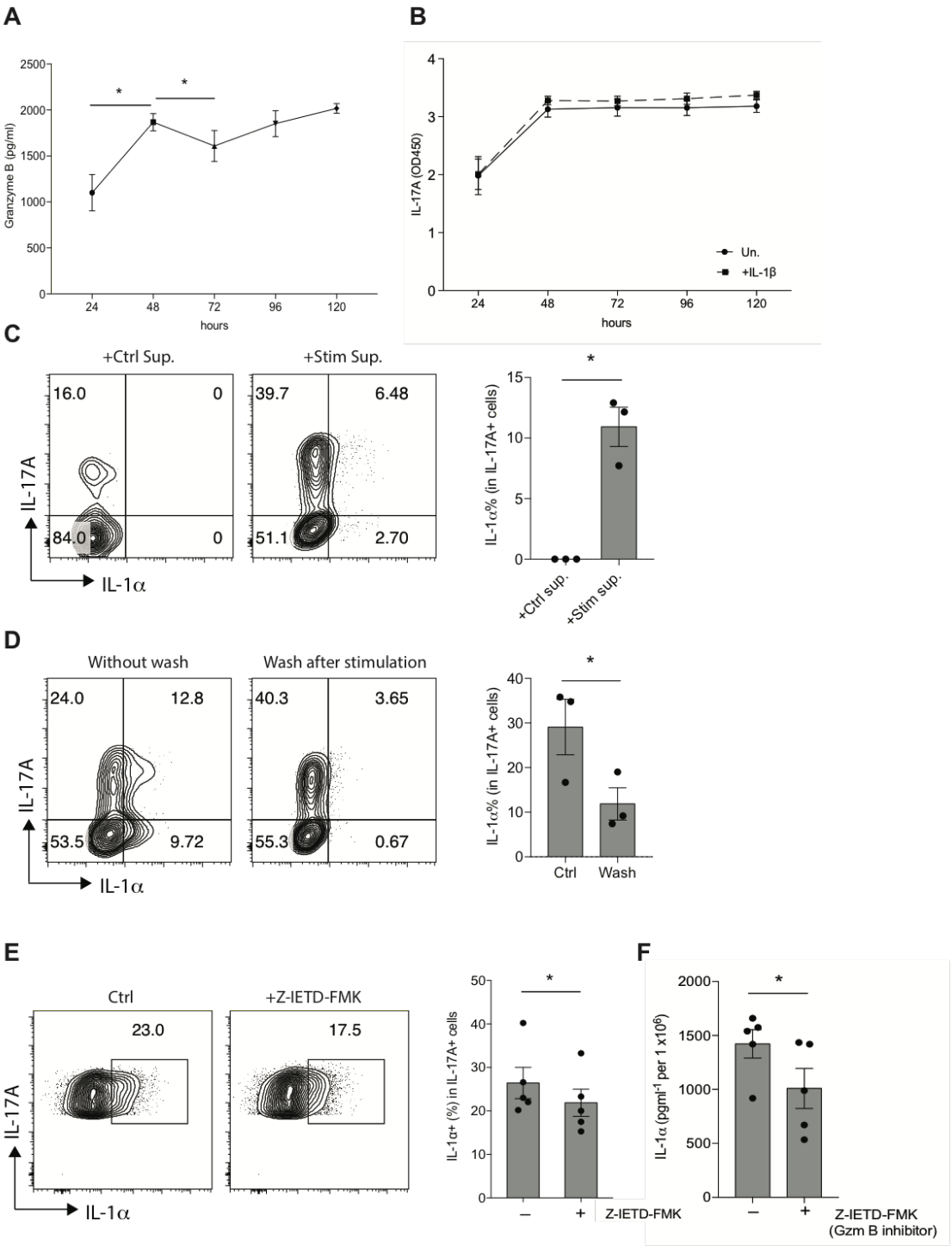

Figure 2.14 See next page for caption.

Figure 2.14 Granzyme B secreted from T cells may contributes to IL-1α production.

(A and B) Th17 cells were stimulated with anti-CD3/CD28. Granzyme B and IL-17A levels were detected at different time points during the Th17 culture and analyzed by ELISA (n = 3, paired Student's t-test, * $p < 0.05$). (C) Isolated Th17 cells were treated with control or stimulated-supernatants (48 hrs) for 3 days. Cells were collected to perform intracellular staining. The bar graphs show IL-1α percentages within IL-17A$^+$ cells (n = 3, paired Student's t-test, * $p < 0.05$). (D) Th17 cells were stimulated with anti-CD3/CD28 for 48 hours, washed with complete medium, and cultured for 3 more days. Cells were collected to perform intracellular staining. The bar graph shows IL-1α percentage within IL-17A$^+$ cells (n = 3, paired Student's t-test, * $p < 0.05$). (E) Th17 cells were sorted and pre-incubated with Z-IETD-FMK (20 μM) for 3 hours, and stimulated with anti-CD3/CD28 for 5 days. The bar graph shows the IL-1α percentage within IL-17A$^+$ cells. (n = 5, paired Student's t-test, * $p < 0.05$). (F) Supernatants were collected and analyzed by ELISA and normalized against cell number (n = 5, paired Student's t-test, * $p < 0.05$).

2.2.2 The role of the innate inflammasome machinery in T cells and its role in the production and secretion of IL-1α

The secretion of IL-1α is not only associated with passive release from dying cells but may also be associated with the regulation by the inflammasome, which has been studied more profoundly in innate immune cells (Bhan et al., 2013; Fettelschoss et al., 2011). Recently, increasing evidence has supported the existence of inflammasome activation, resulting in downstream components being expressed in Th cells (Arbore et al., 2016; Bruchard et al., 2015; Doitsh et al., 2014). To determine the role played by the inflammasome, I first blocked caspase activities, which may be involved downstream of inflammasome activation. However, using the pan-caspases inhibitor, Z-VAD-FMK, hardly any conclusions could be made due to the variable responses between donors (Figure 2.15A). Thus, I focused on the caspases, which were activated by the canonical inflammasome pathway. Caspase-1 has been shown to be the final executor of the inflammasome activation and is expressed by Th cells (Gao et al., 2020). However, the inhibition of caspase-1 enzymatic activity, using Ac-YVAD-CMK, failed to diminish IL-1α secretion (Figure 2.15B). Consistent with this finding, an equivalent level of enzymatically active caspase-1 (479 ± 325 pg/mL in ctrl monocytes and 325 ± 70 pg/mL in untreated Th17 cells) and a relatively low expression of endogenous caspase-1 protein were observed compared with unstimulated monocytes (Figure 2.15C and E). These results suggested that the overall expression of the enzymatically active form of caspase-1 is lower in Th17 cells and that blocking its enzymatic function does not affect IL-1α secretion.

NLRP3, one of the most studied members of the NLR family, has been shown to be expressed in human CD4 T cells (Bruchard et al., 2015; Doitsh et al., 2014). Surprisingly, by inhibiting NLRP3 with a potent small-molecule drug, MCC950 (Coll et al., 2015), I observed the decreased secretion of IL-1α (Figure 2.15D). The role of the NLRP3 receptor in IL-1α secretion suggested that IL-1α might be released from a cell undergoing pyroptosis, which is a unique form of cell death that is triggered by NLRP3 inflammasome activation (Bergsbaken, Fink, & Cookson, 2009).

In recent years, increasing evidence has indicated that gasdermin D (GSDMD) executes pyroptosis and that it is recruited to the NLRP3 inflammasome upon the cells receiving danger signals. Pore formation, mediated by N-terminal GSDMD, represents the final step in the pyroptosis process that facilitates the release of inflammatory cytokines [e.g., IL-1β, IL-18, and lactate dehydrogenase (LDH)] (W. T. He et al., 2015; Shi et al., 2015). To evaluate the role played by GSDMD in Th17 cells, I examined GSDMD protein expression in Th17 cells. As a control, the expression of GSDMD was examined in human monocytes stimulated to induce pyroptosis (Figure 2.15E). I observed that N-GSDMD is absent in Th17, whereas this protein could be detected in activated monocytes (Figure 2.15E). However, the full-length GSDMD protein was detectable in Th17 cells (Figure 2.15E). To examine whether Th17 cells form pores other than the GSDMD pore, the cells were treated with the cytoprotective agent glycine, which prevents the loss of membrane integrity during pyroptosis, through currently undefined mechanisms (Fink, Bergsbaken, & Cookson, 2008).

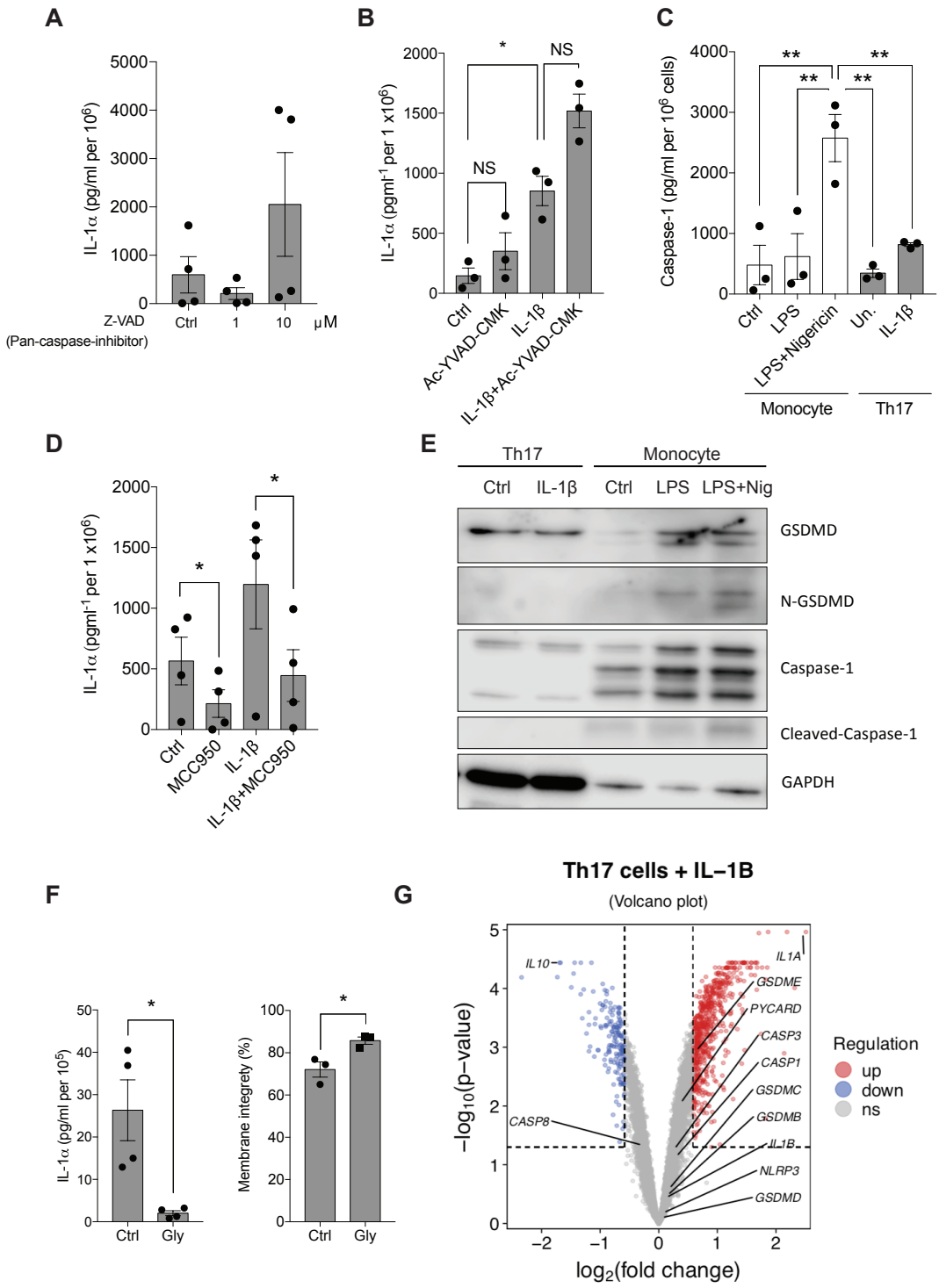

Figure 2.15 See next page for caption.

Figure 2.15 IL-1α secretion is caspase-1 independent but NLRP3-involved.

(A) Isolated Th17 cells were pre-treated with the pan-caspase inhibitor Z-VAD for 3 hours and then stimulated with anti-CD3/CD28 for 5 days. Supernatants were collected on day 5, and analyzed by ELISA, and normalized against cell number (n = 4, one-way ANOVA). (B) Isolated Th17 cells were pre-treated with a caspase-1 inhibitor (Ac-YVAD-CMK) at 50 μM and then stimulated with anti-CD3/CD28, for 5 days. Supernatants were collected on day 5, analyzed by ELISA, and normalized against cell number (n=3, one-way ANOVA, NS, not significant, * $p < 0.05$, ** $p < 0.01$). (C) Monocytes were isolated from $CD14^+$ cells and stimulated with LPS (1 μg/mL) for 24 hours and Nigericin (Nig) (10 μM) for 30 mins. Th17 cells were isolated and stimulated with anti-CD3/CD28 (2 μg/mL) for 5 days. Supernatants were collected and analyzed with caspase-1 ELISA. Concentrations were normalized against cell numbers. Data are presented as the means ± SEM (n = 3, one-way ANOVA, * $p < 0.05$). (D) Isolated Th17 cells were pre-treated with NLRP3 inhibitor (MCC950) at 10 μM and stimulated with anti-CD3/CD28 for 5 days. Supernatants were collected on day 5, analyzed by ELISA and normalized against cell number (n = 4, one-way ANOVA, * $p < 0.05$). (E) Immunoblot analysis of gasdermin D (GSDMD), caspase-1, and GAPDH, in monocytes treated with LPS and LPS+Nigericin and in Th17 cells, treated with or without IL-1β. (F) Isolated Th17 cells were stimulated with anti-CD3/CD28 and treated with 500 μM Glycine, for 5 days. Supernatants were collected on day 5, and analyzed by ELISA, and normalized against cell number (n = 4, paired Student's t-test, * $p < 0.05$). (G) Microarray analysis between pro- and anti-inflammatory Th17 subsets. Pro- and anti- inflammatory Th17 subsets were generated in the presence or absence of IL1β and were stimulated with anti-CD3/CD28 (n=3) . Genes of interest are labeled. Colors indicate upregulation (Red) or downregulation (Blue).

Interestingly, IL-1α secretion was hampered by glycine treatment (Figure 2.15F), suggesting that changes in membrane integrity may regulate the secretion of IL-1α.

To better understand the involvement of the inflammasome in human Th17 cells, I attempted to extract inflammasome-related genes from our gene expression analysis. Some inflammasome-related genes were upregulated with IL-1β treatment, such as *PYCARD* (a gene encoding a critical component of NLRP3 assembly) (Figure 2.15G). I also isolated Th17 cells and treated them with TGF-β, which induces IL-1α production, according to our previous observations. Candidate genes known to regulate inflammasomes were selected and validated by PCR analysis. In accordance with increased protein levels, *IL1A* was also highly increased in the TGF-β-treated group. Moreover, *NLRP3* was also upregulated by TGF-β treatment (Figure 2.16A). However, no differences were observed in *IL1B, PYCARD, CASP1*, and *GSDMD* expression levels in response to cytokine treatment (Figure 2.16A). When we analyzed our transcriptome data using gene set enrichment analysis, based on published inflammasome datasets, I did not observe any enrichments in inflammasome-related genes in our gene sets (Figure 2.16B and C). To summarize, I identified a potential role for NLRP3 in the mechanism underlying IL-1α secretion from Th17 cells; however, the classic tools used to analyze inflammasomes in innate cells have not provided strong evidence to support this relationship.

IL-1β is an inflammasome-inducing cytokine that can be co-produced with IL-1α in innate immune cells. To determine whether this occurs in Th17 cells, I co-stained IL-1α and IL-1β in Th17 cells. I found that neither intracellular nor extracellular IL-1β could be detected in Th17 cells and clones (Figure 2.17), suggesting that the underlying secretion mechanisms for IL-1α in T cells may be distinct from that in innate immune cells.

2.2.3 Reactive oxygen species participate in the production and secretion of IL-1α in Th17 cells.

Previous studies have indicated that reactive oxygen species (ROS) are generated after TCR stimulation in human and murine primary T cells (Devadas, Zaritskaya, Rhee, Oberley, & Williams, 2002; Simeoni & Bogeski, 2015). Some studies have indicated that ROS may play a role in the regulation of signaling during T-cell activation and the control of cytokine production and cell viability (Devadas et al., 2002; Kaminski et al., 2010). Furthermore, ROS can be produced by the NLRP3 inflammasomes activators and have been shown to be a critical mechanism for triggering NLRP3 inflammasome activation in innate immune cells (Cruz et al., 2007; Tschopp & Schroder, 2010). Therefore, I explored ROS signaling and its role in the activation of the NLRP3 inflammasome in Th17 cells. Gene set enrichment analysis was performed to obtain a preliminary impression (2.18A and B), and ROS signaling gene sets were strongly enriched in the IL-1β treatment group. Following the Inhibition of ROS in Th17 cells with the antioxidant N-acetyl cysteine (NAC), IL-1α production and secretion were significantly decreased (Figure 2.18C and D), suggesting that ROS play a role in IL-1α production in Th17 cells.

2.2.4 Gasdermin E (GSDME), a pyroptosis-determining protein, is expressed on Th17 cells and may form a pore for IL-1α release.

Because the pore-forming component of GSDMD was undetectable in Th17 cells (Figure 2.15E), I speculated that another pore-forming protein may be involved in the IL-1α secretion mechanism. Transcriptome analysis suggested that GSDME, another pore-forming protein that drives apoptosis into pyroptosis, via an unknown mechanism, was detected in the IL-1β-treated group, associated with a significant fold change compared with the control group (Figure 2.15G). During the stimulation timeline of the culture (Figure 2.19A), the secretion level of IL-1α slowly and continuously increases, and a similar trend was observed for the accumulation of N-terminal GSDME (Figure 2.19B), whereas N-GSDMD remained absent. Because the cleavage of GSDME has

been shown to be dependent on the caspase-8-caspase-3-axis (Figure 2.19D), we also detected the concentration of cleaved caspase-8 and cleaved caspase-3. Cleaved caspase-8 can be detected at 48 hours, whereas little cleaved-caspase 3 could be detected at this time point. The addition of a caspase-3 inhibitor (Z-DEVD-FMK) did not affect intracellular or secreted levels of IL-1α (Figure 2.20A and B). In addition, cell viability and N-GSDME levels were also unaffected by caspase-3 inhibition. Thus, the cleavage of GSDME might occur through a caspase-3 independent machanism.

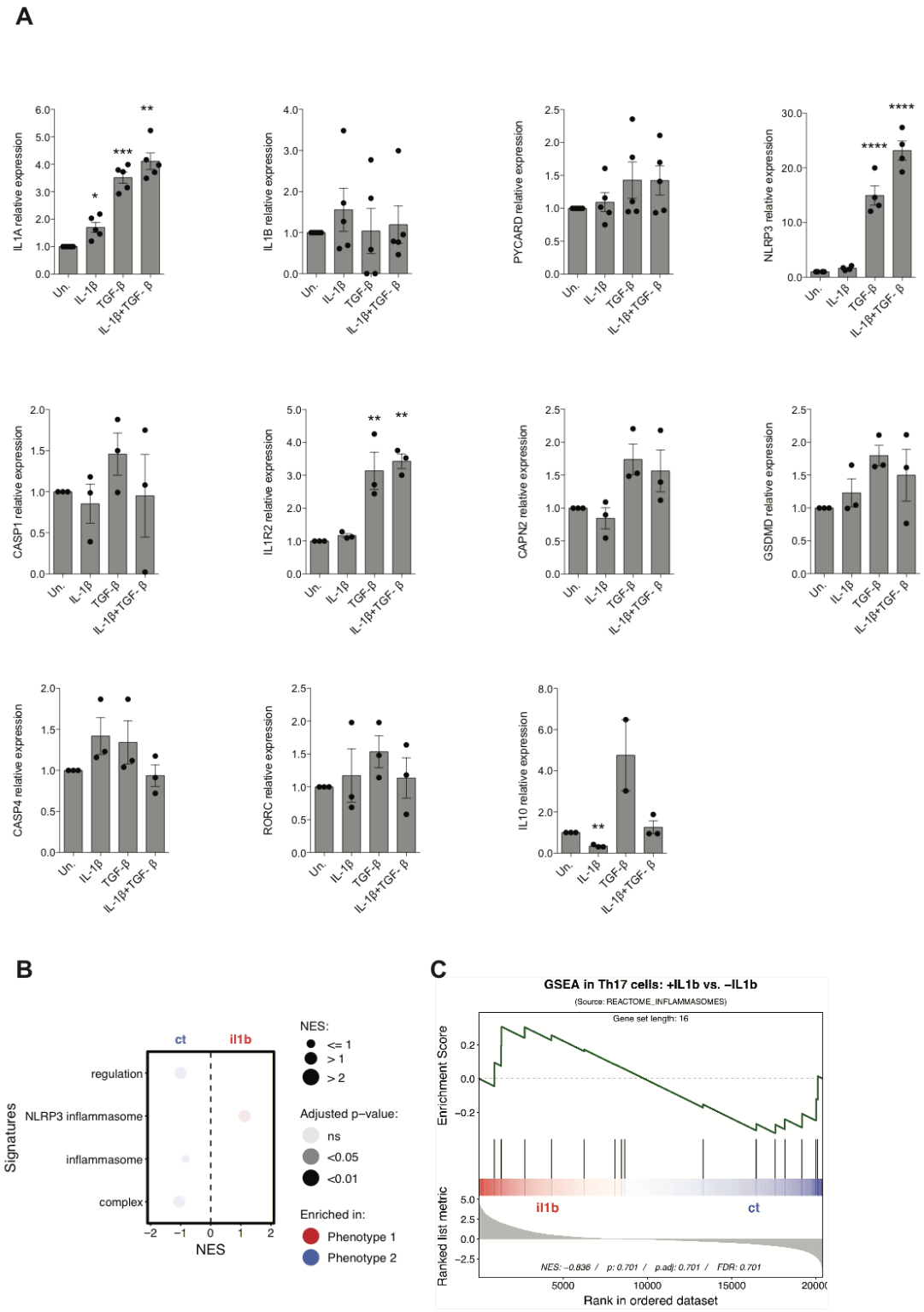

Figure 2.16 See next page for caption.

Figure 2.16 NLRP3 inflammasome-related genes.

(A) Real-time polymerase chain reaction (PCR) analysis examining the expression *IL1A, IL1B, PYCARD, NLRP3, CASP1, IL1R2, CAPN2, GSDMD, CASP4, RORC,* and *IL-10* in sorted Th17 cells stimulated with CD3/CD28 and treated with the indicated cytokines for 5 days. Cultured T cells were collected on day 5 and re-stimulated for 3 hours with phorbol 12-myristate 13-acetate (PMA)/ ionomycin before RNA extraction (n=3–5, one-way ANOVA, * $p < 0.05$, ** $p < 0.01$, *** $p < 0.001$, **** $p < 0.0001$). (B and C) Transcriptome analysis and gene set enrichment analysis of inflammasome-related genes in Th17 cells after IL-1β treatment, compare with untreated cells.

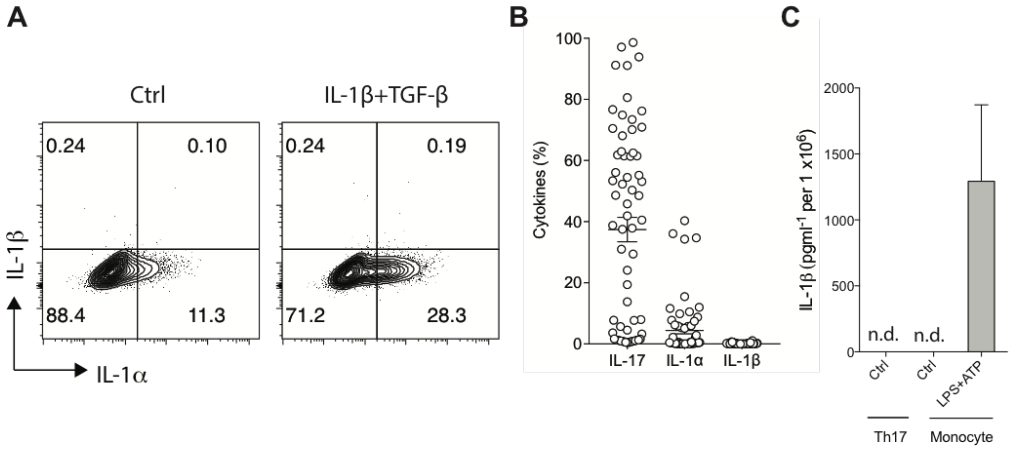

Figure 2.17 IL-1β is not detectable in human Th17 cells.

(A) Isolated Th17 cells were stimulated and treated with IL-1β and TGF-β for 5 days. The IL-1β percentage was determined by intracellular staining (n = 3). (B) IL-1β is not produced by Th17 clones. Th17 clones were generated by the direct cloning of $CCR6^+CCR4^+$ memory $CD4^+$ T cells. Cytokines staining was performed on day 12. The graph show frequencies of IL-17A, IL-1α and IL-1β detection among the Th17 clones. Each symbol represents an individual T cell clone. (n=64) (C) Monocytes were isolated from $CD14^+$ cells, stimulated with LPS (1 μg/mL) for 24 hours and ATP (5 mM) for 30

mins. Th17 cells were isolated, stimulated with anti-CD3/CD28 (2 μg/mL) for 2 days, and rested for 3 days. Supernatants were collected and analyzed for IL-1β expression by ELISA. Concentrations were normalized against cell numbers. Data are presented as the means ± SEM (n = 3).

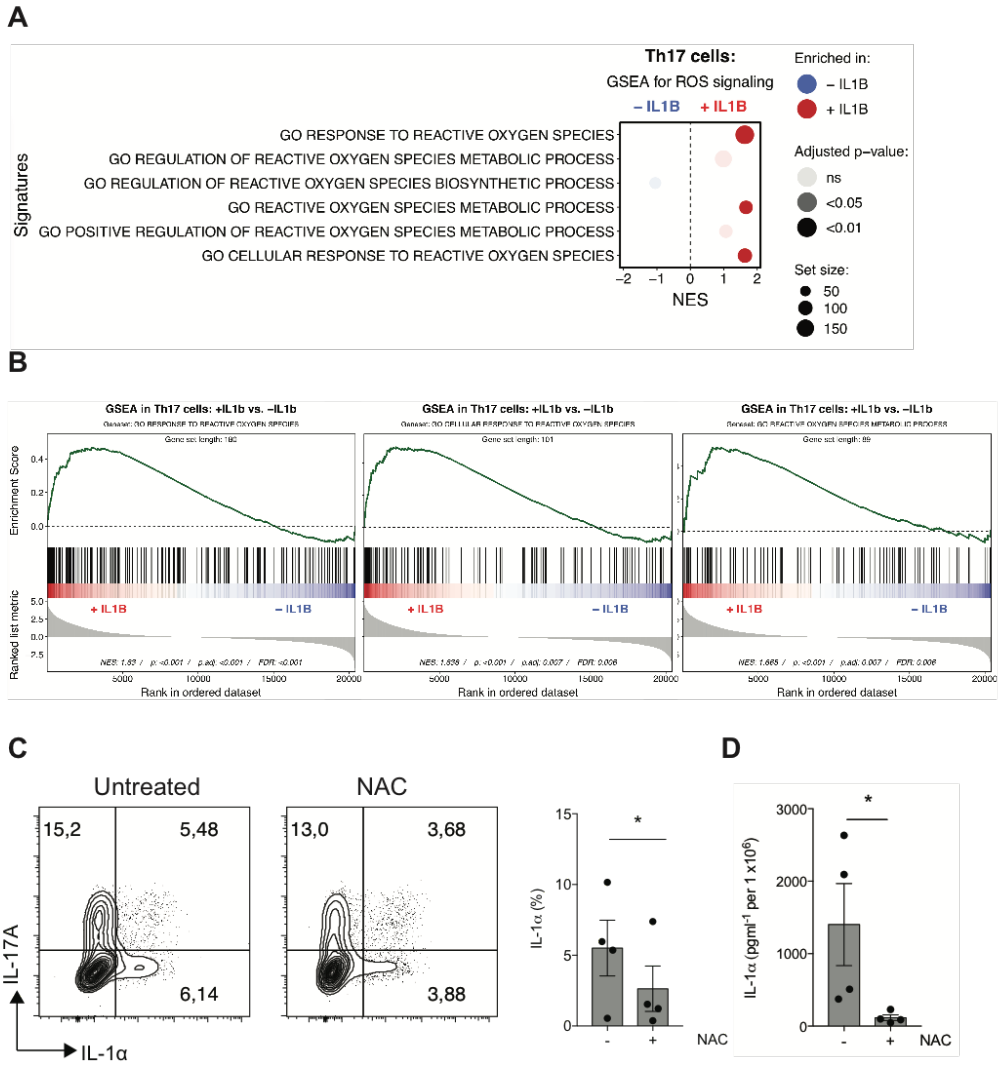

Figure 2.18 See next page for caption.

Figure 2.18 ROS signaling contributes to IL-1α production.

(A and B) Transcriptome analysis and gene set enrichment analysis of ROS-related genes in Th17 cells after IL-1β treatment compare with untreated cells. (C) Isolated Th17 cells were stimulated and treated with 20 mM N-acetylcysteine (NAC) for 5 days. Cells were collected to perform intracellular staining. The bar graph shows the IL-1α percentage (n = 4, paired Student's t-test, * $p < 0.05$). (D) Supernatants were collected on day 5, analyzed by ELISA, and normalized against cell number (n = 4, paired Student's t-test, * $p < 0.05$).

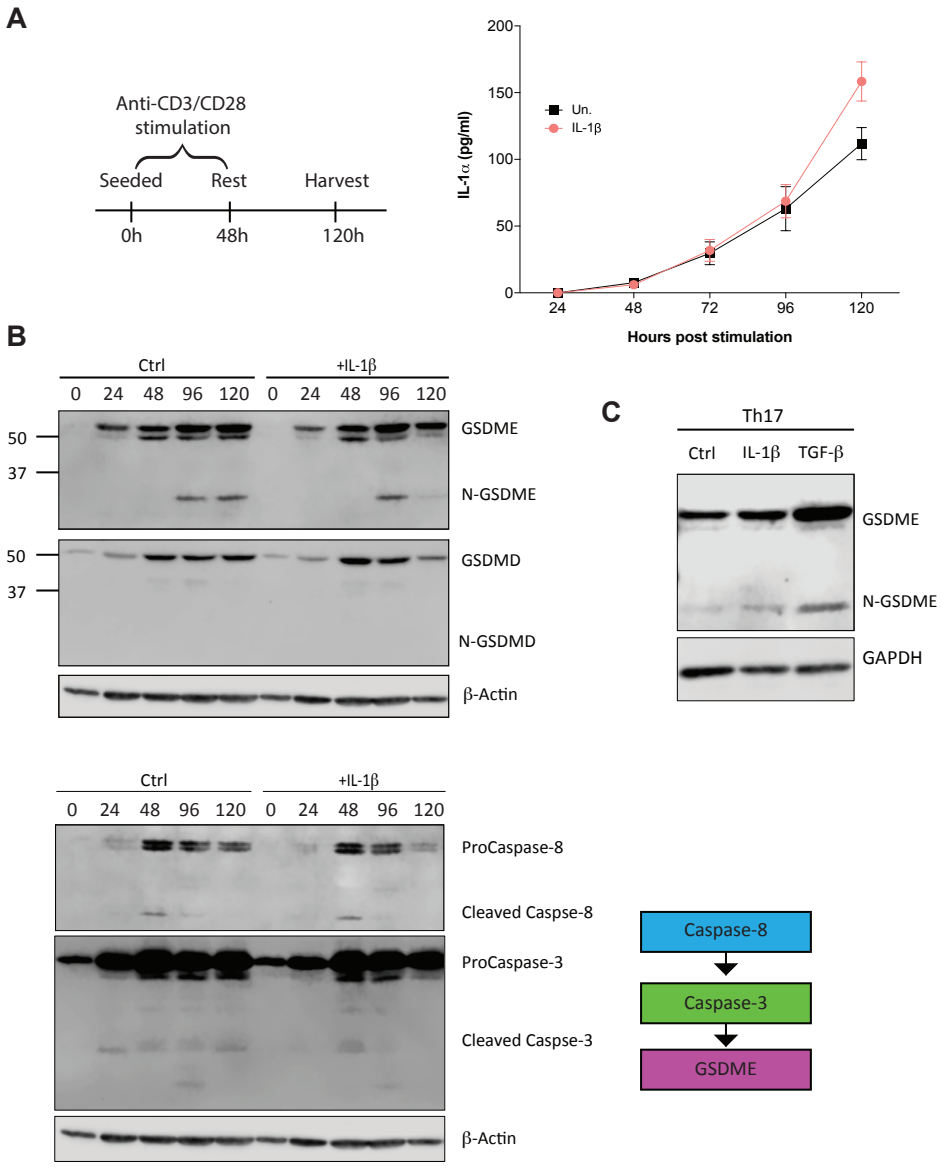

Figure 2.19 GSDME-N can be detected 96 hours after stimulation.

(A) IL-1α levels were detected at different time points during culture and analyzed by ELISA (n = 3, paired Student's t-test). (B) Immunoblots analysis of GSDMD, GSDME, Caspase-8, Caspase-1 and β-actin proteins in Th17 cells. Cells were sorted and stimulated with anti-CD3/CD28, in the presence or abscence of IL-1β (20 ng/mL) for 24–120 hours. (C) Immunoblots against GSDME and GAPDH in Th17 cells, treated with IL-1β (20 ng/mL) or TGF-β (20 ng/mL) for 5 days.

2.3 Cell viability upon IL-1α secretion

Because previous studies have associated the secretion of IL-1α with cell death, I examined the cell status after IL-1α secretion. I isolated eight IL-1α positive and eight IL-1α-negative clones, pooled them together into one group and compared the expression of apoptosis-related genes. I observed a trend toward apoptosis-related gene upregulation in IL-1α-positive clones (Figure 2.21A). Likewise, Gene set enrichment analysis also showed the enrichment of apoptosis signatures in the IL-1β-treated group (Figure 2.21B and C). However, when I had examined which genes were regulated, key apoptosis genes (Caspase-3, Bcl2, etc.) did not show a significant difference between these two groups, suggesting that an atypical cell death pathway may be involved. Tumor necrosis factor (TNF)-α has been identified as a potential Th17-pathogenicity-tuning cytokines, and blocking TNF-α has been shown to dramatically alleviates rheumatoid arthritis by altering Th17 differentiation (Hyrich, Watson, Silman, Symmons, & British Society for Rheumatology Biologics, 2006; Y. C. Lin et al., 2017). However, TNF-α can also trigger a primary pathway, leading to the apoptosis of numerous cell types (Brenner, Blaser, & Mak, 2015), and CD4 T cells from aged humans and HIV-infected CD4 T cells have been associated with increased levels of TNF-α-induced apoptosis (Aggarwal, Gollapudi, & Gupta, 1999; Gupta, 2002; Klein et al., 1996), implying a potential role for TNF-α in activated T cells. To examine the effects of TNF-α on IL-1α secretion, I treated cells with TNF-α or with neutralizing antibodies against TNF-α, and found that altering the TNF-α levels had no effects on IL-1α secretion (Figure 2.22 A), suggesting that the IL-1α secretion mechanism is TNF-α-independent.

To examine the occurrence of necroptosis, a programmed form of necrosis, or inflammatory cell death, I also attempted to visualize the presence of necroptosis-related genes by preforming a Kyoto Encyclopedia of Genes and Genomes (KEGG) pathway analysis (Figure 2.23A). Several genes are upregulated after IL-1β treatment in Th17 cells. Although the addition of the necroptosis inhibitor, necrostatin-1 did not

suppress extracellular IL-1α levels (Figure 2.23A), I observed reduced intracellular IL-1α levels and increased activated caspase-8 (Figure 2.23B and C), indicating the potential induction of apoptosis when cells are protected from necroptosis. The potential for cross-talk between various cell death pathways will be addressed in the discussion section of this thesis.

Because the secretion of IL-1a in Th cells represent a relatively long-term process (>3 days), the methods that are commonly used to address cell death in innate immune cells are not appropriate for our purposes. For example, the small populations of dying T cells may be masked by the growth of activated T cells; therefore, assessing cell viability among Th17 cells secreting IL-1α can be challenging. To overcome this challenge, I established a single-cell-based re-cloning method, grounded in the ability of live T cells to generate clones upon re-stimulation. I initially screened for IL-1α production ability in each individual clone and seeded single cells into one well each. Cell growth within a given well indicated the viability of the seeded cell, and counting the number of wells showing growth can provide a live cell percentage for the whole population of seeded cells (clone-efficiency) (Figure 2.24). I found a significant negative correlation between IL-1α expression and re-clone efficiency (Figure 2.24A); however, this phenomenon was not observed for IFN-γ and IL-17A expression (Figure 2.24 B and C). These results support the idea that IL-1α-producing cells are prone to cell death.

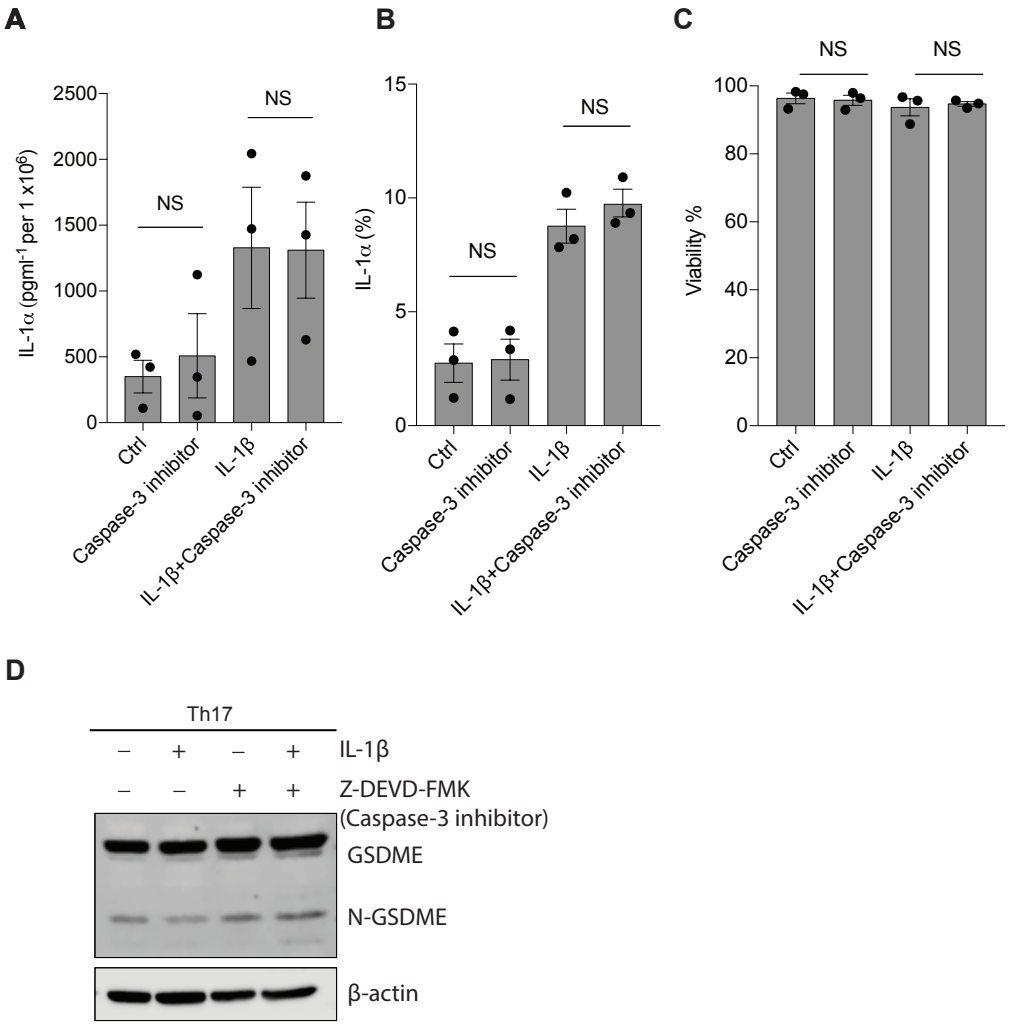

Figure 2.20 IL-1α secretion is caspase-3 independent.

(A) Isolated Th17 cells were pre-treated with a caspase-3 inhibitor (Z-DEVD-FMK), at 20 μM, for 3 hours and stimulated with anti-CD3/CD28. Supernatants were collected on day 5, analyzed by ELISA, and normalized against cell number (n = 3, paired Student's t-test). (B) The bar graph shows the IL-1α percentage within the total cell population (n = 3, paired Student's t-test). (C) Cell viability was determined by staining with zombie dye. (n = 3, paired Student's t-test) (D) Immunoblots examining GSDME protein levels in Th17 cell lysates treated with IL-1β and/or the caspase-3 inhibitor Z-DEVD-FMK for 5 days.

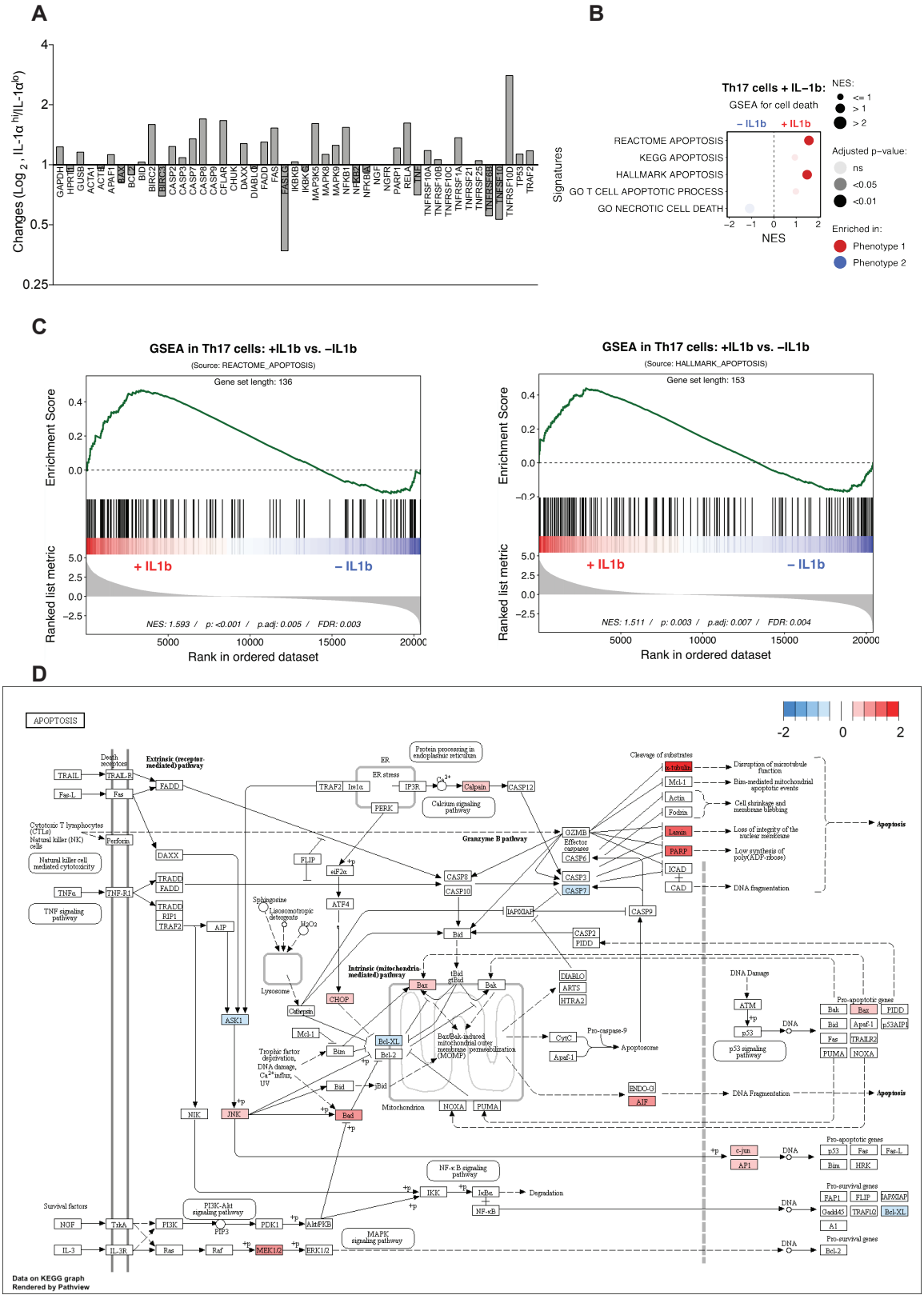

Figure 2.21 See next page for caption.

Figure 2.21 Genes related to apoptosis are enriched in Th17 cells treated with IL-1β.

(A) TaqMan™ Array Human Apoptosis 96-well Plate was performed using pooled Th17 IL-1α-positive (hi) and -negative (lo) clones (8 clones of each type were pooled). Values were normalized against 18S gene expression levels. T cell clones were collected and restimulated for 3 hours with PMA/ionomycin before RNA extraction (n=1). (B and C) Gene set enrichment analysis (GSEA) for apoptosis-related genes in Th17 cells after IL-1β treatment, compared with untreated cells. (D) KEGG pathway analysis for apoptosis-related genes. Colors indicated upregulated (red) or downregulated (blue) genes after IL-1β treatment.

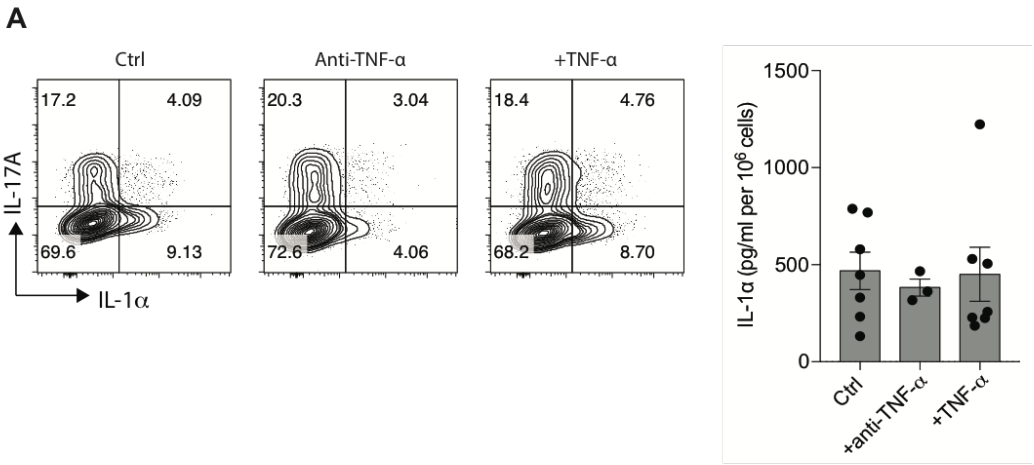

Figure 2.22 IL-1α secretion occurs via TNF-α-independent pathway.

(A) Th17 cells were stimulated and treated with anti-TNF-α antibody (5 μg/mL) or TNF-α (20 ng/mL) for 5 days. Supernatants were collected and analyzed by ELISA. Concentrations were normalized against cell numbers (n = 3–7, one-way ANOVA).

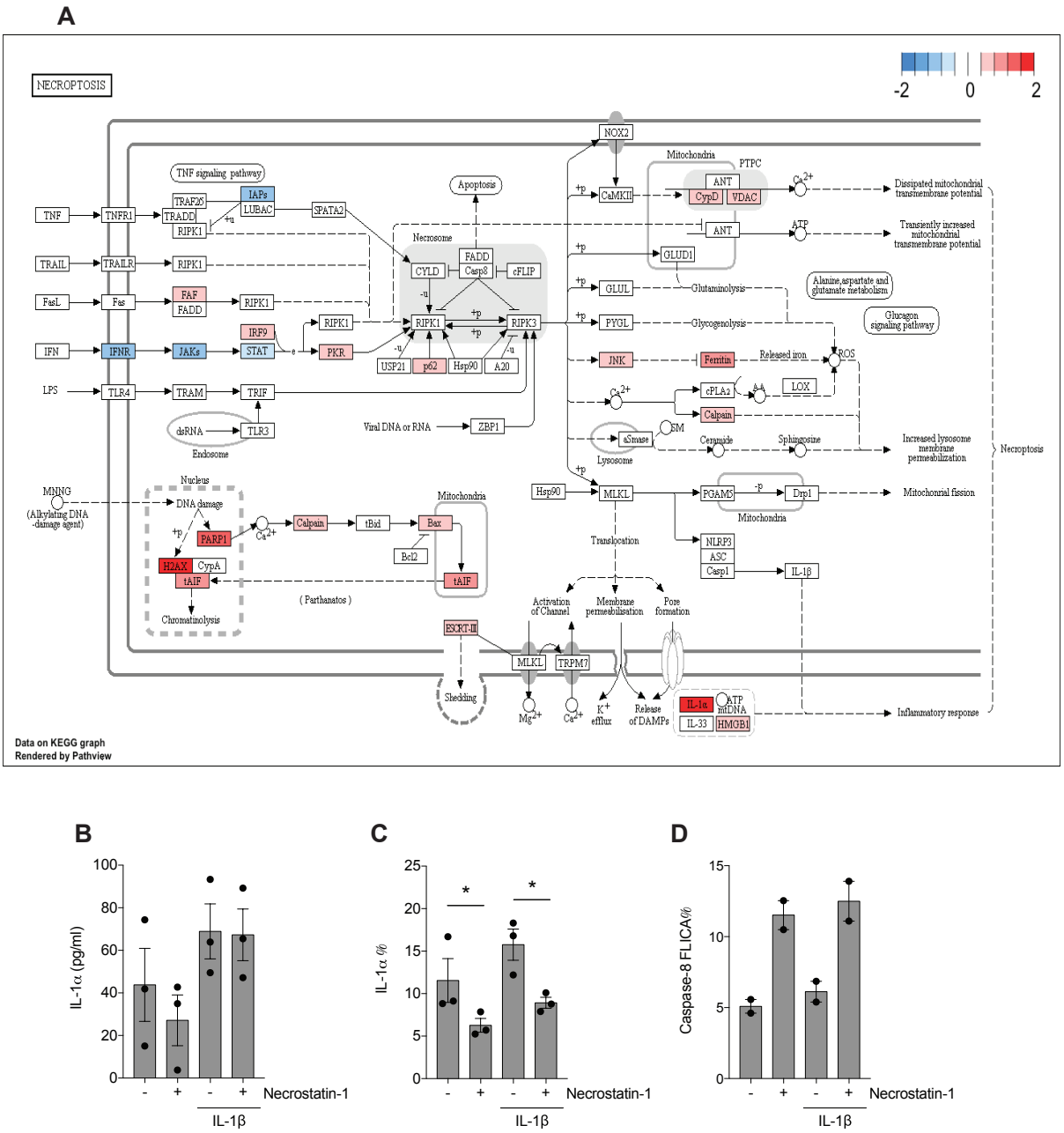

Figure 2.23 The role of necroptosis in IL-1α production.

(A) KEGG pathway analysis for necroptosis-related genes. Colors indicate the upregulation (red) or downregulation (blue) of genes after IL-1β treatment. (B) Isolated Th17 cells were pre-treated with Necrestatin-1 (10 μM), for 3 hours, and stimulated with anti-CD3/CD28. Supernatants were collected on day 5, analyzed by ELISA, and normalized against cell number (n = 3, paired Student's t-test). (C) The bar graph shows

the IL-1α percentage within the total cell population (n=3, paired Student's t-test, * p < 0.05). (D) Cells were stained with FLICA-caspase-8 on day 5 (n=2).

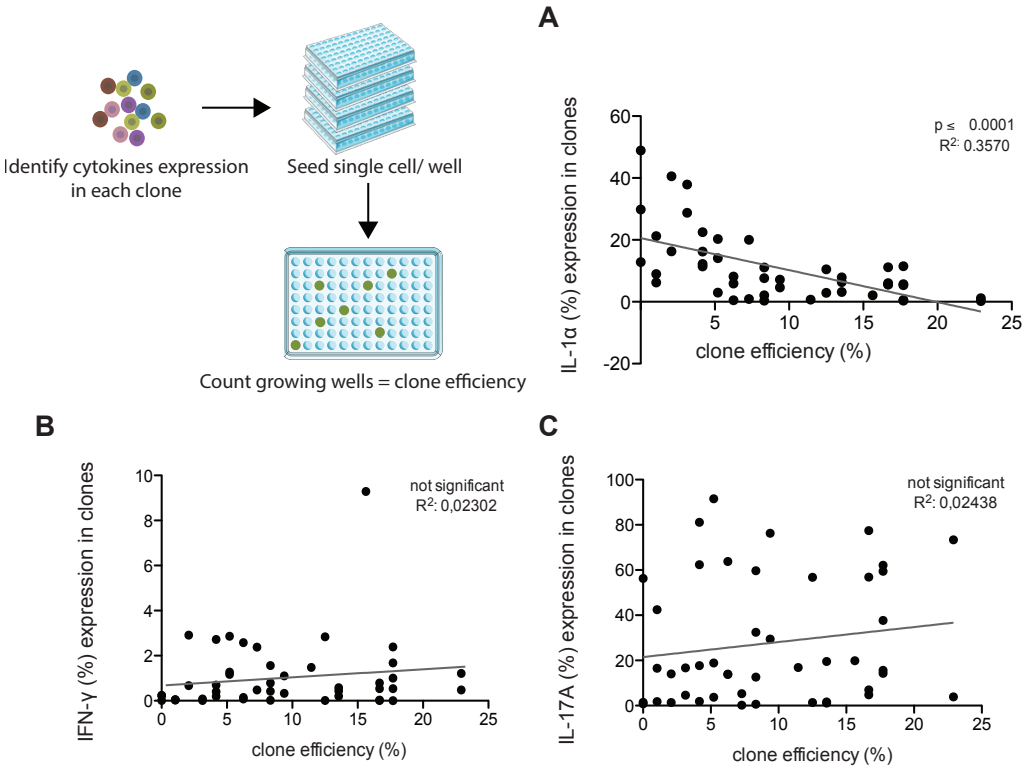

Figure 2.24 Clones that produced increased levels of IL-1α showed lower re-cloning efficiency.

(A–C) Th17 clones were generated, and several clones were selected and analyzed for IL-1α, IFN-γ and IL-17A expression at the resting state. Single cells from each clone were then seeded into a 384 well plate by limiting dilution and were stimulated with allogeneic peripheral blood mononuclear cells (PBMCs). Clone efficiency was determined by calculated the number of growing wells relative to the number of total seeded wells. Data points were obtained from three independent experiments and were pooled for statistical analyses.

2.4 Physiological and pathophysiological significance of IL-1α producing human Th cells

2.4.1 Physiological relevance of IL-1α-producing human Th cells

We previously showed that innate IL-1β suppresses IL-10 production in Th17 cells, rendering them pathogenic (Noster et al., 2016; Zielinski et al., 2012). I hypothesized that autocrine IL-1α secretion can also suppress IL-10 and contributes to the pathogenicity of Th17 cells, due to the shared IL-1R1 receptor.

I found that following external IL-1α treatment, IL-10 was downregulated (Figure 2.25A). The absence of IL-1β further validated the previous results that IL-1α secretion from Th17 cells is IL-1β independent. I further examined additional pro-inflammatory cytokines, and found that the levels of IL-1α itself, IFN-γ, and IL-17A increased (Figure 2.25B). IL-1R1, a shared receptor between IL-1α and IL-1β signaling, was also upregulated by IL-1α signaling (Figure 2.25C). These data indicated the presence of a positive feedback loop, initiated by extrinsic IL-1β and amplified by intrinsic IL-1α, which further enhances the pathogenicity of Th17 cells. Upon the specific blockade of IL-1α, the cells were able to restore IL-10 secretion (Figure 2.25D), even when the pro-inflammatory initiating signal IL-1β was present. Taken together, these results suggesting that IL-1α and IL-1β play similar roles in determining the functionality of the Th cell compartment, particular with respect to the anti-inflammatory IL-10 expression, however, different expression patterns were observed between these two IL-1 isoforms in human Th cells.

2.4.2 The contribution of IL-1α-producing Th17 cells to the pathogenesis of autoinflammatory syndromes

Autoinflammatory syndromes are often characterized by the overproduction of IL-1α, due to aberrant gene mutations in the inflammasome or other molecular alterations related to the innate immune system (de Jesus, Canna, Liu, & Goldbach-Mansky,

2015). Because I observed that IL-1β can induce and enhance IL-1α production by T cells, I examined the effects of IL-1α expression in autoinflammatory syndrome patients treated with IL-1β-blocking therapies. Our laboratory previously collected PBMC samples from patients diagnosed with Schnitzler syndrome, who were treated with the IL-1β blockade drug, canakinumab. Using these patient samples, we aimed to investigate whether IL-1α production levels were altered following IL-1β blocking treatment. I observed the isolated Th17 cells from patients showed lower IL-1α level after canakinumab treatment (Figure 2.26A and B), in addition to reduced level of pro-inflammatory cytokines, such as IL-17A and IFN-γ. I also cloned Th17 cells from an adult-onset Still's disease (AOSD) patient, and observed the reduced production of IL-1α from Th17 clones after anakinra treatment (Figure 2.26C), which targets IL-1R and, therefore, blocks both IL-1α- and IL-1β-signaling simultaneously. Together, these results support the regulation of IL-1α expression by T cells, *in vivo*.

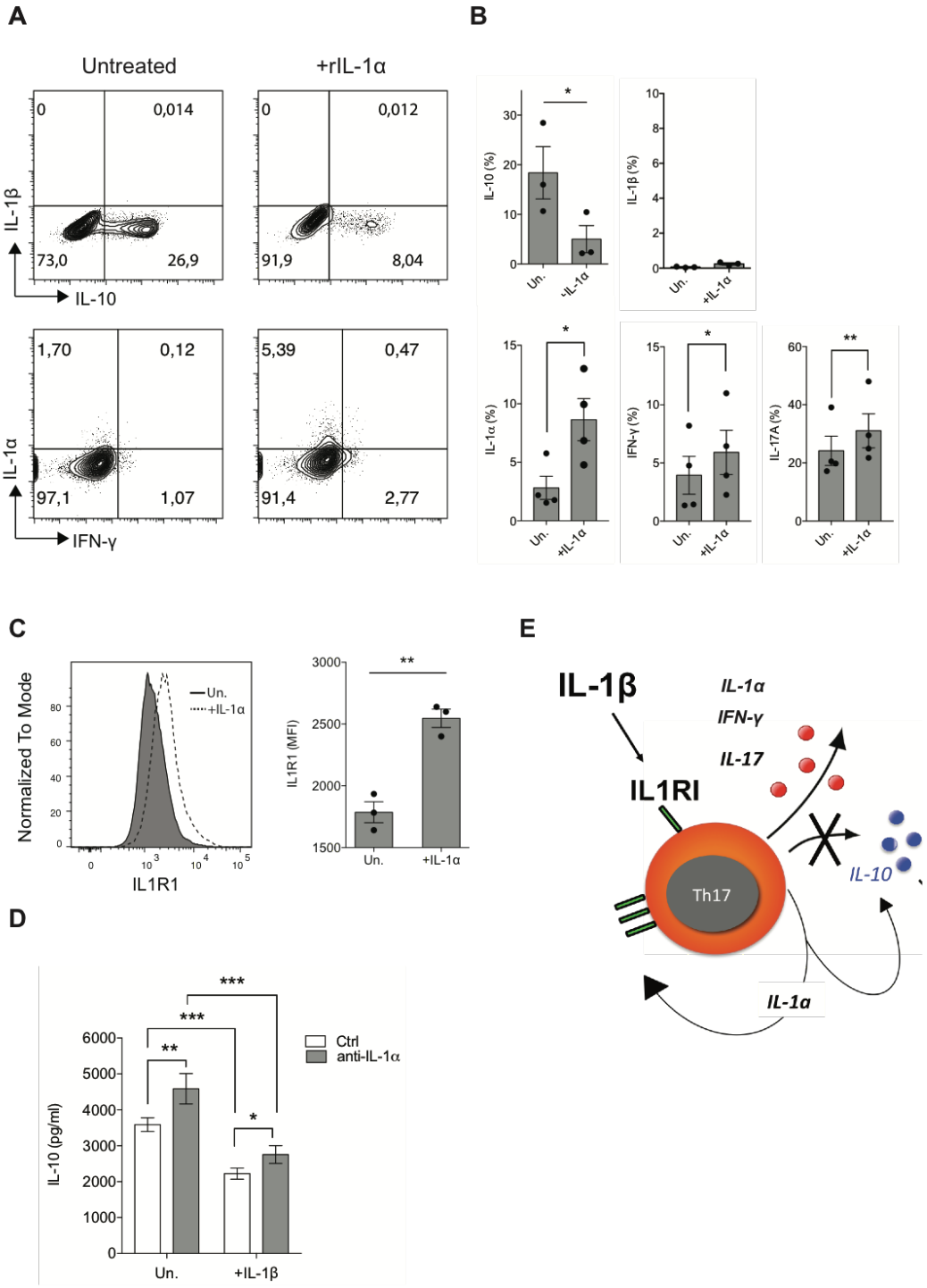

Figure 2.25 See next page for caption.

Figure 2.25 Autocrine IL-1α amplifies the pathogenicity of Th17 cells through the downregulation of IL-10.

(A) Sorted Th17 cells were stimulated and treated with or without IL-1α (20 ng/mL). A representative flowcytometry graph shows the intracellular staining of IL-10 and IL-1β as well as IL-1α and IFN-γ. (B) Quantification of the percentage of IL-10-, IL-1β-, IL-1α- IFN-γ- and IL-17A-producing cells. Data are presented as the mean ± SEM (n=3–4, paired Student's t-test, * $p < 0.05$, ** $p < 0.01$). (C) IL1R1 is upregulated by IL-1α. Sorted Th17 cells were stimulated and treated with or without IL-1α (20 ng/mL). Data are presented as the mean ± SEM (n = 3, paired Student's t-test, * $p < 0.05$, ** $p < 0.01$). (D) Blocking IL-1α rescues the inhibition of IL-10 by IL-1β treatment. Sorted Th17 cells were activated and treated with IL-1α neutralization antibody (10 μg/mL) in the presence or absence of IL-1β (20 ng/mL). Supernatants were collected after 5 days of culture (n = 5, Two-way ANOVA, * $p < 0.05$, ** $p < 0.01$, *** $p < 0.001$) (E) Schematic showing the autocrine IL-1α mechanism.

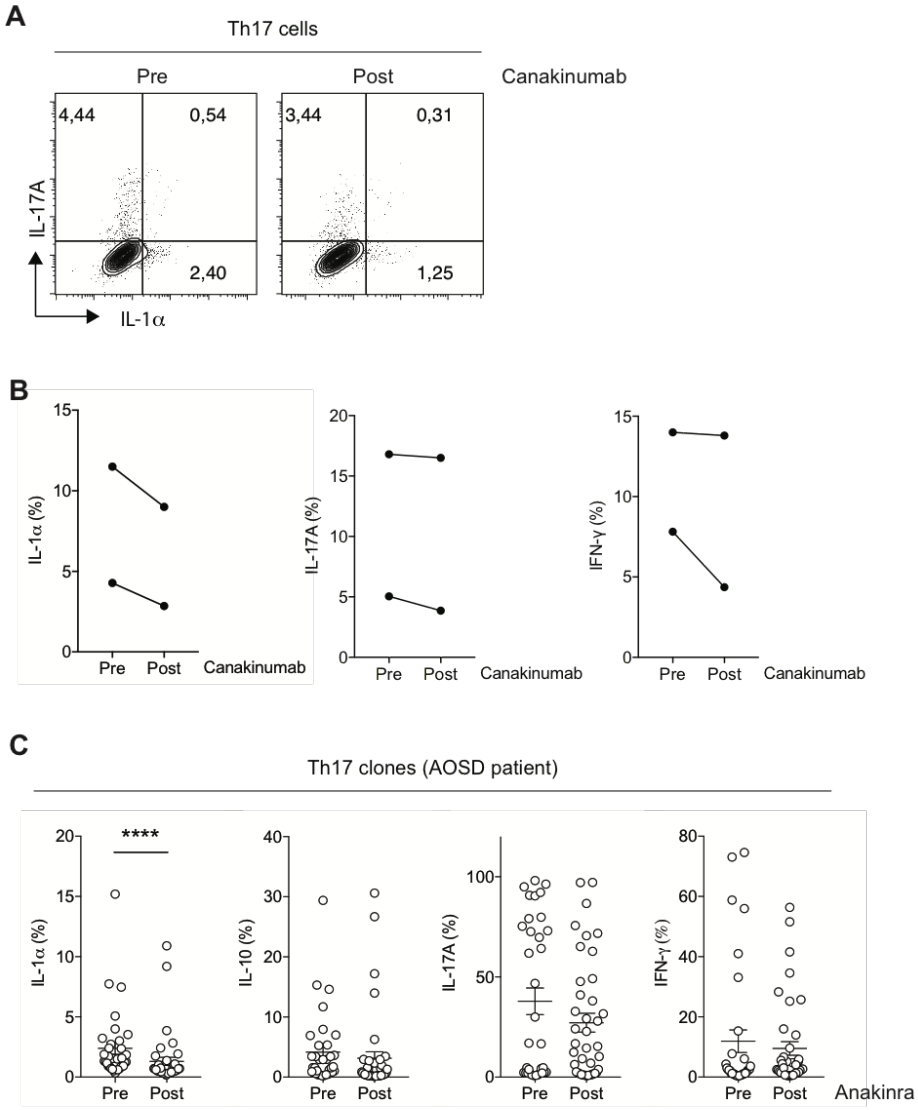

Figure 2.26 IL-1α is downregulated in patients with Schnitzler syndrome following IL-1β-blocking treatments.

(A) Th17 cells isolated from patients with Schnitzler syndrome, before and after treatment with canakinumab. Cells were stimulated with anti-CD3/CD28 for 5 days. (B) Quantification of the percentage of IL-1α- IFN-γ- and IL-17A-producing cells. (n=2). Patients with Schnitzler syndrome and matched control patients (matched pairs) were examined after at least 6 months of treatment with canakinumab, associated with a complete clinical response. (C) Th17 clones were generated from an AOSD patient, before and after treatment with anakinra (pre, n = 34; post, n = 40, Mann-Whitney U test, ns, not significant, * $p < 0.05$, ** $p < 0.01$, *** $p < 0.001$, **** $p < 0.0001$).

3 Discussion

3.1 Why have we overlooked IL-1α secretion from T cells for so long?

In the first part of the Results, I demonstrated that T helper cells, especially the Th17 subset, has an increased ability to produce IL-1α. This effect has been overlooked in most of the literature for various possible reasons, described below.

The first article that described IL-1α being produced by T cells was published in 1991 by Daniel Olive's group (Cerdan et al., 1991). They showed that IL-1α mRNA levels in T cells were upregulated upon treatment with anti-CD2 plus anti-CD28. The process is, therefore, independent of monocyte stimulation and represents a slow and prolonged procedure (> 48 hours). Two years later, the same group found that both IL-1α gene expression levels and protein secretion were upregulated (Costello et al., 1993). At that time, the conclusion was made that "monokines", such as IL-1α can be secreted from T cells. However, the cell isolation strategy they used might have been a confounding factor; contamination of myeloid cells is difficult to avoid with the method they used. Since those initial studies, no further work has been invested in establishing the mechanism of IL-1α secretion from T cells.

Another study was published 10 years later describing the discovery of IL-1α gene expression in human CD4 T cell clones (Th0, Th1, and Th2) that was monoallelic. The purpose of cytokines being regulated through monoallelic expression remains unclear. However, the study did not investigate the protein levels of IL-1α secreted by the T cells (Bayley et al., 2003). After this, IL-1α production and secretion were primarily studied in antigen presenting cells and often linked with IL-1β co-expression and regulation.

When checking public datasets for gene expression levels in different immune cell types, T cells often show low baseline levels of IL-1α. However, our results indicate that for maximal expression and secretion of IL-1α, the TCR signal strength and activation times of T cells are critical (Figures 2.5 and 2.10). These data also agree

with the results from the first publication in 1991. There is a recently published dataset that also supports this hypothesis; the authors profiled the patterns of gene expression with and without proper activation in different immune cell types. The *IL1A* gene was only detected in activated T cells, not in resting T cells (Calderon et al., 2019).

Taken together, the special requirements for the production and secretion of IL-1α by T cells, plus the fact that only a small subpopulation shows this capacity, make the study of this effect quite challenging.

3.2 The production mechanism of IL-1α in T cells might be distinct from the more commonly known IL-1α-producing cell types.

Here, I would like to focus on the intracellular regulation of IL-1α production. As an alarmin, IL-1α production is known to begin promptly in response to stress-associated stimuli. When looking at the promoter region of the *IL1A* gene, the lack of TATA and CAAT boxes and the Sp1 transcription factor binding site imply that IL-1α expression is subject to housekeeping-like regulation (McDowell, Symons, & Duff, 2005). Later, AP1 and NF-κB binding sites were also discovered (Bailly, Fay, Israël, & Gougerot-Pocidalo, 1996; Zaldivar, Nugent, Imfeld, & Berman, 2002), which implies that a spectrum of stimuli induce *IL1A*. In T cells. I also observed that several cytokines, such as IL-1α itself, IL-1β, TGF-β, and IL-2 (Figures 2.25, 2.7, and 2.11), as well as TLR ligands (Figures 2.6C and 2.7C) induce IL-1α intracellularly. The potential mechanism is that IL-1 proteins and CpG-ODNs could promote IL-1α production through the Myd88-signaling pathway and downstream molecules, such as AP1 and NF-κB. Our results also suggest that STAT-JAK signaling is important in IL-1α production, with evidence of a trend for positive regulation from IL-2-STAT5 signaling (Figure 2.11) and the inhibitory effects of all the STAT3-related cytokines, such as IL-6 and IL-23 (Figure 2.7). As the *IL1A* promotor has no known STAT binding site, the effect of STAT families on promoting IL-1α could be indirect. Besides, TGF-β, which is regarded as an anti-inflammatory cytokine, has shown the capacity to promote IL-1α production intracellularly (Figures 2.3 and 2.7), but not extracellularly (Preliminary Data Figure 1),

and the effect is IL-1R1-independent (Figure S1B). When we analyzed the protein-DNA interaction network using CoRegNet analysis, it was interesting to see that there is a possible interaction of Smad3 with the *IL1A* promotor (Figure S1C); however, whether this is a true interaction and whether it acts positively or negatively still need to be investigated. The inhibitory effect of TGF-β on IL-1α release is also interesting; this could be explained by IL-1R2 expression, which is induced by TGF-β (Figure 2.16A) and protects IL-1α from cleavage and secretion (Zheng et al., 2013). However, the binding of IL-1α to IL-1R2 in T cells has not been addressed, and further work is needed to determine the inhibiting role of TGF-β on IL-1α secretion.

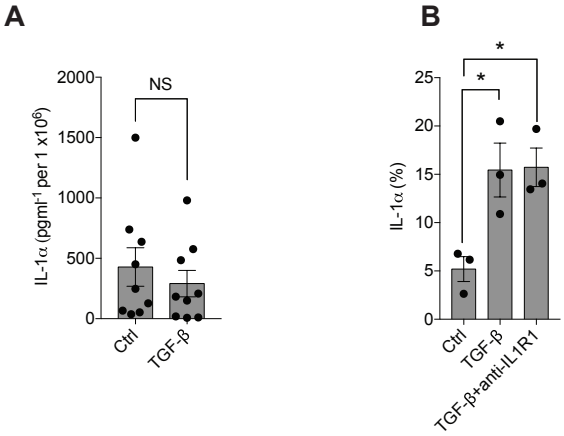

C

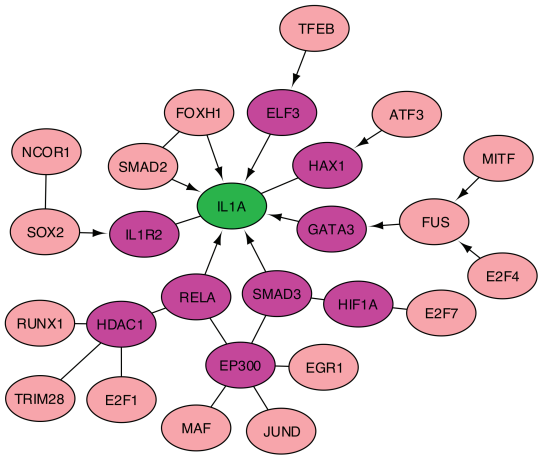

ID1	ID2	edgeProbability	interaction	redundancy	pubmedID
E2F7	HIF1A	0.564165	0.564165	0.572408	26681691
EGR1	EP300	0.991672	0.991672	0.00836259	9806899 15225550 20018936 20089040
JUND	EP300	0.972367	0.972367	0.028022	16264271 17510411 21937452
ATF3	HAX1	0.6	0.6	0.510826	PDI:23680149 27146783
NCOR1	SOX2	0.837476	0.837476	0.177363	21532573 23667531 28794006
E2F4	FUS	0.6	0.6	0.510826	PDI:17652178 21247883
E2F1	HDAC1	0.999268	0.999268	7.32E-04	10734134 17980157 26468294 9468139 9468140
MITF	FUS	0.6	0.6	0.510826	PDI:21258399
FUS	GATA3	0.6	0.6	0.510826	PDI:26573619
TRIM28	HDAC1	0.964522	0.964522	0.0361226	21669397 23060449 22863883
FOXH1	IL1A	0.6	0.6	0.510826	PDI:21741376
SOX2	IL1R2	0.6	0.6	0.510826	PDI:20726797
RUNX1	HDAC1	0.961492	0.961492	0.0392693	16652147 21059642 22498736 26598521
SMAD2	IL1A	0.6	0.6	0.510826	PDI:18955504
SMAD2	FOXH1	1	1	5.96E-08	10199400 9858566 9389648 10938097 9288972 12732634 21828274 16916642 15750622 9702198 unassigned1304
MAF	EP300	0.629023	0.629023	0.463588	11943779
TFEB	ELF3	0.6	0.6	0.510826	PDI:21752829
HDAC1	RELA	1	1	4.77E-07	12419806 11931769 11564889 20001970 17000776 16483679 15192014 17827154 21983014 27012186 30670829 16291753
HIF1A	SMAD3	0.999631	0.999631	3.69E-04	11486006 12228247 14741200 28471448
EP300	SMAD3	1	1	1.00E-10	16876108 15623506 11058129 10575014 15133024 20564330 9679056 10497242 16109717 15345715 9843571 11134049 12743039 15824515 21567395 17469184 15588252
EP300	RELA	1	1	1.00E-10	12419806 9096323 12403783 11585920 11567019 18280497 15192014 10235267 20333651 20154269 17692505 17982102 12960163 21187066 18397880 12456660 25074812 23999430 25400040 16135789 12471036 21483817 11533489 16291753
IL1R2	IL1A	0.9709	0.9709	0.029532	25241761 16971486
RELA	IL1A	0.6	0.6	0.510826	PDI:24523406
ELF3	IL1A	0.6	0.6	0.510826	PDI:26769127
HAX1	IL1A	0.984225	0.984225	0.0159003	11554782 25416956 16971486
SMAD3	IL1A	0.6	0.6	0.510826	PDI:18955504
GATA3	IL1A	0.6	0.6	0.510826	PDI:21878914

Preliminary Data Figure 1. TGF-β does not induce extracellular levels of IL-1α. (A) Isolated Th17 cells were stimulated with anti-CD3 and anti-CD28 in the presence TGF-β (20 ng/mL) for 5 days. Supernatants were collected on day 5 and analyzed by enzyme-linked immunosorbent assay (ELISA) and normalized to the cell number (n = 9, mean ± SEM, paired Student's t-test). (B) Isolated Th17 cells were stimulated with anti-CD3 and anti-CD28 in the presence of TGF-β (20 ng/mL) and anti-IL1R1 for 5 days. The bar graph shows IL-1α percentage within total cells. (n = 3, One-way ANOVA) (C) The transcription factors that influence *IL1A* gene expression were identified in the CoRegNet analysis, with FDR < 0.05 and |FC| > 1.5 used as input for this analysis. *IL1A* was set as the end point.

Even though IL-1α can be expressed as a membrane-bound or secreted form, I could not detect surface IL-1α (Figure 2.5). In some cell lines, surface-bound IL-1α has been shown to act in a juxtacrine manner as a result of cell senescence (Orjalo, Bhaumik, Gengler, Scott, & Campisi, 2009). I have no clear evidence showing that our cells underwent senescence, but my preliminary results showed the production of IL-1α was detected in CTV-negative cells (Preliminary Data Figure 2), suggesting that IL-1α might be produced by proliferating cells. To better address the possible senescence of T cells, future work might check for the presence of some typical senescence markers, such as Ki67, p21 (CDKN1A), and γH2AX, combined with IL-1α staining (Lawless et al., 2010). The phenomenon of T cells lacking surface-bound IL-1α might indicate the autocrine or paracrine action of IL-1α from migrating T cells. Surface-bound IL-1α is known to be an upstream regulator of IL-6 and IL-8 production (Orjalo et al., 2009). As T cells have not been found to secrete IL-6, I measured IL-8 in different Th subsets and found that IL-8 is upregulated with IL-1β treatment (Preliminary Data Figure 3B). Similar results were observed by Gasch et al. IL-8 secretion was detected in Th17-polarizing conditions (TGF-β, IL-1β, and IL-23), and found to be driven by the aryl hydrocarbon receptor (AHR) (Gasch et al., 2014). Thus, the hypothesis that IL-1α can also induce IL-8 in human T cells needed to be investigated carefully, considering that cell-type specific regulation of IL-8 occurs and the effects might be IL-1α-independent.

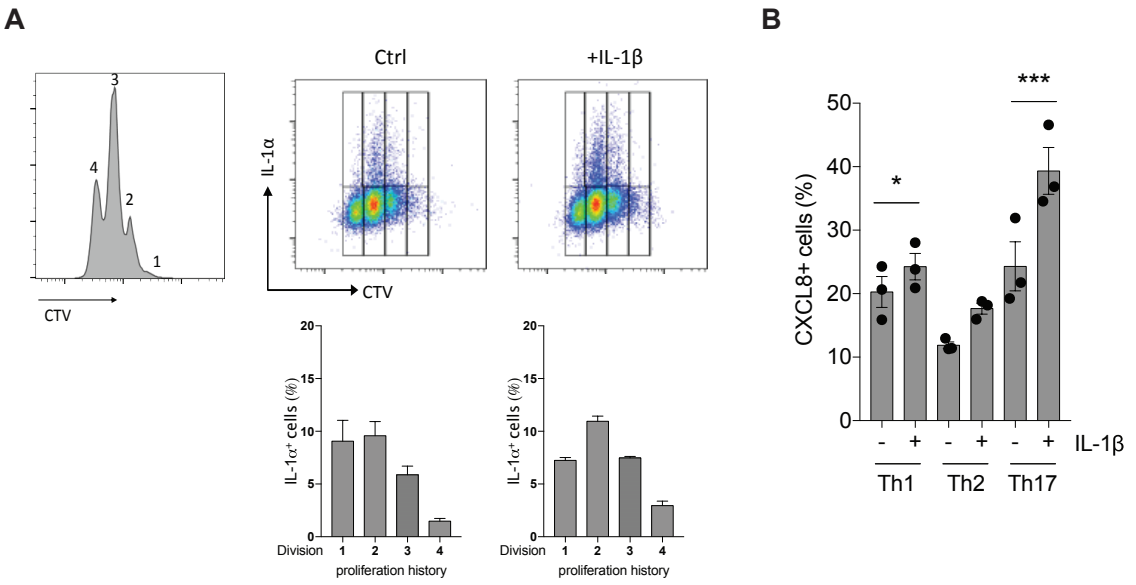

Preliminary Data Figure 2. (A) Isolated Th17 cells were stained with CellTrace Violet and stimulated with anti-CD3 and anti-CD28 in the presence or absence of IL-1β (20 ng/mL) for 5 days. Cells were gated according to the divided peaks; percentages represent the IL-1α portion in each division. (B) Th1, Th2, and Th17 cells were isolated and stimulated with anti-CD3 and anti-CD28 in the presence or absence of IL-1β (20 ng/mL) for 5 days. CXCL8 (IL-8) was analyzed with ICCS. Data show mean ± SEM (n = 3, paired Student's t-test, * $p < 0.05$, ** $p < 0.01$, *** $p < 0.001$).

3.3 The innate inflammasome machinery might participate in IL-1α secretion mechanism in T cells.

The Inflammasome is crucial in the processing and release of IL-1β in myeloid immune cells; however, this seems not to be the case in human T cells, as we were unable to detect IL-1β secretion from human T cells (Figure 2.17). The autocrine induction of *IL1B* gene expression after IL-1β treatment was observed in a monocyte cell line (Toda et al., 2002), but was absent in Th17 cells (Figure 2.16), suggesting that IL-1β secretion and the autocrine regulation of *IL1B* gene expression might be myeloid cell-restricted.

Nevertheless, there are data reported in previous studies showing that IL-1β is secreted from HIV-infected, CAPS, and RA patient T cells (Arbore et al., 2016; Doitsh et al., 2014; Li et al., 2019). This disparate finding might be due to cell death or some exceptional requirements for T cell activation, which need to be closely investigated. In a previous study with mouse models, it has been identified that IL-1β can be produced by Th17 cells and that it mediated experimental autoimmune encephalomyelitis (EAE) (Martin et al., 2016). The Th17-derived IL-1β was produced by the ASC-NLRP3 inflammasome. Since I did not observe IL-1β secretion by the human T helper cells from our system, I tried to investigate whether intrinsic NLRP3 inflammasome is present in our Th17 cells and plays a role in IL-1α secretion instead of IL-1β.

Indeed, our observation that the NLRP3 inhibitor, MCC950, reduced IL-1α secretion suggested the potential inflammasome activation in T cells. However, our data shows that inflammasome activation does not rely on the classical downstream executor, caspase-1 (Figures 2.15 B and C). It may be prudent to examine the alternative downstream executor of the activated inflammasome, caspase-8. Several studies have demonstrated that the caspase-8-derived inflammasome occurs in human monocytes or in the absence of caspase-1 (Gaidt et al., 2016; Schneider et al., 2017) and murine Th17 cells (Martin et al., 2016). I also detected a higher level of activated caspase-8 in Th17 cells compared with caspase-1 (Preliminary Data Figure 4A), which might support NLRP3-caspase-8 inflammasome activation. However, as caspase-8 is also important in several cell death pathways (Bossaller et al., 2012), and IL-1α is known to be secreted from dying cells, the interaction between NLRP3 and caspase-8 in T cells might be interesting to investigate.

The target of MCC950 has been shown to directly interact with the NLRP3 NACHT domain, both in its active and inactive states (Coll et al., 2019). Our results show a pronounced upregulation of *NLRP3* gene expression after TGF-β treatment, as well as IL-1β + TGF-β treatment (Figure 2.16A), which has not been reported before in the literature. The NLRP3 protein has not only been identified as a component of the

inflammasome but also acts as a transcription factor, which translocates to the nucleus and regulates T helper cell differentiation (Bruchard et al., 2015). The effect of MCC950 does not exclude the possibility that the conformational changes of NLRP3 might also change its transcriptional factor activities. Together, our results imply that NLRP3 in Th17 cells might act as a component of the inflammasome or a transcription factor, influencing IL-1α secretion.

3.4 Cleavage of IL-1α

3.4.1 The role of calpain

The dominant form of IL-1α that is secreted from Th17 cells is cleaved (~15 kDa) (Figure 2.12), suggesting that the processing of IL-1α takes place before IL-1α secretion. The best-known protease for IL-1α cleavage is calpain (Y Kobayashi, 1990). By inhibiting calpain activity, I detected lower levels of IL-1α, indicating the role of calpain in IL-1α secretion. When I tried to investigate the role of calpain and GSDME in the formation of pores, which leads to the secretion of IL-1α, I was surprised to see that calpain inhibitor induced caspase-3 activation, but not GSDME cleavage (Preliminary Data Figure 3A and B, preliminary data, n=1). This could be because calpain inhibitor induces apoptosis, which is known to be triggered by active caspase-3; therefore, the cell membrane remains intact. On the other hand, caspase-3 is known to cleave GSDME (Rogers et al., 2019; Yu et al., 2019), yet it is still not know to what extent activated caspase-3 contributes to pore formation in the membrane. Section 3.5 will go into more detail about GSDME pore formation in Th17 cells. Here I would like to raise the possibility of another function of calpain in IL-1α secretion; in addition to cleaving pro-IL-1α to make it small enough to exit the pore, it can also control cell apoptosis and pyroptosis, as implied by our results.

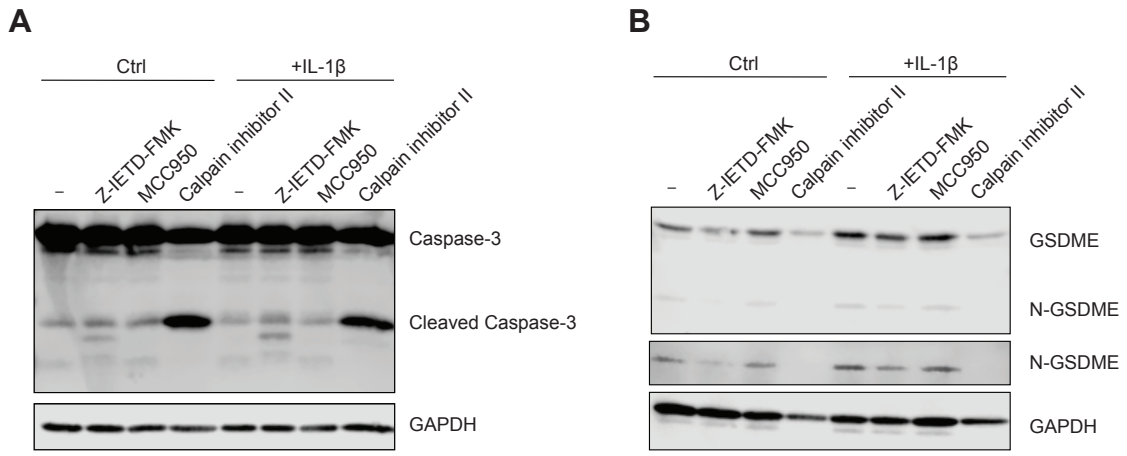

Preliminary Data Figure 3. (A) Immunoblot of caspase-3, (B) GSDME, and GAPDH in Th17 cells treated with or without IL-1β (20 ng/mL) and indicated inhibitors for 5 days.

3.4.2 The role of granzyme B and caspase-5

In addition to a calplain cleavage site, Pro-IL-1α has been shown to be cleaved by granzyme B and the newly discovered caspase-5 (Afonina et al., 2011; Wiggins et al., 2019). The possible involvement of these two proteases is interesting, because a recent publication demonstrated that granzyme B could also cleave GSDME, which suggests another possible mechanism of IL-1α secretion (Zhang et al., 2020). The fact that CD4 T cells can secrete granzyme B was observed in a previous report (L. Lin et al., 2014) and also in our current study (Figure 2.14C). Nonetheless, the loss-of-function assay for granzyme B might be crucial for determining its role, as the inhibitor I used for granzyme B also inhibits caspase-8 activity (Yang, Pemberton, Morrison, & Connelley, 2019).

Caspase-5 and caspase-4 are known to initiate non-canonical inflammasomes and also engage in activation of NLRP3 in human monocytes/macrophages (Casson et al., 2015; Vigano et al., 2015). I also attempted to inhibit caspase-4/5 using Z-LEVD-FMK and found that IL-1α is indeed reduced when caspase-4/5 is inactive (Preliminary Data Figure 4B).

In summary, our results suggest that there is more than one protease that cleaves IL-1α to facilitate its release from cells.

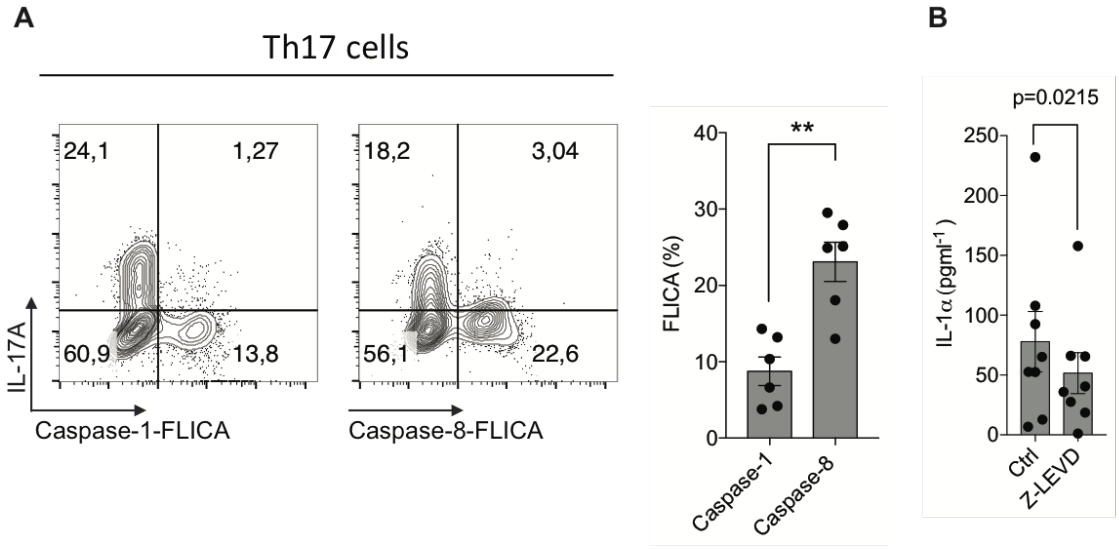

Preliminary Data Figure 4. (A) Isolated Th17 cells were stimulated with anti-CD3 and anti-CD28 5 days, cells were then re-stimulated with PMA plus ionomycin for 5 hours and cytokine-staining and Caspase-FLICA were performed. (n = 6, Mann-Whitney U-test, * $p < 0.05$, ** $p < 0.01$) (B) Isolated Th17 cells were pre-treated with Z-LEVD-FMK (2 μM) for 3 hours and then stimulated with anti-CD3 and anti-CD28 for 2 days and then rested for 3 days. Supernatants were collected on day 5 and analyzed by ELISA. (n = 8, paired Student's t-test).

3.5 The GSDME pore formation

3.5.1 GSDME pores and IL-1α secretion

One of the most striking findings in my thesis is that T cells form GSDME pores upon activation (Figure 2.19B). GSDME belongs to the gasdermin (GSDM) family. Proteins in this family are known to form pores in the cellular membrane or the mitochondrial membrane (Broz, Pelegrin, & Shao, 2020; Liu & Lieberman, 2017). In the GSDM family, the most well-known protein is GSDMD, which we discussed in the Introduction. GSDMD has been known to be cleaved by caspases-1/4/5/8 (Kayagaki et al., 2015;

Sarhan et al., 2018; Shi et al., 2015), which have been shown to be upstream and downstream mediators of NLRP3 activation. I first thought that GSDMD might be the crucial mediator of IL-1α secretion by T cells, based on the previous observation made in myeloid cells (Evavold et al., 2018) and on the data supporting the hypothesis that NLRP3 activation takes place in Th17 cells. Despite evidence of a role for caspase-4/5 and caspase-8 in IL-1α secretion, I could not detect the N-terminal GSDMD in Th17 cells (Figure 2.19B), suggesting that GSDMD pores might not be involved in IL-1α secretion. Nevertheless, I detected full-length GSDMD after cells were activated. Whether the full-length GSDMD is cleaved at some point or what function it may have in Th17 cells is unclear.

The detection of N-GSDME sheds light on how IL-1α can be released from Th17 cells. GSDME protein, which has been known to cause an autosomal dominant form of hearing impairment (de Beeck, Van Laer, & Van Camp, 2012), has recently been studied for its tumor-suppressive role (Rogers et al., 2019; Zhang et al., 2020). These studies demonstrated that tumor cells expressing GSDME pores showed less proliferation and implied that the substances secreted from the pore recruit CD8 T cells and NK cells for tumor cell killing (Zhang et al., 2020). Our results showed that GSDME pores in immune cells may result in IL-1α release and thereby alter their functions. The N-terminal GSDME is inserted into the plasma membrane and can also permeabilize the mitochondrial membrane and augment inflammasome activation (Rogers et al., 2019); therefore, it might be interesting to check the pore-forming sites in the cells.

3.5.2 Regulation of GSDME expression in Th17 cells.

Our transcriptomic data show that GSDME gene expression is significantly upregulated when Th17 cells receive IL-1β signals (Figure 2.15G). The protein expression levels also showed the same trend (Figures 2.19 B and C, Figure S3B). This implies that IL-1β not only induces GSDME gene expression, but also promotes its cleavage; data that correlate with the higher IL-1α secretion in the IL-1β treated group (Figures 2.3H and 2.15B). Moreover, Z-IETD-FMK or MCC950, which lowered

IL-1α secretion (Figures 2.14F and 2.15D), also decreased the levels of N-terminal GSDME expression (Preliminary Data Figure 3B). These data indicate a correlation between IL-1α secretion and GSDME pore formation, yet, I observed a discrepancy in the TGF-β treated group, in which I saw low IL-1α secretion but higher levels of N-terminal GSDME (Preliminary Data Figure 1A and Figure 2.19C). I speculate that this could be due to the inhibitory effect of IL1R2, as discussed in section 3.2.

Caspase-3 was once thought to be the only protease to cleave GSDME; however, a recent publication by Zhang et al. suggested that another protease, granzyme B, also has a cleavage site in GSDME (Zhang et al., 2020). Our finding that a caspase-3 inhibitor had no effect on GSDME cleavage supports the idea that cleavage of GSDME proceeds through a caspase-3 independent mechanism (Figure 2.20D). Whether it is through granzyme B or another protease, demands more investigation. Compared to GSDMD, the cleavage and regulation of GSDME has been studied less, and more research should be conducted into its tumor-suppressive role.

3.6 Cell death and IL-1α secretion

IL-1α secretion is often linked to cell death, as discussed in the section 1.3.4. and as shown in our findings that activated T cells are able to secrete IL-1α (Figure 2.10), suggesting the likely occurrence of activation-induced cell death (AICD). During an immune response and after clonal expansion, ACID has been found to participate in controlling the number of proliferating T cells in the contraction phase (Brenner, Krammer, & Arnold, 2008). Under this concept, programmed cell death (apoptosis) should take place to shut-down the immune response. Different forms of cell death might give rise to diverse clearance outcomes. Apoptosis has been assumed to be silent because it does not trigger an inflammatory response. In the Gene Set Enriched Analysis (GSEA), I found that some apoptosis genes were enriched in the IL-1β-treated group (upregulation of *BAX* and downregulation of *BCL2L1* (Figure 2.21D). In contrast, key caspases involved in apoptosis were not detected, and a caspase-3 inhibitor did not influence IL-1α secretion (Figure 2.20A), which implied there might be an atypical

apoptosis pathway controlling the IL-1α secretion. The GSDME pores support the idea that Th17 cells might start to lose their membrane integrity after they are stimulated, and they are known to convert non-inflammatory apoptosis to pyroptosis. Our results support the idea that pyroptosis takes place in Th17 cells while they secrete IL-1α.

I also performed several classical cell-death assays to determine if the cells were undergoing apoptosis. However, compared to monocytes, which showed lower ATP levels and higher LDH levels upon NLRP3 activation, human CD4 T cells showed similar levels of ATP and LDH in the control and the IL-1β-treated group, implying that cell viability was comparable (Preliminary Data Figure 5). I propose that the secreting cells make up a very small proportion and determining the cell death issues with bulk populations may underrate the phenomenon at the single-cell scale. Single-cell-based and real-time detection methods are required to better characterize cell death upon IL-1α secretion, which I will discuss in section 3.6.2.

Necroptosis is another well-known type of programmed cell death and is also triggered by external death receptors (TNF, Fas, TRAIL and TLR) and occurs when caspase activity, required for apoptosis, is impeded (Kearney & Martin, 2017). Necroptosis is considered as a pro-phase for the initiation of pro-inflammatory responses because it triggers the release of several danger signals. I also examined the role of necroptosis in IL-1α secretion by adding a necroptosis inhibitor, Necrostatin-1, and found that necroptosis does not affect the secretion of IL-1α (Figure 2.23), although some necroptosis-related genes were found to be upregulated in the KEGG pathway analysis (Figure 2.23).

3.6.1 Death receptors and the role of IL-1α secretion

AICD can involve the engagement of death receptors, such as CD95 (Apo-1/Fas) and the TNF-α receptor. I also observed the upregulation of several death receptor genes in IL-1α-high producing clones (Figure 2.21A). Furthermore, TNF-α does not participates in regulating IL-1α secretion (Figure 2.22A); therefore, it would be interesting to determine the role of Fas.

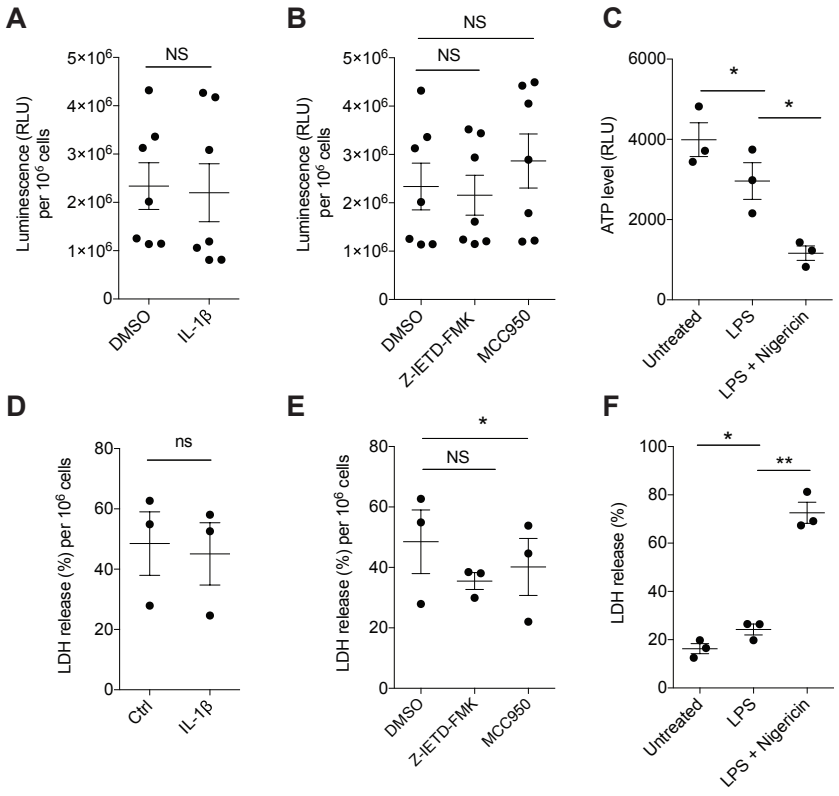

Preliminary Data Figure 5. (A and B) CD4 memory cells were isolated and pretreated with Z-IETD-FMK (20 μM) or MCC950 (10 μM) inhibitor for 3 hours and then stimulated with anti-CD3 and anti-CD28 for 5 days. Cells were collected on day 5 and the ATP-assay was performed. Readout was normalized against cell numbers (n = 7, paired Student's t-test, NS, not significant, * $p < 0.05$). (D and E) Supernatants were collected and an LDH assay was performed. Readout was normalized with cell numbers (n = 3, paired Student's t-test). (C and F) CD14 monocytes were used as control and stimulated with LPS and LPS+Nigericin (n = 3, paired Student's t-test, * $p < 0.05$, ** $p < 0.01$).

3.6.2 Cell viability upon IL-1α secretion

Determining the cell viability will provide further information, such as whether the cells are still alive upon IL-1α secretion, which could be a mechanism that is exclusively observed in human T cells; this could also mean that IL-1α is part of a cytokine profile belonging to pro-inflammatory Th17 cells. On the other hand, if cells die upon secretion, that would denote T cell response suppression, and may indicate that cells die via pyroptosis.

Nevertheless, several difficulties arise when applying the commonly used cell-death indicators to lymphocytes. For example, the IL-1α secretion process in T cells is long (> 48 hours) compared with monocytes, which takes no longer then 24 hours. Additionally, the proliferation rate of T cells is much higher than that of monocytes, which means that growing T cells might mask the dying cells and cause misinterpretation. With these problems, we must address the question at the single-cell level.

In order to resolve these problems, I cloned single IL-1α-producing or non-producing T cells. The growth of the clones from single cells indicates T cell viability. By performing experiment, I successfully established a correlation between cell viability and IL-1α (Figure 2.24A). Meanwhile, I also observed that the re-clone efficiency from IL-1α non-producing clones was low (~25%), which means there might be some room for technical improvements. To make a solid conclusion, I expected the low-level producing clones to reach a clone efficiency of greater than 80%.

Nevertheless, the negative correlation between cytokine secretion and clone efficiency was only observed for IL-1α, not for IFN-γ or IL-17A, suggesting that IL-1α secretion affects T cells proliferation (Figure 2.24). One more strategy that could be carried out in our study is a live-imaging system. By detecting real-time images with secretion of IL-1α could provide us with direct evidence of cell viability upon IL-1α secretion. This technique, together with nucleic acid staining, has been used in monocytes and

showed IL-1β secretion dynamics (Shirasaki et al., 2014), thereby allowing the simultaneous assessment of the real-time cell status and cytokine secretion.

3.7 Pathological role of IL-1α in autoinflammatory syndromes

Our previous publication demonstrated that IL-10 production from Th17 cells was diminished in Schnitzler syndrome patients (Noster et al., 2016). Now, with evidence that IL-1α production takes place in pro-inflammatory Th17 cells, we would like to determine whether IL-1α producing Th17 cells contribute to the pathogenesis of autoinflammatory syndromes. Indeed, we found an autocrine feedback loop for IL-1α in Th17 cells (Figure 2.25B), and blocking IL-1α significantly restored IL-10 production in Th17 cells (Figure 2.25D). These results support that IL-1α from TH17 cells might be a pathogenic cytokine in disease settings. After IL-1 blockade therapies, we also observed a decrease in IL-1α production levels, along with alleviated symptoms (Figure 2.26). It would be interesting to study other autoinflammatory syndromes, as the role of IL-1α in human Th17 cells has been overlooked for a long time.

3.8 Final evaluation and outlook

Once thought of as innate alarmin, IL-1α has now been shown, in our studies, to have a role in the human adaptive immune system. I attempted to dissect the regulation of IL-1α production in T cells; I found that it is co-regulated with the Th17 program and is produced primarily in Th17 cells. I also showed that TCR signaling is required for IL-1α production in T cells, and the innate immune machinery of the inflammasome might have a role in its production, although how it regulates the release of IL-1α remains elusive. However, IL-1α secretion from Th17 cells increases their pro-inflammatory properties, as evidenced by the upregulation of several pro-inflammatory cytokines, such as IL-1α itself, IFN-γ, and IL-17A. IL-1α secretion also hindered the production of the anti-inflammatory cytokine IL-10. Strikingly, GSDME pores, which have never been detected in T cells before, also contribute to IL-1α secretion, raising several questions for future outlooks. Other questions that might be interesting to follow up on are: Do

GSDME pores contribute to cell death in Th17 cells after they facilitate IL-1α release from Th17 cells? Do GSDME pores take part in the pathogenic role of Th17 cells? If so, would blocking the GSDME pores be a potential target for clinical applications? The representative scheme shows a summary of my results and illustrates further potential mechanisms.

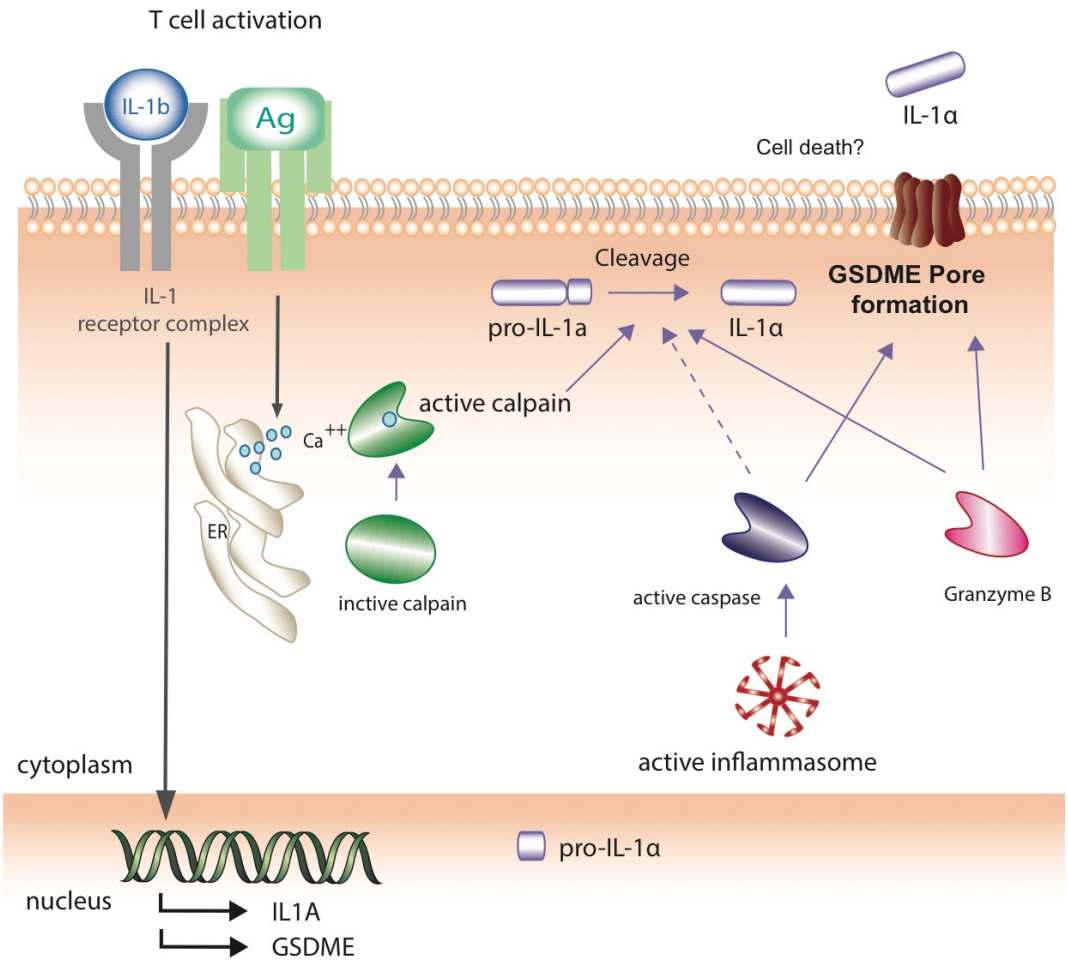

Summary Figure. TCR signaling is required for IL-1α production in T cells, whereas IL-1 signaling promotes GSDME protein expression. The expression of GSDME protein is then available for further cleavage and facilitates IL-1α release. NLRP3-inflammasome activation may help the secretion of IL-1α; however, the downstream mechanism remains elusive.

4 Materials and Methods

4.1 Materials

4.1.1 Chemicals and reagents

Name	Source	Identifier
10x Tris/Glycine Buffer	Bio-Rad	Cat#1610771
2-Mercaptoethanol (50 mM)	ThermoFisher Scientific	Cat#31350010
40% Acylamide/Bis Solution	Bio-Rad	Cat#1610144
4x Laemmli Sample Buffer	Bio-Rad	Cat#1610747
Accell Human DFNA5 (1687) siRNA, SMARTpool, 5 nmol	Dharmacon	Cat#E-011844-00-0005
Accell siRNA Delivery Media, 100 mL	Dharmacon	Cat#B-005000-100
Anti-Sodium Potassium ATPase antibody [EP1845Y] - Plasma Membrane Loading Control (ab76020)	Abcam	Cat#ab76020
ATP Solution (100mM)	ThermoFisher Scientific	Cat#R0441
Biocoll (1,077 g/mL)	Biochrom	Cat#L6115
Bovine Serum Albumin (BSA)	Sigma-Aldrich	Cat#A4612-100G
Brefeldin A	Sigma-Aldrich	Cat#B7651-5MG
CD3 (human) monoclonal antibody (TR66)	enzolifesciences	Cat#ALX-804-822-C100
Chloroform	Merck	Cat#1.02445

CountBright Absoulute Counting Beads	ThermoFisher Scientific	Cat#C36950
Dulbecco's Phosphate Buffered Saline, modified, without $MgCl_2$ and $CaCl_2$	Sigma-Aldrich	Cat#D8537-500ML
Dulbecco's Phosphate Buffered Saline, with $MgCl_2$ and $CaCl_2$	Sigma-Aldrich	Cat#D8662-500ML
Ethanol, absolute for analysis EMSURE® ACS,ISO,Reag. Ph Eur	Merck	Cat#1.00983
Fetal bovine serum	Biochrom	Cat#S0015
GlutaMAX™ Supplement	ThermoFisher Scientific	Cat#35050061
Glycine	Roth	Cat#3187.4
Human serum	Sigma-Aldrich	Cat#H6914-100ML
Ionomycin	Sigma-Aldrich	Cat#I0634-1MG
LPS-EB Ultrapure (E. coli O111:B4)	Invivogen	Cat#tlrl-3pelps
MEM Non-Essential Amino Acids Solution (100X)	ThermoFisher Scientific	Cat#11140050
Methanol	Merck Millipore	Cat#1060092511
Milk powder	Roth	Cat#T145.3
Nigericin, sodium salt	Invivogen	Cat#28643-80-3
Nuclease-free water	Qiagen	Cat#129114

PageRuler Prestained Protein Ladder, 10 to 180 kDa	ThermoFisher Scientific	Cat#26616
Penicillin/Streptomycin	Biochrom	Cat#A2212
Phorbol 12-myristate 13-acetate	Sigma-Aldrich	Cat#P8139-5MG
Purified NA/LE Mouse Anti-Human CD28	BD Pharmingen™	Cat#555725
RPMI 1640 Medium w/o glutamine	ThermoFisher	Cat#31870074
RPMI 1640 Medium with 20mM HEPES	Biochrom	Cat#F1235
Sodium Chloride	Sigma-Aldrich	Cat#746398-1KG
Sodium Pyruvate (100 mM)	ThermoFisher Scientific	Cat#11360070
Streptavidin Conjuction Kit	Abcam	Cat#ab102921
Sulfo-NHS-LC-Biotin	Abcam	Cat#ab145611
TEMED	Bio-Rad	Cat#1610800
Thermo Scientific™ Remel™ PHA Purified	ThermoFisher Scientific	Cat#10082333
Tris-base	Sigma-Aldrich	Cat#T1503-5KG
TRIzolTM Reagent	Invitrogen	Cat#1559602
Tween® 20	Roth	Cat#9127.2
PhosSTOP EASYpack	Roche	Cat#04906837001
cOmplete Tablets, Mini EDTA-free, EASYpack	Roche	Cat#04693159001

4.1.2 Oligonucleotides

Name	Source	Identifier
Taqman Assay IL1A	Thermo Fisher	HS00174092-m1
Taqman Assay IL1B	Thermo Fisher	Hs01555410_m1
Taqman Assay PYCARD	Thermo Fisher	Hs01547324_gH
Taqman Assay NLRP3	Thermo Fisher	Hs00918082_m1
Taqman Assay CASP1	Thermo Fisher	Hs00354836_m1
Taqman Assay IL1R2	Thermo Fisher	Hs00174759_m1
Taqman Assay CAPN2	Thermo Fisher	Hs00965097_m1
Taqman Assay GSDMD	Thermo Fisher	Hs00986739_g1
Taqman Assay CASP4	Thermo Fisher	Hs01031951_m1
Taqman Assay RORC	Thermo Fisher	Hs01076122_m1
Taqman Assay IL10	Thermo Fisher	Hs00961622 _m1
Taqman Assay 18S	Thermo Fisher	Hs03928990_g1

4.1.3 Cytokines and neutralizing Antibodies

Name	Working concentration	Source	Identifier
Human IL-1β	20 ng/mL	R&D	Cat#201-LB
Human IL-1α	20 ng/mL	Miltenyi biotec	Cat#130-093-893
Human TGF-β	20 ng/mL	R&D	Cat#240-B

Human IL-4	10 ng/mL	Miltenyi biotec	Cat#130-093-919
Human IL-12	8 ng/mL	R&D	Cat#219-IL
Human IL-6	50 ng/mLl	Miltenyi biotec	Cat#130-095-352
Human IL-23	50 ng/mL	R&D	Cat#1290-IL
Human IL-2	500 Unit	produced in cell culture in house	-
anti-IL1-α	10 µg/mL	R&D	Cat#NF-200NA
anti-TNF-α	5 µg/mL	R&D	Cat#MAB610

4.1.4 Inhibitors

Name	Source	Identifier
Ac-YVAD-cmk	Sigma-Aldrich	Cat#SML0429-1MG
Calpain Inhibitor I	Sigma-Aldrich	Cat#A6185-5MG
Calpain inhibitor II	Sigma-Aldrich	Cat#A6060 SIGMA
Caspase-3 Inhibitor Z-DEVD-FMK	R&D Systems	Cat#FMK004
Necrostatin-1	Tocris a biotechne brand	Cat#4311-88-0
STAT5 inhibitor	Calbiochem	Cat#573108
Z-IETD-FMK	R&D systems	Cat#FMK007
Z-YVAD-FMK (10mM)	Enzo Life Sciences	Cat#ALX-260-154- R020

N-Acetyl-L-cysteine,cell culture tested, BioReagent	Sigma-Aldrich	Cat#A9165-5G
MCC950	Sigma Aldrich	Cat#PZ0280-5MG
Z-LEVD-FMK Casp4/5 inhibitor	enzolifesciences	Cat#ALX-260-142
GSK2981278	Cayman	Cat#20974
Z-VAD-FMK	enzolifesciences	Cat#ALX-260-020-M001

4.1.5 Critical commercial assays

Name	Source	Identifier
Western Blotting Kit V RD (TBS/PVDF)	LI-COR Biosciences	Cat#926-35010
Plasma Membrane Protein Extraction Kit	Abcam	Cat#ab65400
High Capacity cDNA Reverse Transcription Kits	Applied Biosystems	Cat#4368814
Calpain Activity Assay Kit	Abcam	Cat#ab65308
FAM-FLICA caspase-1,4,5 assays	ImmunoChemistry technologies	Cat#98
FAM-FLICA caspase-8 assays	ImmunoChemistry technologies	Cat#910
Fixation/Permeabilization Solution Kit	BD Biosciences	Cat#554714
Human Caspase-1 SimpleStep ELISA Kit	Abcam	Cat#ab219633
Human IL-1 alpha/IL-1F1 DuoSet ELISA	R&D Systems	Cat#DY200
Human IL-1 beta/IL-1F2 DuoSet ELISA	R&D Systems	Cat#DY201-05

Human Granzyme B Duoset ELISA	R&D Systems	Cat#DY2906-05
Human IL-10 Duoset ELISA	R&D Systems	Cat#DY217B-05
Human IL-17 Duoset ELISA	R&D Systems	Cat#DY317-05
Human IFN-γ Duoset ELISA	R&D Systems	Cat#DY285-05
Human IL-1α ELISpot BASIC (ALP)	Mabtech	Cat#3414-2A
Pierce BCA Protein Assay Kit	ThermoFisher Scientific	Cat#23225
Zombie AquaTM Fixable Viability Kit	BioLegend	Cat#423101
Zombie YellowTM Fixable Viability Kit	BioLegend	Cat#423103

4.1.6 Antibodies

Magnetic beads		
Name	**Source**	**Identifier**
CD14 Microbeads, human	Miltenyi Biotec	Cat#130-050-201
CD4 Microbeads, human	Miltenyi Biotec	Cat#130-045-101
CD8 Microbeads, human	Miltenyi Biotec	Cat#130-045-201

Western blot antibodies			
Name	**Dilution**	**Source**	**Identifier**
Anti-rabbit IgG, HRP linked Antibody	1:1000 1:5000	Cell signaling	Cat#7074S

	(β-Action or GADPH)		
Anti-Glyceraldehyde-3-Phosphate Dehydrogenase Antibody	1:1000	Sigma-Aldrich	Cat#MAB374
Caspase-1 Antibody	1:1000	Cell signaling	Cat#2225
Caspase-3 Antibody	1:1000	Cell signaling	Cat#9662
Caspase-8 Mouse mAb	1:1000	Cell signaling	Cat#9746
DFNA5/GSDME antibody [EPR19859] -N-terminal	1:1000	Abcam	Cat#ab215191
Gasdermin D Antibody	1:1000	Cell signaling	Cat#96458
IL-1 alpha antibody	1:1000	Abcam	Cat#ab134908
IRDye® 680RD Goat anti-Rabbit IgG Secondary Antibody	1:1000	LI-COR	Cat#926-68071
IRDye® 800CW Goat anti-Mouse IgG Secondary Antibody	1:1000	LI-COR	Cat#926-32210
β-Actin (13E5) Rabbit mAb	1:2000	Cell signaling	Cat#4970S

Flow antibodies			
Name	**Dilution**	**Source**	**Identifier**
Alexa Fluor® 488 Mouse Anti-Human CD183	1:20	BD	Cat#558047
Alexa Fluor® 647 anti-human CD127 (IL-7Rα)	1:50	Biolegend	Cat#351318

Antibody			
Alexa Fluor® 647 anti-human IL-17A Antibody	1:100	Biolegend	Cat#512310
Alexa Fluor® 647 anti-human IL-1β Antibody	1:50	Biolegend	Cat#508207
APC Mouse Anti-Human CD183	1:10	BD	Cat#550967
APC/Cyanine7 anti-human CD4 Antibody	1:300	Biolegend	Cat#317418
APC/Cyanine7 anti-human IFN-γ Antibody	1:100	Biolegend	Cat#502530
Brilliant Violet 421™ anti-human CD196 (CCR6) Antibody	1:100	Biolegend	Cat#353408
Brilliant Violet 421™ anti-human CD25 Antibody	1:100	Biolegend	Cat#302630
Brilliant Violet 650™ anti-human CD45RA Antibody	1:50	Biolegend	Cat#304136
FITC anti-human CD45RA Antibody	1:100	Biolegend	Cat#304106
FITC anti-human IL-1β Antibody	1:50	Biolegend	Cat#508206
FITC anti-human IL-4 Antibody	1:600	Biolegend	Cat#500807
FITC anti-human IL-8 Antibody	1:50	Biolegend	Cat#514604
IL-1 alpha Monoclonal Antibody (364/3B3-14), FITC, eBioscience™	1:50	eBioscience	Cat#11-7118-82
IL-1α Antibody, anti-human, APC	1:50	Miltenyi	Cat#130-109-227
Pacific Blue™ anti-human CD14 Antibody	1:200	Biolegend	Cat#325616
Pacific Blue™ anti-human CD8 Antibody	1:200	Biolegend	Cat#344718

Pacific Blue™ anti-human IL-17A Antibody	1:300	Biolegend	Cat#512311
PE anti-human CD197 (CCR7) Antibody	1:50	Biolegend	Cat#353203
PE anti-human IL-1α Antibody	1:50	Biolegend	Cat#500106
PE/Cyanine7 anti-human IL-10 Antibody	1:50	Biolegend	Cat#501420
PerCP anti-human CD14 Antibody	1:100	Biolegend	Cat#325632
PerCP/Cyanine5.5 anti-human CD8a Antibody	1:100	Biolegend	Cat#301032

4.1.7 Medium and Buffers

Buffer	Composition
Cloning medium	RPMI 1640 Medium with Sodium-bicarbonate without Hepes
	5% human serum
	1% GlutaMAX™ Supplement (100X)
	1% MEM Non-Essential Amino Acids Solution (100X)
	0.1% 2-Mercaptoethanol
	500 units IL-2
	1% Sodium Pyruvate (100 mM)
	1%Penicillin/Streptomycin
Complete medium	RPMI 1640 Medium with Sodium-bicarbonate without Hepes
	10% FBS

	1% GlutaMAX™ Supplement
	1% MEM Non-Essential Amino Acids Solution (100X)
	0.1% 2-Mercaptoethanol
	1% Sodium Pyruvate (100 mM)
	1%Penicillin/Streptomycin
Culture medium for monocytes	RPMI 1640 Medium with Sodium-bicarbonate without Hepes
	10% FBS (heat-inactivated at 56°C for 30 min)
	1% Penicillin/Streptomycin
Wash buffer	RPMI1640 with HEPES
	1% FCS
MACS buffer	DPBS w/o $MgCl_2$ and $CaCl_2$ 1%FCS
	2mM EDTA
ELISA reagent diluent	DPBS
	1% BSA
	pH adjusted to 7,2 – 7,4 filtered (0.2 µm)
ELISA wash buffer	DPBS
	0.05% Tween®20
	pH adjusted to 7,2 – 7,4
TBST (10x)	80 g NaCl

	24.2 g Tris-base
	10 mL Tween® 20
	in 1000 mL ddH_2O
Medium for monocytes	RPMI 1640 Medium w/o glutamine
	1% FBS (heat-inactivated at 56°C for 30min)
Western blot transfer buffer (10x)	30.33 g Tris-base
	144 g Glycine
	in 1000 mL ddH2O
	1x buffer supplied with 10% Methanol
RIPA buffer	Tris-HCl pH7.6
	NaCl 150 mM
	1% TritonX-100
	0.1%SDS
	0.5% Sodium Deoxycholate

4.1.8 Consumables

Name	Source	Identifier
Falcon® 12-well Clear Flat Bottom TC-treated Multiwell Cell Culture Plate	Falcon	Cat#353043
15mL tubes	Greiner-Bio-one	Cat#188271

Falcon® 24-well Clear Flat Bottom TC-treated Multiwell Cell Culture Plate	Falcon	Cat#353047
50mL tubes	Greiner Bio-one	Cat#227261
Falcon® 96-well Clear Round Bottom TC-treated Cell Culture Microplate	Falcon	Cat#353077
Cell strainer, 70µM	Omnilab	Cat#FALC352350
Corning® 384 well plates	Sigma-Aldrich	Cat#CLS3701-100EA
Falcon Round-Bottom tubes	BD Biosciences	Cat#352054
Half area microplates	Greiner Bio-one	Cat#675061
Immun-Blot® PVDF Membrane	Bio-Rad	Cat#1620177
Nunc MaxiSorpTM flat-bottom 96 well plate	ThermoFisher Scientific	Cat#44-2404-21
Pipette tips, 10µl	Sarstedt	Cat#70.113
Pipette tips, 1000µl	Sarstedt	Cat#70.762
Pipette tips, 200µl	Sarstedt	Cat#70.760.502
Reaction tubes, 0.5mL	Omnilab	Cat#5283547
Reaction tubes, 1.5mL	Omnilab	Cat#5283548
Reaction tubes, 2mL	Omnilab	Cat#5283549
Serological pipettes, 10mL	Greiner-Bio-one	Cat#607160

Serological pipettes, 25mL	Greiner-Bio-one	Cat#760160
Serological pipettes, 2mL	Greiner-Bio-one	Cat#710160
Serological pipettes, 5mL	Greiner-Bio-one	Cat#606160
Sterile filters, 500mL, 0,22µm, PES)	Omnilab	Cat#CORN431097
Microcentrifuge tubes, protein LoBind / DNA LoBind	Eppendorf	Cat#525-0130
Western blotting filter paper	ThermoFisher Scientific	Cat#88600
Filter Tip 20µl	Sarstedt	Cat#70.760.213
Biosphere® LowRet FilTip 200	Sarstedt	Cat#70.760.216
Biosphere® LowRet FilTip 1000	Sarstedt	Cat#70.762.216

4.1.9 Devices

Instrument	Supplier
Centrifuge 5427R	Eppendorf
Centrifuge 5810R	Eppendorf
Centrifuge 5424 R	Eppendorf
Infinite® M Nano plate reader	Tecan
The BD FACSAria™ III sorter	BD Biosciences
Pipette, 0,5-10µl	Gilson
Pipette, 100-1000µl	Gilson

Pipette, 20-200µl	Gilson
Pipetting controller	Integra
Thermomixer compact	Eppendorf
LightCycler® 480 II	Roche
MACS separator	Miltenyi
CLARIOstar multi-mode microplate reader	BMG Labtech
NanoPhotometer® N60/N50	Implen
Odyssey® Fc Imaging System	LI-COR
BD FACSAriaTM Fusion	BD Biosciences
Mini-PROTEAN Tetra Vertical Electrophoresis Cell	Bio-rad
PowerPac Power Supplies	Bio-rad

4.1.10 Software

Name	Supplier
Flowjo version 10.6.2	Treestar
Prism 7	Graphpad Software, Inc.
Image Studio Lite	LI-COR

4.2 Methods

4.2.1 PBMC isolation

4.2.1.1 PBMC isolation from fresh blood

Peripheral blood was collected into a vacutainer containing heparin (0.1 ml for 50 ml blood) and diluted 1:1 with PBS. 35 ml of diluted blood was carefully layered on top of 12 ml Biocoll separating solution (density 1.077 g/ml) in a 50 ml falcon tube and centrifuged (805 rcf, 30 min, RT, no brake). The PBMC fraction was enriched within the white ring between plasma and Biocoll layers. The cell ring was then transferred into a new 50 ml falcon tube and filled up to 50 ml with MACS buffer. After the centrifugation, cells were washed twice with wash buffer and used for downstream applications.

4.2.1.2 PBMC isolation from blood cones

Cones were carefully cut from the top and bottom of the tube, in order to let the blood out of the cones and subsequently dilute it 1:10 with PBS. Loading of the blood onto the Biocoll solution followed the same procedure as described above for PBMC isolation from fresh blood.

4.2.2 Cell sorting

4.2.2.1 Magnetic-activated cell sorting

Isolated PBMCs were incubated with 200 µl microbeads per total PBMCs isolated from 500 ml fresh blood. Cells went through a cell strainer (70 µm) and were placed in AutoMACS and sorted in the positive selection mode. Positive fractions were washed with MACS buffer and used for downstream applications.

4.2.2.2 Fluorescence-activated cell sorting

Isolated PBMCs or cells obtained from a MACS sort were stained with different combinations of fluorochrome-conjugated antibodies (see staining panels). Zombie

dye was used to exclude dead cells if needed. For surface staining, cells were stained on ice for 30 mins and washed with MACS buffer and sorted on a BD FACSAria™ III sorter, BD FACSAria™ Fusion or BD FACSMelody™.

4.2.2.3 Sorting strategy for Th subsets

Naive T cells were sorted as $CD14^{-}CD8^{-}CD45RA^{+}$, whereas $CD45RA^{-}CD14^{-}CD8^{-}$ memory T cell subsets were sorted according to the differential expression of CXCR3, CCR4 and CCR6. Treg cells were sorted as $CD14^{-}CD8^{-}CD4^{+}CD25^{hi}CD127^{-}$ as illustrated in Figure 4.2, and Th1, Th2 and Th17 cells were sorted as indicated in Figures 4.1 and 4.2.

Table 1. Staining panel for Naïve, Th1, Th2 and Th17 sorting

Antibody	Fluorophore	Dilution
anti-CD45RA	FITC	1:100
anti-CD4	APC-Cy7	1:300
anti-CD8	Pacific Blue	1:200
anti-CD14	Pacific Blue	1:200
anti-CCR4	PE-Cy7	1:200
anti-CCR6	PE	1:50
anti-CXCR3	APC	1:30

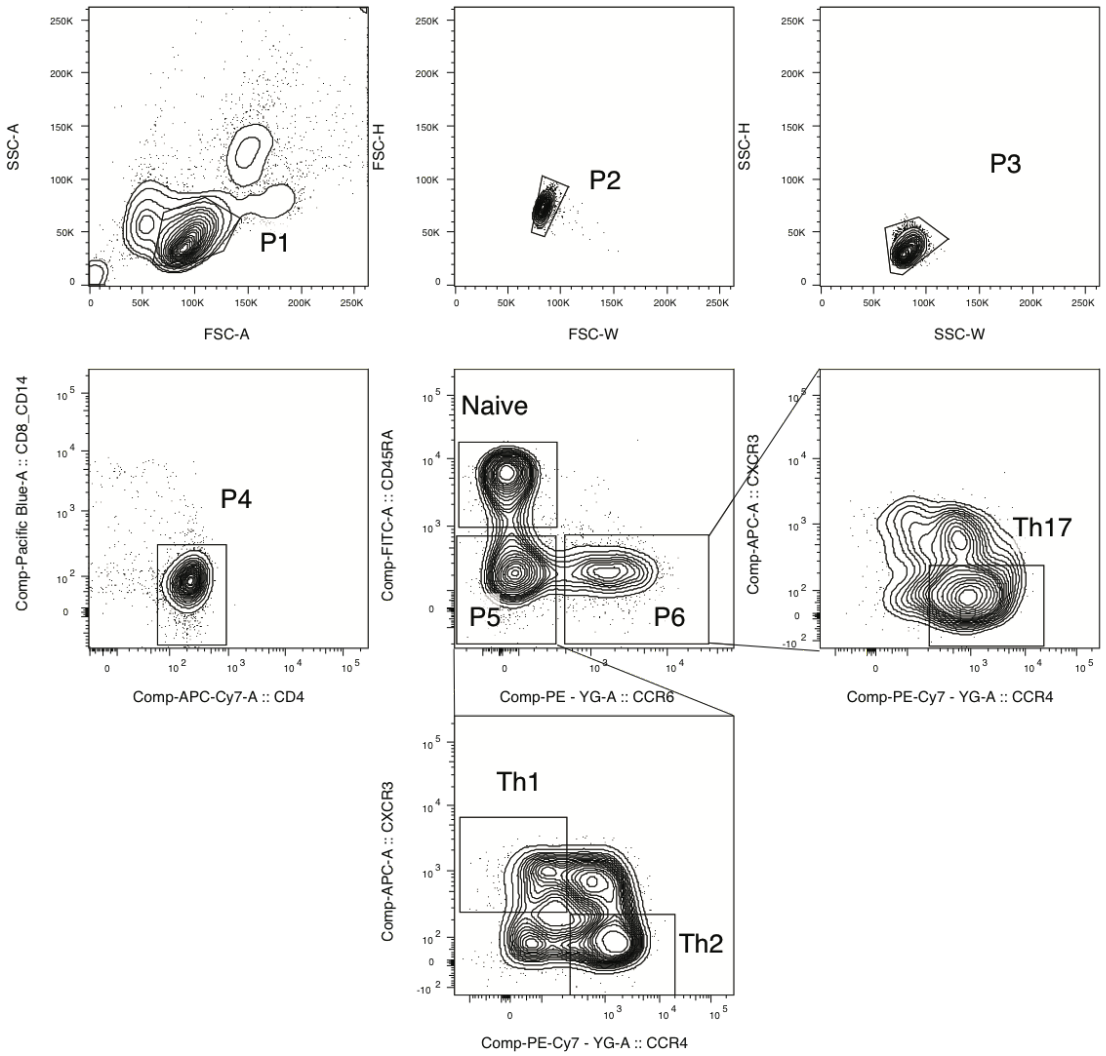

Figure 4. 1.Gating strategy for Naïve CD4 Tcells, Th1, Th2 and Th17 subsets

Table 2. Staining panel for chemokine receptors sorting.

Antibody	Fluorophore	Dilution
anti-CD45RA	FITC	1:100
anti-CD14	PerCP	1:100
anti-CCR7	PE	1:50
anti-CCR4	PE-Cy7	1:200

anti-CCR6	BV421	1:100
anti-CXCR3	APC	1:30

Table 3. Staining panel for Th1, Th2, Th17 and Treg sorting

Antibody	Fluorophore	Dilution
anti-CD45RA	BV650	1:50
anti-CD4	APC-Cy7	1:300
anti-CD8	PerCP	1:100
anti-CD14	PerCP	1:100
anti-CCR4	PE-Cy7	1:200
anti-CCR6	PE	1:50
anti-CXCR3	AF488	1:20
anti-CD25	BV421	1:100
anti-CD127	AF647	1:50

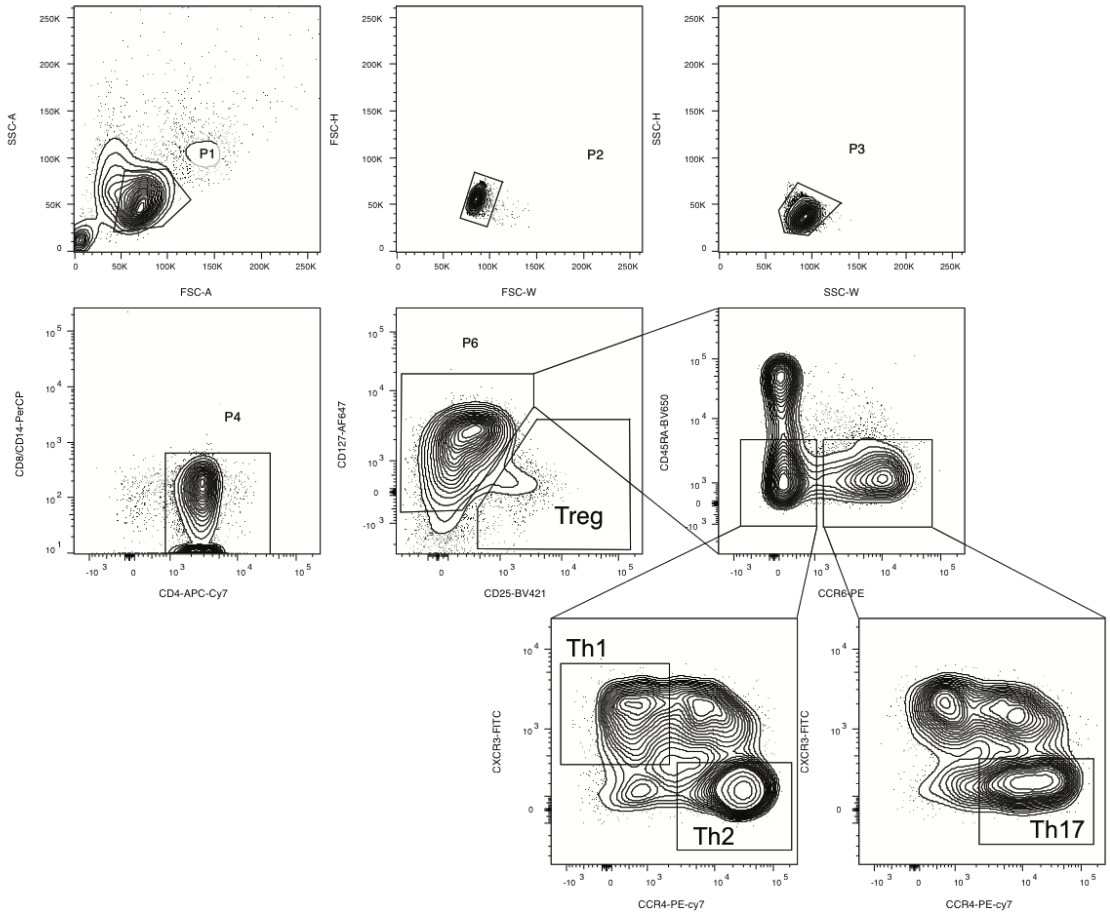

Figure 4. 2 Gating strategy for Treg, Th1, Th2 and Th17 subsets

4.2.3 Cell culture

4.2.3.1 In vitro Monocyte stimulation

Human monocytes were incubated with or without inhibitors for 3 hours and then cultured with or without 1 μg/mL ultrapure LPS-EB (tlrl-3pelps, Invivogen) for 24 hours and Nigericin (10 μg/mL) or ATP (5 mM) or 30 mins.

4.2.3.2 In vitro expansion and stimulation of T cells

96-well MicroWell™ MaxiSorp™ flat bottom plates were coated with anti-CD3 and anti-CD28 antibodies (at the indicated concentrations diluted in PBS and incubated overnight at 4°C). Before the addition of cells, the wells were washed twice with wash buffer. Freshly isolated T cells (5 x 10^4 cell/well) were seeded onto the plate. The desired cytokines (see table 4.1.3) were prepared as 10 times concentration and added immediately at 1/10 of the final volume on top of the culture medium with T cells. After 48 hours incubation, cells were then transferred to 96 well u-bottom well plates and cultured for 3 more days before FACS analysis.

4.2.3.3 T cell cloning

Cells of the purified Th subsets were counted and diluted to 200 cells/mL by 1:10 serial dilution. The 1 ml of final dilution were added to irradiated allogenic PBMC (2 x 10^7) and PHA in cloning medium. Cells with irradiated feeder PMBC were seeded onto 384 well plates with 50 µL/well. Plates were incubated at 37 °C, 5% CO_2 for at least 10 days.

4.2.3.4 Inhibitor treatments

Isolated T cells were seeded at 5 x 10^4 in 200 µl of complete RPMI1640 medium with 10% FCS and containing inhibitors dissolved in DMSO. Cells were incubated for 3 hours (at 37 °C, 5% CO_2), and stimulated for a total culture period of 5 days with anti-CD3 and anti-CD28 monoclonal antibody (plate-bound) for 48 hours.

4.2.4 Flow cytometry analysis

4.2.4.1 Zombie dye live/dead staining

Cells were collected at the end point of incubation and washed with PBS to remove protein and then resuspended in Zombie dye diluted in PBS (1:300) and incubated on ice for 20 min. Cells were then washed once with PBS and once with MACS buffer,

followed by surface staining or intracellular staining, depending on the experimental design.

4.2.4.2 Absolute cell counting beads

CountBrightTM absolute counting beads (Thermo Fisher Scientific) was resuspended completely and added to the cells at the end point of incubation (beads number varies with batch). At least 5 µL of beads mix was added to fulfill the criteria for correct counting (collected beads counts must exceed 1000), absolute cells numbers were calculated as follows:

$\frac{A}{B} \times \frac{C}{D}$ = concentration of sample as cells/µL

A= number of cell events

B= number of bead events

C= bead count of the lot (beads/50 µL)

D=volume of sample (µL)

4.2.4.3 Surface staining

Expression makers on human T cells were determined by FACS analysis. Cells were stained with specific anti-human Abs conjugated with fluorochromes (see tables in section 4.2.2.3) diluted in MACS Buffer and incubated on ice for 30 mins.

4.2.4.4 Intracellular cytokine staining

Human T cells were restimulated for 5 hours with phorbol 12-myristate 13-acetate (PMA) and ionomycin in the presence of brefeldin A (all from Sigma-Aldrich) for the final 2.5 hours of culture. Cells were fixed and permeabilized with Cytofix/Cytoperm, and Perm/Wash buffer according to the manufacturer's instructions (BD Biosciences).

Cells were stained with anti-human Abs conjugated with fluorochromes (see table 4.1.5), diluted in Perm/Wash buffer for 30 mins on ice and analyzed by flow cytometry.

4.2.4.5 FAM FLICA staining

The FAM FLICA Caspase-1 Assay Kit and the Caspase-8 Assay Kit (ImmunoChemistry Technologies) were used to evaluate the presence of catalytically active forms of Caspase-1 (p10 and p12) and Caspase-8. Th17 cells were stimulated and incubated with different cytokines for 5 days. The cells were washed and resuspended in RPMI1640 medium with 10% FBS with PMA and Ionomycin for 4.5 h and stained with 30x FAM-VAD-FMK for 30 min at 37 °C. Afterwards, the cells were also stained with the Intracellular cytokine cocktail, following the procedure described above. Cells were analyzed by flow cytometry.

4.2.4.6 Cell tracker Violet staining

Isolated cells were washed with PBS firstly to remove FCS, resuspended with Cell trace violet staining solution, and incubated for 20 min at 37°C. Stained cells were then washed with MACS buffer to absorb unbound dye and resuspended in RPMI1640 complete medium. Cells were ready for the further stimulation or cell culture.

4.2.5 Molecular biological methods

4.2.4.2 Total protein extraction

Cells were washed once with cold PBS and lysed in RIPA buffer (50mM Tris, 150mM NaCl, 1 mM EDTA, 0.1% NP-40, pH 7.5) containing protease inhibitor and phosphoSTOP (all from Roche) on ice. Cell lysates were then centrifuged at 14,000 rpm for 15 minutes at 4°C, supernatants were collected for Pierce BCA Protein Assay.

4.2.4.3 Pierce BCA Protein Assay.

10 µL of each standard (20-2000 µg/ml) or sample extracts were pipetted into a microplate well, followed by addition of 200 µl of BCA working reagent (50 parts of

BCA Reagent A and 1 part of BCA Reagent B). After 30 min of incubation at 37 °C the absorbance at 562 nm was measured and protein concentration was calculated by the standard curve.

4.2.4.3 SDS-PAGE

Gels were prepared with 12.5% SDS for separating and 4% for stacking. 20-40 µg of total protein extracts were loaded into wells. For time course experiments, total cells were collected from 4 wells ($5x10^4$ were seeded initially) at 5 different time points. Samples were then boiled in 4x Laemmli buffer with 2-ME for 10 min at 99°C. and run at 80 v for stacking and 100 v for separating. After fractionation, gels were then transferred to PVDF membranes (0.2 µm, Merck Millipore) and blocked with Odyssey blocking buffer for 1 hour and probed with primary antibody (used dilution see table 4.1.5) overnight and fluorescently-labeled secondary antibody (1:1000 dilution, Odyssey) for 1 hour. Images were analysed with Odyssey® Fc Imaging System (LI-COR) and quantified with Image Studio™ Software.

4.2.4.4 RNA extraction and convertion to cDNA

At the end point of incubation, cultured T cells were washed once with wash buffer and stimulated with PMA plus ionomycin for 3 hours. Total RNA was extracted from the stimulated cells by using TRIzol reagent (Invitrogen) according to the manufacturer's instructions. RNA concentration and purity were measured with Nanodrop and diluted to the same concentration within the same sample group. The conversion of cDNA from RNA was performed by using High capacity cDNA Reverse transcription kits (Applied Biosystems). The master mix was as indicated here:

Component	Volume/Reaction(µL)
10X RT	2.0
25X dNTP	0.8
10X RT	2.0
Reverse	1.0

RNase	1.0
Nuclease-	3.2
Total per	10.0

Thermal cycler conditions for performing reverse transcription:

	Step 1	Step 2	Step 3	Step 4
Temperature (°C)	25	37	85	4
Time	10 min	120 min	5 min	∞

4.2.4.5 Quantitative PCR

Quantitative PCR was performed in a reaction including 5 µl Taqman® Universal PCR Master Mix (2X), 0.5 µl of Taqman® gene Expression assay mix (20X) and 4.5 µl sample (1-100 ng total cDNA). The PCR reactions were run on the Roche LightCycler 480 Real-Time PCR system. The thermal cycling parameters were the following:

	Polymerase	PCR	
	Hold	Denature	Anneal/extend
Temperature (°C)	95	95	60
Time	10 min	15 sec	1 min

4.2.6 Calpain activity assay

Cells were harvested and washed with cold PBS. Then cells were resuspended in Extraction Buffer (Abcam) and centrifuged at 14,000 rpm. Supernatants were collected and measure the protein concentration with Pierce BCA Protein Assay. 40 µg cell lysates were adjusted to 85 µL/well from each group. 10 µL 10x Reaction Buffer and 5 µL calpain substrate were added into each well. 1-2 µL of active Calpain was used as the positive control. 1µL calpain inhibitor was used as the negative control. Lysates

and calpain substrate were incubated at 37°C for 60 min. Fluorometric signal was detected at Ex/Em 400/505 nm.

4.2.7 ELISA

Captured antibodies were diluted in PBS and coated in a half-area high-binding 96 well plate (Greiner Bio-One) overnight at room temperature. Plates were then blocked with reagent diluent (1% BSA in PBS) at room temperature for 1 hour. Samples were loaded in duplicates and incubated for 2 hours. Detection antibodies were used according to the manufacturer's instructions (R&D systems). Plates were washed three times between steps with wash buffer (0.05% Tween 20 in PBS). In the final step, plates were read at 450 nm and 540 nm were used as reference. Standard curve was created by Microsoft Excel by generating a four-parameter logistic (4-PL) curve-fit.

4.2.8 Microarray analysis

The microarray analyses were done by Dr. Gustavo Almeida. In brief, total RNA was extracted using the RNA MiniPrep kit and hybridized to Genechip Human Genome U133 Plus 2.0 Arrays (Affymetrix) according to the manufacturer's instructions for the whole-transcriptome pico Kit. Raw signals were processed by the affy R package (PMID:14960456) and normalized using the robust multi-array average (RMA) expression measure with background correction and cross- chip quantile normalization. The limma R package (PMID:25605792) was applied to identify differentially expressed genes using linear model fit and adjusting for differences between biological replicates. Empirical Bayes Statistics was used for moderation of standard errors and p-values were adjusted with the Benjamini & Hochberg method. A false discovery rate (FDR) smaller than 0.05 and a fold change cutoff of 2 were used to define the differentially expressed genes.

5 Table of figures

6 References

Afonina, I. S., Tynan, G. A., Logue, S. E., Cullen, S. P., Bots, M., Luthi, A. U., . . . Martin, S. J. (2011). Granzyme B-dependent proteolysis acts as a switch to enhance the proinflammatory activity of IL-1alpha. *Mol Cell, 44*(2), 265-278. doi:10.1016/j.molcel.2011.07.037

Aggarwal, S., Gollapudi, S., & Gupta, S. (1999). Increased TNF-alpha-induced apoptosis in lymphocytes from aged humans: changes in TNF-alpha receptor expression and activation of caspases. *J Immunol, 162*(4), 2154-2161.

Agostini, L., Martinon, F., Burns, K., McDermott, M. F., Hawkins, P. N., & Tschopp, J. (2004). NALP3 forms an IL-1beta-processing inflammasome with increased activity in Muckle-Wells autoinflammatory disorder. *Immunity, 20*(3), 319-325. doi:10.1016/s1074-7613(04)00046-9

Ara, A., Ahmed, K. A., & Xiang, J. (2018). Mannose-6-phosphate receptor: a novel regulator of T cell immunity. *Cell Mol Immunol, 15*(11), 986-988. doi:10.1038/s41423-018-0031-1

Arbore, G., West, E. E., Spolski, R., Robertson, A. A. B., Klos, A., Rheinheimer, C., . . . Kemper, C. (2016). T helper 1 immunity requires complement-driven NLRP3 inflammasome activity in CD4(+) T cells. *Science, 352*(6292), aad1210. doi:10.1126/science.aad1210

Ariel Werman, R. W.-V., Rosalyn White, Jae-Kwon Lee, Batsheva Werman, Yakov Krelin, Elena Voronov, Charles A. Dinarello, and Ron N. Apte. (2004). The precursor form of IL-1 is an intracrine proinflammatory activator of transcription. *Proc Natl Acad Sci USA., 101*, 2434-2439.

Aschenbrenner, D., Foglierini, M., Jarrossay, D., Hu, D., Weiner, H. L., Kuchroo, V. K., . . . Sallusto, F. (2018). An immunoregulatory and tissue-residency program modulated by c-MAF in human TH17 cells. *Nat Immunol, 19*(10), 1126-1136. doi:10.1038/s41590-018-0200-5

Bailly, S., Fay, M., Israël, N., & Gougerot-Pocidalo, M. A. (1996). The transcription factor AP-1 binds to the human interleukin 1 alpha promoter. *Eur Cytokine Netw, 7*(2), 125-128.

Bayley, J. P., van Rietschoten, J. G., Bakker, A. M., van Baarsen, L., Kaijzel, E. L., Wierenga, E. A., . . . Verweij, C. L. (2003). Allele-specific expression of the IL-1 alpha gene in human CD4+ T cell clones. *J Immunol, 171*(5), 2349-2353. doi:10.4049/jimmunol.171.5.2349

Bergsbaken, T., Fink, S. L., & Cookson, B. T. (2009). Pyroptosis: host cell death and inflammation. *Nat Rev Microbiol, 7*(2), 99-109. doi:10.1038/nrmicro2070

Bhan, U., Newstead, M. J., Zeng, X., Podsaid, A., Goswami, M., Ballinger, M. N., . . . Standiford, T. J. (2013). TLR9-dependent IL-23/IL-17 is required for the generation of Stachybotrys chartarum-induced hypersensitivity pneumonitis. *J Immunol, 190*(1), 349-356. doi:10.4049/jimmunol.1202225

Bossaller, L., Chiang, P. I., Schmidt-Lauber, C., Ganesan, S., Kaiser, W. J., Rathinam, V. A., . . . Latz, E. (2012). Cutting edge: FAS (CD95) mediates noncanonical IL-1beta and IL-18 maturation via caspase-8 in an RIP3-independent manner. *J Immunol, 189*(12), 5508-5512. doi:10.4049/jimmunol.1202121

Brenner, D., Blaser, H., & Mak, T. W. (2015). Regulation of tumour necrosis factor signalling: live or let die. *Nat Rev Immunol, 15*(6), 362-374. doi:10.1038/nri3834

Brenner, D., Krammer, P. H., & Arnold, R. (2008). Concepts of activated T cell death. *Crit Rev Oncol Hematol, 66*(1), 52-64. doi:10.1016/j.critrevonc.2008.01.002

Broz, P., & Dixit, V. M. (2016). Inflammasomes: mechanism of assembly, regulation and signalling. *Nat Rev Immunol, 16*(7), 407-420. doi:10.1038/nri.2016.58

Broz, P., Pelegrin, P., & Shao, F. (2020). The gasdermins, a protein family executing cell death and inflammation. *Nat Rev Immunol, 20*(3), 143-157. doi:10.1038/s41577-019-0228-2

Bruchard, M., Rebe, C., Derangere, V., Togbe, D., Ryffel, B., Boidot, R., . . . Ghiringhelli, F. (2015). The receptor NLRP3 is a transcriptional regulator of TH2 differentiation. *Nat Immunol, 16*(8), 859-870. doi:10.1038/ni.3202

Burzynski, L. C., Humphry, M., Pyrillou, K., Wiggins, K. A., Chan, J. N. E., Figg, N., . . . Clarke, M. C. H. (2019). The Coagulation and Immune Systems Are Directly Linked through the Activation of Interleukin-1alpha by Thrombin. *Immunity, 50*(4), 1033-1042 e1036. doi:10.1016/j.immuni.2019.03.003

Calderon, D., Nguyen, M. L. T., Mezger, A., Kathiria, A., Müller, F., Nguyen, V., . . . Pritchard, J. K. (2019). Landscape of stimulation-responsive chromatin across diverse human immune cells. *Nat Genet, 51*(10), 1494-1505. doi:10.1038/s41588-019-0505-9

Carruth LM, D. S., Mizel SB. (1991). Involvement of a calpain-like protease in the processing of the murine interleukin 1 alpha precursor. *J Biol Chem., 266*, 12162-12167.

Casson, C. N., Yu, J., Reyes, V. M., Taschuk, F. O., Yadav, A., Copenhaver, A. M., . . . Shin, S. (2015). Human caspase-4 mediates noncanonical inflammasome activation against gram-negative bacterial pathogens. *Proc Natl Acad Sci U S A, 112*(21), 6688-6693. doi:10.1073/pnas.1421699112

Cerdan, C., Martin, Y., Brailly, H., Courcoul, M., Flavetta, S., Costello, R., . . . Olive, D. (1991). IL-1 alpha is produced by T lymphocytes activated via the CD2 plus CD28 pathways. *J Immunol, 146*(2), 560-564.

Chen, C. J., Kono, H., Golenbock, D., Reed, G., Akira, S., & Rock, K. L. (2007). Identification of a key pathway required for the sterile inflammatory response triggered by dying cells. *Nat Med, 13*(7), 851-856. doi:10.1038/nm1603

Chen, D. Y., Chen, Y. M., Lan, J. L., Lin, C. C., Chen, H. H., & Hsieh, C. W. (2010). Potential role of Th17 cells in the pathogenesis of adult-onset Still's disease. *Rheumatology (Oxford), 49*(12), 2305-2312. doi:10.1093/rheumatology/keq284

Chen, M., Xing, Y., Lu, A., Fang, W., Sun, B., Chen, C., . . . Meng, G. (2015). Internalized Cryptococcus neoformans Activates the Canonical Caspase-1 and the Noncanonical Caspase-8 Inflammasomes. *J Immunol, 195*(10), 4962-4972. doi:10.4049/jimmunol.1500865

Chung, Y., Chang, S. H., Martinez, G. J., Yang, X. O., Nurieva, R., Kang, H. S., . . . Dong, C. (2009). Critical regulation of early Th17 cell differentiation by interleukin-1 signaling. *Immunity, 30*(4), 576-587. doi:10.1016/j.immuni.2009.02.007

Cohen, S., Bigazzi, P. E., & Yoshida, T. (1974). Commentary. Similarities of T cell function in cell-mediated immunity and antibody production. *Cell Immunol, 12*(1), 150-159. doi:10.1016/0008-8749(74)90066-5

Coll, R. C., Hill, J. R., Day, C. J., Zamoshnikova, A., Boucher, D., Massey, N. L., . . . Schroder, K. (2019). MCC950 directly targets the NLRP3 ATP-hydrolysis motif for inflammasome inhibition. *Nat Chem Biol, 15*(6), 556-559. doi:10.1038/s41589-019-0277-7

Coll, R. C., Robertson, A. A., Chae, J. J., Higgins, S. C., Munoz-Planillo, R., Inserra, M. C., . . . O'Neill, L. A. (2015). A small-molecule inhibitor of the NLRP3 inflammasome for the treatment of inflammatory diseases. *Nat Med, 21*(3), 248-255. doi:10.1038/nm.3806

Costello, R., Cerdan, C., Pavon, C., Brailly, H., Hurpin, C., Mawas, C., & Olive, D. (1993). The CD2 and CD28 adhesion molecules induce long-term autocrine proliferation of CD4+ T cells. *Eur J Immunol, 23*(3), 608-613. doi:10.1002/eji.1830230304

Cruz, C. M., Rinna, A., Forman, H. J., Ventura, A. L., Persechini, P. M., & Ojcius, D. M. (2007). ATP activates a reactive oxygen species-dependent oxidative stress response and secretion of proinflammatory cytokines in macrophages. *J Biol Chem, 282*(5), 2871-2879. doi:10.1074/jbc.M608083200

Cua, D. J., Sherlock, J., Chen, Y., Murphy, C. A., Joyce, B., Seymour, B., . . . Sedgwick, J. D. (2003). Interleukin-23 rather than interleukin-12 is the critical cytokine for autoimmune inflammation of the brain. *Nature, 421*(6924), 744-748. doi:10.1038/nature01355

Daniels, M. J., & Brough, D. (2017). Unconventional Pathways of Secretion Contribute to Inflammation. *Int J Mol Sci, 18*(1). doi:10.3390/ijms18010102

de Beeck, K. O., Van Laer, L., & Van Camp, G. (2012). DFNA5, a gene involved in hearing loss and cancer: a review. *Ann Otol Rhinol Laryngol, 121*(3), 197-207. doi:10.1177/000348941212100310

de Jesus, A. A., Canna, S. W., Liu, Y., & Goldbach-Mansky, R. (2015). Molecular mechanisms in genetically defined autoinflammatory diseases: disorders of amplified danger signaling. *Annu Rev Immunol, 33*, 823-874. doi:10.1146/annurev-immunol-032414-112227

Devadas, S., Zaritskaya, L., Rhee, S. G., Oberley, L., & Williams, M. S. (2002). Discrete generation of superoxide and hydrogen peroxide by T cell receptor stimulation: selective regulation of mitogen-activated protein kinase activation and fas ligand expression. *J Exp Med, 195*(1), 59-70. doi:10.1084/jem.20010659

Di Paolo, N. C., & Shayakhmetov, D. M. (2016). Interleukin 1alpha and the inflammatory process. *Nat Immunol, 17*(8), 906-913. doi:10.1038/ni.3503

Dinarello, C. A., Goldin, N. P., & Wolff, S. M. (1974). Demonstration and characterization of two distinct human leukocytic pyrogens. *J Exp Med, 139*(6), 1369-1381. doi:10.1084/jem.139.6.1369

Doitsh, G., Galloway, N. L., Geng, X., Yang, Z., Monroe, K. M., Zepeda, O., . . . Greene, W. C. (2014). Cell death by pyroptosis drives CD4 T-cell depletion in HIV-1 infection. *Nature, 505*(7484), 509-514. doi:10.1038/nature12940

Eigenbrod, T., Park, J. H., Harder, J., Iwakura, Y., & Núñez, G. (2008). Cutting edge: critical role for mesothelial cells in necrosis-induced inflammation through the recognition of IL-1 alpha released from dying cells. *J Immunol, 181*(12), 8194-8198. doi:10.4049/jimmunol.181.12.8194

England, H., Summersgill, H. R., Edye, M. E., Rothwell, N. J., & Brough, D. (2014). Release of interleukin-1alpha or interleukin-1beta depends on mechanism of cell death. *J Biol Chem, 289*(23), 15942-15950. doi:10.1074/jbc.M114.557561

Evavold, C. L., Ruan, J., Tan, Y., Xia, S., Wu, H., & Kagan, J. C. (2018). The Pore-Forming Protein Gasdermin D Regulates Interleukin-1 Secretion from Living Macrophages. *Immunity, 48*(1), 35-44 e36. doi:10.1016/j.immuni.2017.11.013

Eyerich, S., & Zielinski, C. E. (2014). Defining Th-cell subsets in a classical and tissue-specific manner: Examples from the skin. *Eur J Immunol, 44*(12), 3475-3483. doi:10.1002/eji.201444891

Fettelschoss, A., Kistowska, M., LeibundGut-Landmann, S., Beer, H. D., Johansen, P., Senti, G., . . . Kundig, T. M. (2011). Inflammasome activation and IL-1beta target IL-1alpha for secretion as opposed to surface expression. *Proc Natl Acad Sci U S A, 108*(44), 18055-18060. doi:10.1073/pnas.1109176108

Fink, S. L., Bergsbaken, T., & Cookson, B. T. (2008). Anthrax lethal toxin and Salmonella elicit the common cell death pathway of caspase-1-dependent pyroptosis via distinct mechanisms. *Proc Natl Acad Sci U S A, 105*(11), 4312-4317. doi:10.1073/pnas.0707370105

Gaidt, M. M., Ebert, T. S., Chauhan, D., Schmidt, T., Schmid-Burgk, J. L., Rapino, F., . . . Hornung, V. (2016). Human Monocytes Engage an Alternative Inflammasome Pathway. *Immunity, 44*(4), 833-846. doi:10.1016/j.immuni.2016.01.012

Gao, Y., Deason, K., Jain, A., Irizarry-Caro, R. A., Dozmorov, I., Coughlin, L. A., . . . Pasare, C. (2020). Transcriptional profiling identifies caspase-1 as a T cell-intrinsic regulator of Th17 differentiation. *J Exp Med, 217*(4). doi:10.1084/jem.20190476

Garlanda, C., Dinarello, C. A., & Mantovani, A. (2013). The interleukin-1 family: back to the future. *Immunity, 39*(6), 1003-1018. doi:10.1016/j.immuni.2013.11.010

Gasch, M., Goroll, T., Bauer, M., Hinz, D., Schutze, N., Polte, T., . . . Herberth, G. (2014). Generation of IL-8 and IL-9 producing CD4(+) T cells is affected by Th17 polarizing conditions and AHR ligands. *Mediators Inflamm, 2014*, 182549. doi:10.1155/2014/182549

Goldbach-Mansky, R., & Kastner, D. L. (2009). Autoinflammation: the prominent role of IL-1 in monogenic autoinflammatory diseases and implications for common illnesses. *J Allergy Clin Immunol, 124*(6), 1141-1149; quiz 1150-1141. doi:10.1016/j.jaci.2009.11.016

Gupta, S. (2002). Tumor necrosis factor-alpha-induced apoptosis in T cells from aged humans: a role of TNFR-I and downstream signaling molecules. *Exp Gerontol, 37*(2-3), 293-299. doi:10.1016/s0531-5565(01)00195-4

Harrington, L. E., Hatton, R. D., Mangan, P. R., Turner, H., Murphy, T. L., Murphy, K. M., & Weaver, C. T. (2005). Interleukin 17-producing CD4+ effector T cells develop via a lineage distinct from the T helper type 1 and 2 lineages. *Nat Immunol, 6*(11), 1123-1132. doi:10.1038/ni1254

He, W. T., Wan, H., Hu, L., Chen, P., Wang, X., Huang, Z., . . . Han, J. (2015). Gasdermin D is an executor of pyroptosis and required for interleukin-1beta secretion. *Cell Res, 25*(12), 1285-1298. doi:10.1038/cr.2015.139

He, Y., Hara, H., & Nunez, G. (2016). Mechanism and Regulation of NLRP3 Inflammasome Activation. *Trends Biochem Sci, 41*(12), 1012-1021. doi:10.1016/j.tibs.2016.09.002

Hyrich, K. L., Watson, K. D., Silman, A. J., Symmons, D. P., & British Society for Rheumatology Biologics, R. (2006). Predictors of response to anti-TNF-alpha therapy among patients with rheumatoid arthritis: results from the British Society for Rheumatology Biologics Register. *Rheumatology (Oxford), 45*(12), 1558-1565. doi:10.1093/rheumatology/kel149

Ivanov, II, McKenzie, B. S., Zhou, L., Tadokoro, C. E., Lepelley, A., Lafaille, J. J., . . . Littman, D. R. (2006). The orphan nuclear receptor RORgammat directs the differentiation program of proinflammatory IL-17+ T helper cells. *Cell, 126*(6), 1121-1133. doi:10.1016/j.cell.2006.07.035

Kaminski, M. M., Sauer, S. W., Klemke, C. D., Suss, D., Okun, J. G., Krammer, P. H., & Gulow, K. (2010). Mitochondrial reactive oxygen species control T cell activation by regulating IL-2 and IL-4 expression: mechanism of ciprofloxacin-mediated immunosuppression. *J Immunol, 184*(9), 4827-4841. doi:10.4049/jimmunol.0901662

Kayagaki, N., Stowe, I. B., Lee, B. L., O'Rourke, K., Anderson, K., Warming, S., . . . Dixit, V. M. (2015). Caspase-11 cleaves gasdermin D for non-canonical inflammasome signalling. *Nature, 526*(7575), 666-671. doi:10.1038/nature15541

Kearney, C. J., & Martin, S. J. (2017). An Inflammatory Perspective on Necroptosis. *Mol Cell, 65*(6), 965-973. doi:10.1016/j.molcel.2017.02.024

Keller, M., Ruegg, A., Werner, S., & Beer, H. D. (2008). Active caspase-1 is a regulator of unconventional protein secretion. *Cell, 132*(5), 818-831. doi:10.1016/j.cell.2007.12.040

Klein, S. A., Dobmeyer, J. M., Dobmeyer, T. S., Falke, D., Kabelitz, D., Friese, K., . . . Rossol-Voth, R. (1996). TNF-alpha mediated apoptosis of CD4 positive T-lymphocytes. A model of T-cell depletion in HIV infected individuals. *European journal of medical research, 1*(5), 249-258. Retrieved from http://europepmc.org/abstract/MED/9374446

Kurt-Jones, E. A., Beller, D. I., Mizel, S. B., & Unanue, E. R. (1985). Identification of a membrane-associated interleukin 1 in macrophages. *Proc Natl Acad Sci U S A, 82*(4), 1204-1208. doi:10.1073/pnas.82.4.1204

Langrish, C. L., Chen, Y., Blumenschein, W. M., Mattson, J., Basham, B., Sedgwick, J. D., . . . Cua, D. J. (2005). IL-23 drives a pathogenic T cell population that induces autoimmune inflammation. *J Exp Med, 201*(2), 233-240. doi:10.1084/jem.20041257

Lawless, C., Wang, C., Jurk, D., Merz, A., Zglinicki, T., & Passos, J. F. (2010). Quantitative assessment of markers for cell senescence. *Exp Gerontol, 45*(10), 772-778. doi:10.1016/j.exger.2010.01.018

Lever, W. F. (1953). Pemphigus. *Medicine (Baltimore), 32*(1), 1-123. doi:10.1097/00005792-195302000-00001

Li, Y., Shen, Y., Jin, K., Wen, Z., Cao, W., Wu, B., . . . Weyand, C. M. (2019). The DNA Repair Nuclease MRE11A Functions as a Mitochondrial Protector and Prevents

T Cell Pyroptosis and Tissue Inflammation. *Cell Metab, 30*(3), 477-492 e476. doi:10.1016/j.cmet.2019.06.016

Lin, L., Couturier, J., Yu, X., Medina, M. A., Kozinetz, C. A., & Lewis, D. E. (2014). Granzyme B secretion by human memory CD4 T cells is less strictly regulated compared to memory CD8 T cells. *BMC Immunol, 15*, 36. doi:10.1186/s12865-014-0036-1

Lin, Y. C., Lin, Y. C., Wu, C. C., Huang, M. Y., Tsai, W. C., Hung, C. H., & Kuo, P. L. (2017). The immunomodulatory effects of TNF-α inhibitors on human Th17 cells via RORγt histone acetylation. *Oncotarget, 8*(5), 7559-7571. doi:10.18632/oncotarget.13791

Liu, X., & Lieberman, J. (2017). A Mechanistic Understanding of Pyroptosis: The Fiery Death Triggered by Invasive Infection. *Adv Immunol, 135*, 81-117. doi:10.1016/bs.ai.2017.02.002

Mahnke, Y. D., Brodie, T. M., Sallusto, F., Roederer, M., & Lugli, E. (2013). The who's who of T-cell differentiation: human memory T-cell subsets. *Eur J Immunol, 43*(11), 2797-2809. doi:10.1002/eji.201343751

Mangan, P. R., Harrington, L. E., O'Quinn, D. B., Helms, W. S., Bullard, D. C., Elson, C. O., . . . Weaver, C. T. (2006). Transforming growth factor-beta induces development of the T(H)17 lineage. *Nature, 441*(7090), 231-234. doi:10.1038/nature04754

Mariathasan, S., Newton, K., Monack, D. M., Vucic, D., French, D. M., Lee, W. P., . . . Dixit, V. M. (2004). Differential activation of the inflammasome by caspase-1 adaptors ASC and Ipaf. *Nature, 430*(6996), 213-218. doi:10.1038/nature02664

Marta, M., Andersson, A., Isaksson, M., Kampe, O., & Lobell, A. (2008). Unexpected regulatory roles of TLR4 and TLR9 in experimental autoimmune encephalomyelitis. *Eur J Immunol, 38*(2), 565-575. doi:10.1002/eji.200737187

Martin, B. N., Wang, C., Zhang, C. J., Kang, Z., Gulen, M. F., Zepp, J. A., . . . Li, X. (2016). T cell-intrinsic ASC critically promotes T(H)17-mediated experimental autoimmune encephalomyelitis. *Nat Immunol, 17*(5), 583-592. doi:10.1038/ni.3389

Martinon, F., Burns, K., & Tschopp, J. (2002). The inflammasome: a molecular platform triggering activation of inflammatory caspases and processing of proIL-beta. *Mol Cell, 10*(2), 417-426. doi:10.1016/s1097-2765(02)00599-3

McDowell, T. L., Symons, J. A., & Duff, G. W. (2005). Human interleukin-1 alpha gene expression is regulated by Sp1 and a transcriptional repressor. *Cytokine, 30*(4), 141-153. doi:10.1016/j.cyto.2004.12.010

McGeachy, M. J., Chen, Y., Tato, C. M., Laurence, A., Joyce-Shaikh, B., Blumenschein, W. M., . . . Cua, D. J. (2009). The interleukin 23 receptor is essential for the terminal differentiation of interleukin 17-producing effector T helper cells in vivo. *Nat Immunol, 10*(3), 314-324. doi:10.1038/ni.1698

Mosmann, T. R., Cherwinski, H., Bond, M. W., Giedlin, M. A., & Coffman, R. L. (1986). Two types of murine helper T cell clone. I. Definition according to profiles of lymphokine activities and secreted proteins. *J Immunol, 136*(7), 2348-2357.

Noster, R., de Koning, H. D., Maier, E., Prelog, M., Lainka, E., & Zielinski, C. E. (2016). Dysregulation of proinflammatory versus anti-inflammatory human TH17 cell

functionalities in the autoinflammatory Schnitzler syndrome. *J Allergy Clin Immunol, 138*(4), 1161-1169 e1166. doi:10.1016/j.jaci.2015.12.1338

Orjalo, A. V., Bhaumik, D., Gengler, B. K., Scott, G. K., & Campisi, J. (2009). Cell surface-bound IL-1alpha is an upstream regulator of the senescence-associated IL-6/IL-8 cytokine network. *Proc Natl Acad Sci U S A, 106*(40), 17031-17036. doi:10.1073/pnas.0905299106

Pardo, J., Bosque, A., Brehm, R., Wallich, R., Naval, J., Mullbacher, A., . . . Simon, M. M. (2004). Apoptotic pathways are selectively activated by granzyme A and/or granzyme B in CTL-mediated target cell lysis. *J Cell Biol, 167*(3), 457-468. doi:10.1083/jcb.200406115

Perez, J., Dansou, B., Herve, R., Levi, C., Tamouza, H., Vandermeersch, S., . . . Baud, L. (2016). Calpains Released by T Lymphocytes Cleave TLR2 To Control IL-17 Expression. *J Immunol, 196*(1), 168-181. doi:10.4049/jimmunol.1500749

Peters, V. A., Joesting, J. J., & Freund, G. G. (2013). IL-1 receptor 2 (IL-1R2) and its role in immune regulation. *Brain Behav Immun, 32*, 1-8. doi:10.1016/j.bbi.2012.11.006

Robson, R. L., Westwick, J., & Brown, Z. (1995). Interleukin-1-induced IL-8 and IL-6 gene expression and production in human mesangial cells is differentially regulated by cAMP. *Kidney Int, 48*(6), 1767-1777. doi:10.1038/ki.1995.475

Rogers, C., Erkes, D. A., Nardone, A., Aplin, A. E., Fernandes-Alnemri, T., & Alnemri, E. S. (2019). Gasdermin pores permeabilize mitochondria to augment caspase-3 activation during apoptosis and inflammasome activation. *Nat Commun, 10*(1), 1689. doi:10.1038/s41467-019-09397-2

Sallusto, F., Zielinski, C. E., & Lanzavecchia, A. (2012). Human Th17 subsets. *Eur J Immunol, 42*(9), 2215-2220. doi:10.1002/eji.201242741

Sarhan, J., Liu, B. C., Muendlein, H. I., Li, P., Nilson, R., Tang, A. Y., . . . Poltorak, A. (2018). Caspase-8 induces cleavage of gasdermin D to elicit pyroptosis during Yersinia infection. *Proc Natl Acad Sci U S A, 115*(46), E10888-e10897. doi:10.1073/pnas.1809548115

Schneider, K. S., Gross, C. J., Dreier, R. F., Saller, B. S., Mishra, R., Gorka, O., . . . Gross, O. (2017). The Inflammasome Drives GSDMD-Independent Secondary Pyroptosis and IL-1 Release in the Absence of Caspase-1 Protease Activity. *Cell Rep, 21*(13), 3846-3859. doi:10.1016/j.celrep.2017.12.018

Shi, J., Zhao, Y., Wang, K., Shi, X., Wang, Y., Huang, H., . . . Shao, F. (2015). Cleavage of GSDMD by inflammatory caspases determines pyroptotic cell death. *Nature, 526*(7575), 660-665. doi:10.1038/nature15514

Shimada, K., Crother, T. R., Karlin, J., Dagvadorj, J., Chiba, N., Chen, S., . . . Arditi, M. (2012). Oxidized mitochondrial DNA activates the NLRP3 inflammasome during apoptosis. *Immunity, 36*(3), 401-414. doi:10.1016/j.immuni.2012.01.009

Shirasaki, Y., Yamagishi, M., Suzuki, N., Izawa, K., Nakahara, A., Mizuno, J., . . . Ohara, O. (2014). Real-time single-cell imaging of protein secretion. *Sci Rep, 4*, 4736. doi:10.1038/srep04736

Simeoni, L., & Bogeski, I. (2015). Redox regulation of T-cell receptor signaling. *Biol Chem, 396*(5), 555-568. doi:10.1515/hsz-2014-0312

Smith, S. H., Peredo, C. E., Takeda, Y., Bui, T., Neil, J., Rickard, D., . . . Cote-Sierra, J. (2016). Development of a Topical Treatment for Psoriasis Targeting RORγ:

From Bench to Skin. *PLoS One, 11*(2), e0147979. doi:10.1371/journal.pone.0147979

Sutton, C., Brereton, C., Keogh, B., Mills, K. H., & Lavelle, E. C. (2006). A crucial role for interleukin (IL)-1 in the induction of IL-17-producing T cells that mediate autoimmune encephalomyelitis. *J Exp Med, 203*(7), 1685-1691. doi:10.1084/jem.20060285

Tapia, V. S., Daniels, M. J. D., Palazon-Riquelme, P., Dewhurst, M., Luheshi, N. M., Rivers-Auty, J., . . . Brough, D. (2019). The three cytokines IL-1beta, IL-18, and IL-1alpha share related but distinct secretory routes. *J Biol Chem, 294*(21), 8325-8335. doi:10.1074/jbc.RA119.008009

Toda, Y., Tsukada, J., Misago, M., Kominato, Y., Auron, P. E., & Tanaka, Y. (2002). Autocrine induction of the human pro-IL-1beta gene promoter by IL-1beta in monocytes. *J Immunol, 168*(4), 1984-1991. doi:10.4049/jimmunol.168.4.1984

Tschopp, J., & Schroder, K. (2010). NLRP3 inflammasome activation: The convergence of multiple signalling pathways on ROS production? *Nat Rev Immunol, 10*(3), 210-215. doi:10.1038/nri2725

Veldhoen, M., Hocking, R. J., Atkins, C. J., Locksley, R. M., & Stockinger, B. (2006). TGFbeta in the context of an inflammatory cytokine milieu supports de novo differentiation of IL-17-producing T cells. *Immunity, 24*(2), 179-189. doi:10.1016/j.immuni.2006.01.001

Vigano, E., Diamond, C. E., Spreafico, R., Balachander, A., Sobota, R. M., & Mortellaro, A. (2015). Human caspase-4 and caspase-5 regulate the one-step non-canonical inflammasome activation in monocytes. *Nat Commun, 6*, 8761. doi:10.1038/ncomms9761

Waite, J. C., & Skokos, D. (2012). Th17 response and inflammatory autoimmune diseases. *Int J Inflam, 2012*, 819467. doi:10.1155/2012/819467

Weaver, C. T., Harrington, L. E., Mangan, P. R., Gavrieli, M., & Murphy, K. M. (2006). Th17: an effector CD4 T cell lineage with regulatory T cell ties. *Immunity, 24*(6), 677-688. doi:10.1016/j.immuni.2006.06.002

Wiggins, K. A., Parry, A. J., Cassidy, L. D., Humphry, M., Webster, S. J., Goodall, J. C., . . . Clarke, M. C. H. (2019). IL-1alpha cleavage by inflammatory caspases of the noncanonical inflammasome controls the senescence-associated secretory phenotype. *Aging Cell, 18*(3), e12946. doi:10.1111/acel.12946

Wilson, N. J., Boniface, K., Chan, J. R., McKenzie, B. S., Blumenschein, W. M., Mattson, J. D., . . . de Waal Malefyt, R. (2007). Development, cytokine profile and function of human interleukin 17-producing helper T cells. *Nat Immunol, 8*(9), 950-957. doi:10.1038/ni1497

Y Kobayashi, K. Y., T Saido, H Kawasaki, J J Oppenheim, and K Matsushima. (1990). Identification of calcium-activated neutral protease as a processing enzyme of human interleukin 1 alpha. *Proc Natl Acad Sci USA, 87*, 5548-5552.

Yang, J., Pemberton, A., Morrison, W. I., & Connelley, T. (2019). Granzyme B Is an Essential Mediator in CD8(+) T Cell Killing of Theileria parva-Infected Cells. *Infect Immun, 87*(1). doi:10.1128/IAI.00386-18

Yasuda, K., Takeuchi, Y., & Hirota, K. (2019). The pathogenicity of Th17 cells in autoimmune diseases. *Semin Immunopathol, 41*(3), 283-297. doi:10.1007/s00281-019-00733-8

Yu, J., Li, S., Qi, J., Chen, Z., Wu, Y., Guo, J., . . . Zheng, J. (2019). Cleavage of GSDME by caspase-3 determines lobaplatin-induced pyroptosis in colon cancer cells. *Cell Death Dis, 10*(3), 193. doi:10.1038/s41419-019-1441-4

Zaldivar, F., Nugent, D. J., Imfeld, K., & Berman, M. A. (2002). Identification of a novel regulatory element in the human interleukin 1 alpha (IL-1alpha) gene promoter. *Cytokine, 20*(3), 130-135. doi:10.1006/cyto.2002.1990

Zhang, Z., Zhang, Y., Xia, S., Kong, Q., Li, S., Liu, X., . . . Lieberman, J. (2020). Gasdermin E suppresses tumour growth by activating anti-tumour immunity. *Nature, 579*(7799), 415-420. doi:10.1038/s41586-020-2071-9

Zheng, Y., Danilenko, D. M., Valdez, P., Kasman, I., Eastham-Anderson, J., Wu, J., & Ouyang, W. (2007). Interleukin-22, a T(H)17 cytokine, mediates IL-23-induced dermal inflammation and acanthosis. *Nature, 445*(7128), 648-651. doi:10.1038/nature05505

Zheng, Y., Humphry, M., Maguire, J. J., Bennett, M. R., & Clarke, M. C. (2013). Intracellular interleukin-1 receptor 2 binding prevents cleavage and activity of interleukin-1alpha, controlling necrosis-induced sterile inflammation. *Immunity, 38*(2), 285-295. doi:10.1016/j.immuni.2013.01.008

Zhu, J., & Paul, W. E. (2008). CD4 T cells: fates, functions, and faults. *Blood, 112*(5), 1557-1569. doi:10.1182/blood-2008-05-078154

Zielinski, C. E., Mele, F., Aschenbrenner, D., Jarrossay, D., Ronchi, F., Gattorno, M., . . . Sallusto, F. (2012). Pathogen-induced human TH17 cells produce IFN-gamma or IL-10 and are regulated by IL-1beta. *Nature, 484*(7395), 514-518. doi:10.1038/nature10957

Publications and meetings

a) Publications in peer-reviewed journals

Matthias, J., Heink, S., Picard, F. S., Zeiträg, J., Kolz, A., **Chao, Y. Y.**, Soll, D., de Almeida, G. P., Glasmacher, E., Jacobsen, I. D., Riedel, T., Peters, A., Floess, S., Huehn, J., Baumjohann, D., Huber, M., Korn, T., & Zielinski, C. E. (2020). Salt generates anti-inflammatory Th17 cells but amplifies their pathogenicity in pro-inflammatory cytokine microenvironments. *The Journal of clinical investigation*

Matthias, J., Maul, J., Noster, R., Meinl, H., **Chao, Y. Y.**, Gerstenberg, H., Jeschke, F., Gasparoni, G., Welle, A., Walter, J., Nordström, K., Eberhardt, K., Renisch, D., Donakonda, S., Knolle, P., Soll, D., Grabbe, S., Garzorz-Stark, N., Eyerich, K., Biedermann, T., … Zielinski, C. E. (2019). Sodium chloride is an ionic checkpoint for human T_H2 cells and shapes the atopic skin microenvironment. *Science translational medicine*, *11*(480), eaau0683. https://doi.org/10.1126/scitranslmed.aau0683

Lückel, C., Picard, F., Raifer, H., Campos Carrascosa, L., Guralnik, A., Zhang, Y., Klein, M., Bittner, S., Steffen, F., Moos, S., Marini, F., Gloury, R., Kurschus, F. C., **Chao, Y. Y.**, Bertrams, W., Sexl, V., Schmeck, B., Bonetti, L., Grusdat, M., Lohoff, M., … Huber, M. (2019). IL-17$^+$ CD8$^+$ T cell suppression by dimethyl fumarate associates with clinical response in multiple sclerosis. *Nature communications*, *10*(1), 5722. https://doi.org/10.1038/s41467-019-13731-z

b) Scientific contributions at conferences and symposia

2017 FEBS 19th Immunology Summer School

Poster presentation: Role and regulation of IL-1α production by human T helper cells in health and disease

2018 EMBO workshop: The inflammasomes

Poster presentation: Role and regulation of Innate IL-1a production by human T helper cells in health and disease

2019 IL-17 Summit in Munich

Poster presentation: Role and regulation of Innate IL-1a production by human T helper cells in health and disease

2019 II. Joint Meeting of DGfI and SIICA

Poster presentation: Role and regulation of Innate IL-1a production by human T helper cells in health and disease

Acknowledgements

Foremost, I would like to express my sincere gratitude to my advisor Prof. Christina Zielinski for giving me the chance to work on this exciting project and also for her continuous support of my Ph.D. study. During the period of my Ph.D. research, her enthusiasm and dedication in science encourage and motivate me in discovering unknowns and generating novel ideas. She is always generous in giving me constructive advice and guidance whenever there were bottlenecks and breakthrough needed in findings. As an international student, all of these supports enable me to adapt to the environment faster, thus I was able to start developing this project more independently.

Besides my advisor, I would like to extend the appreciation to my thesis committee: Prof. Groß and Prof. Schmidt-Supprian, for their insightful comment and inputs, and also some intriguing questions.

My sincere thanks to Markus Utzt for helping with cell sort and also instructed me with the cell sorter, Tamara Cikovic, for teaching me Western blot techniques and the collaboration partners, Sabine Helmrath, Eslam Katab, Tomas Seeholzer and Dr. Hanna-Mari Baldauf, for their help throughout this project. Also, as a member of the big group seminar with Prof. Percy Knolle, I would like to thank all the members in the seminar for the significant inputs and sharing.

Without the contributions from Sonja Heine and Claudia Beerweiler, my master students and Lena Träger, my Bachelor student, this project would have not been accomplished at this expected pace. Besides, guiding and monitoring students in doing experiments have taught me the skills of leadership and supervisory.

Furthermore, as a member of SFB1054, I would also like to thank all the members in this scientific group and all the invited speakers for scientific discussions and inputs from every seminar, conferences, and retreats.

I would also like to thanks the formal lab members in our group: Christoph Hauser, for his patience in assisting me to uncover scientific questions and challenged me with several questions as well; Hanna Meinl, her consideration and sincerity always connect all the members together, which inspire me a lot; Ivan Shevchenko and David Frieser, for their warm support and assistance especially at the very early stage of my arrival at this country and city.

I thank my fellow labmates. Andrea Werner, thanks for all the purchase and organizations for our laboratory. A huge thank to Gustavo Almeida, for all the bioinformatics analyses; Gianna Rapp, her generous support eased my stressful moments, such as during thesis writing period; Chang-Feng Chu and Shan Sun, for their generous help and encouragement when I was writing my thesis.

Special thanks to all the members of our neighbor laboratory, Saur's group, for their kindness in sharing accessibility for the analytical instruments, which I needed for my project.

Finally, I must express my very profound gratitude to my parents and my friends for providing me with unfailing support and continuous encouragement throughout the entire period of 4 years of study as well as the process of researching and thesis writing. Last but not the least, Kuan-Wei Chen, Ju-En Chien, and Min-Hui Tou, my flatmates for their accompany and morale support. This accomplishment would not have been possible without them. Thank you.